SAPIENZA
UNIVERSITÀ DI ROMA

Photocatalytic degradation of reactive dyes by visible light and innovative Fe-doped titania catalysts.

Faculty of Civil and Industrial Engineering

Chemical, Material and Environmental Engineering Department

PhD Course in Chemical Engineering

PhD Candidate

Marika Michela Monaco

Supervisor

Prof. Roberto Lavecchia

XXX Cycle

Index

Chapter 2 – Literary review

Chapter 3 – Photocatalytic degradation of Reactive dyes under visible light

List of Figures

List of Tables

List of Symbols and abbreviations

RB4 — Reactive Blue 4

RR120 — Reactive Red 120

RV5 — Reactive Violet 5

CRB4 — Reactive Blue 4 concentration (ppm)

CRR120 — Reactive Red 120 concentration (ppm)

CRV5 — Reactive Violet 5concentration (ppm)

LEDs — Light Emitting Diodes

BL — Blue Light Emitting Diodes

k — rate constant (h^{-1})

m — initial rate constant (h^{-1})

Abs — Absorbance

A/Ao — (Absorbance at time t / Absorbance at time 0)

ID — inner diameter (cm)

H — height (cm)

Qair — air flow (Lh^{-1})

UV — ultra violet

vis — visible

Summary and outline

Problem Formulation

Reactive dyes are the largest class of dyes used in the textile industry. They were selected for the present study because the treatment of wastewaters containing these dyes by conventional methods is often inadequate due to their resistance to biological and chemical degradation. The use of reactive dyes for textile dyeing has increased steadily over the last few years because of theirs cost effectiveness and excellent wash and light fastness properties. However, these dyes exhibit a very low degree of fixation on the fibers, typically between 50 and 90%, which results in the release of substantial amounts of the compounds in the dyeing water. The dyeing water cannot be reused, so dye recovery is not an option with reactive dyes. The high aromaticity and low reactivity of these dyes make them highly resistant to both microbial and chemical degradation. Physical treatments are not efficient because they transfer the toxic dyes from one medium to the other, without converting them to harmless non-toxic substances.

The development of novel treatment methods, called Advanced Oxidation Processes (AOPs), characterized by production of the hydroxyl radical (·OH) as a primary oxidant, could represent a solution. The application of these AOPs, alone or simultaneously, could enhance ·OH radical production leading to higher oxidation rates.

In this work, the photocatalytic oxidative decolorization of various reactive dyes, Reactive Blue 4, Reactive Red 120 and Reactive Violet 5, under exposure to visible light and in the presence of new semiconductor catalysts, was investigated.

The results suggest that Reactive Blue 4 is highly unstable under exposure to visible light, thus the presence of photocatalysts is not necessary for the degradation of this dye.

The Reactive Red 120 cannot be treated by direct irradiation and it cannot be decolorized even in the presence of photocatalysts.

The other results obtained indicate that the photocatalytic treatment under visible light can be an effective method for the removal of Reactive Violet 5from textile effluents.

To enhance the Reactive Violet 5 decolorization yields, the operational parameters such as pH, catalyst loading and hydrogen peroxide concentration, were optimized.

Work Accomplished

The work done in this study has been presented in three chapters as discussed in the following text.

In **Chapter 1** the different types of dyes, particularly the reactive dyes, were described. The traditional methods (physical, biological and chemical) for removal of dyes from wastewaters were also described. Then, new methods for removal of dyes from wastewaters (Advanced Oxidation Processes) were reported. Among them, particular attention were given to the heterogeneous photocatalysis. The different types of catalyst and light sources that can be used, were also described.

In **Chapter 2** the recent advances in synthetic dyes photocatalytic decolorization were reported. The parameters affecting the photocatalytic processes (dye type, dye concentration, catalyst loading, pH, concentration of hydrogen peroxide, aeration, light source) were described. A comparison between the traditional light sources and the new light sources, such as the LEDs, was also reported.

In **Chapter 3** experimental procedures, description of reactor, instruments used and analytical techniques are discussed in detail. The decolorization of Reactive Blue 4, Reactive Red 120 and Reactive Violet 5, respectively, was studied. The influence of the type of catalyst, of pH, of catalyst concentration and hydrogen peroxide concentration, on the photocatalytic process was investigated. The optimal decolorization conditions were found.

The results were compared with those obtained from other authors. Finally, the conclusions and recommendations for future works, were reported.

Chapter 1
Introduction

1.1 Introduction

Textile industries use over 10,000 different dyes and pigments, and over 200,000 tons of these dyes are lost to effluents every year during the dyeing and finishing operations, due to the inefficiency of the dyeing process [1, 2]. Unfortunately, many of these dyes persist in the environment because they have high stability to light, temperature, water, detergents, chemicals and soaps [3]. Moreover, many anti-microbial agents (resistant to biological degradation) are often, used in the manufacture of textiles, especially for natural fibers [3; 4]. The synthetic origin and complex aromatic structure of the dyes make them more recalcitrant to biodegradation [5, 6]. However, environmental legislation obliges industries to eliminate color from their dye-containing effluents, before disposal into water bodies [2; 4].

Dyes not only seriously affect the aesthetic quality and transparency of water bodies like lakes, rivers and others, leading to damage to the aquatic environment [7, 8], but also some of them can show toxic effects, especially carcinogenic and mutagenic events [9, 10]. The removal of the dyes is very difficult because they are designed to be resistant to biodegradation, thus they remain in the environment for a long period of time. For example, the half-life of the hydrolyzed dye Reactive Blue 19 is about 46 years at pH 7 and 25°C [11, 12]. Moreover, Carneiro et al. (2010), have monitored the dyes C.I. Disperse Blue 373 (DB373), C.I. Disperse Orange 37 (DO37) and C.I. Disperse Violet 93 (DV93) in environmental samples. They have found that DB373, DO37 and DV93 were present in both untreated river water and drinking water. This suggests that the traditional effluent treatments (pre-chlorination, flocculation, coagulation and flotation) generally used by drinking water treatment plants, was not completely effective in removing these dyes. The mutagenic activity detected in these effluents confirms these results [13].

1.2 Dyes and Pigments

Organic colorants can be distinguished in two classes, dyes and pigments [14]. They differ because dyes are soluble in water and/or organic solvents, while pigments are insoluble in both types of liquid media. Dyes are used to color substrates to which they have affinity. Pigments can be used to color polymeric substrates. The mechanism is different from that of dyes, because coloration involves the materials surface only.

1.3 Dyes classification

All the aromatic compounds absorb electromagnetic energy, but only those that absorb light with wavelengths in the visible range (~400-700 nm) are colored. A dye molecule is made up of *chromophores*, delocalized electron systems with conjugated double bonds, and *auxochromes*, electron-withdrawing or electron-donating substituents that can cause or intensify the color of the chromophore by modifying the energy of the electron system. Tipycal chromophores are ethylene group (-C=C-), carbon-nitrogen group (-C=N-), carbonyl group (-C=O), azo group (-N=N-), nitro group ($-NO_2$) and aromatic rings. Auxochromes are amino ($–NH_2$), carboxyl (-COOH), sulphonate ($-SO_3H$) and hydroxyl (-OH) groups. There are about thirty different groups of dyes. They can be differentiated by the chemical structure or chromophore.

The chemical classification of dyes is based on the type of chromophore that is in the molecule (i.e. CI Constitution Number such as nitro, azo, carotenoid, diphenylmethane, xanthene, acridine, quinoline, indamine, sulphur, amino- and hydroxy ketone, anthraquinone, indigoid, phthalocyanine, inorganic pigment, etc.). The technical classification is based on the application technique of the dye (i.e. CI Generic Name such as acid, basic, direct, disperse, mordant, reactive, sulphur dye, pigment, vat, azo insoluble). Considering only the general structure, the textile dyes are also classified in anionic, nonionic and cationic dyes. The major anionic dyes are the direct, acid and reactive dyes. The major nonionic dyes are disperse dyes that does not ionised in the aqueous environment. The major cationic dyes are the azo basic, anthraquinone disperse and reactive dyes. Almost two-third of all organic dyes are azo dyes (R_1-N=N-R_2). They are used in a number of different industrial processes such as textile dyeing and printing, color photography, finishing processing of leather, pharmaceutical and cosmethics.

Most notable azo-dyes are: acid dyes, basic dyes (cationic dyes), direct dyes (substantive dyes), disperse dyes (non-ionic dyes), reactive dyes, vat dyes and sulfur dyes.

1.3.1 Reactive Dyes

The reactive dyes form one of largest dye classes. *Reactive dyes* contain reactive groups that are able of forming covalent bonds between carbon atoms of dye molecule and OH-, NH-, or SH- groups in fibres (cotton, wool, silk, nylon).
A reactive dye is characterized by its functional group. The reactive group can be a heterocyclic aromatic ring substituted with a chloride or fluoride atom. Another important reactive group is the vinyl sulphone (─SO_3─CH═CH_2) one.
During dyeing in alkaline conditions (i.e. pH 9-12), at high temperatures (30-70 ºC), and salt concentration from 40-100 g/L, reactive dyes form a reactive vinyl sulfone group, which creates a bond with the textile fibres (Figure 1.1). Anyway, the competition between the dye fixation reaction on the fibres and the undesired hydrolysis of the reactive group, results in a high loss of color (10–50%) in the resulting waters of the process.
To increase the fixation degree of the dye on the fibres, different types of salts (up 60 to 200 g/L) can be added during the dyeing process.

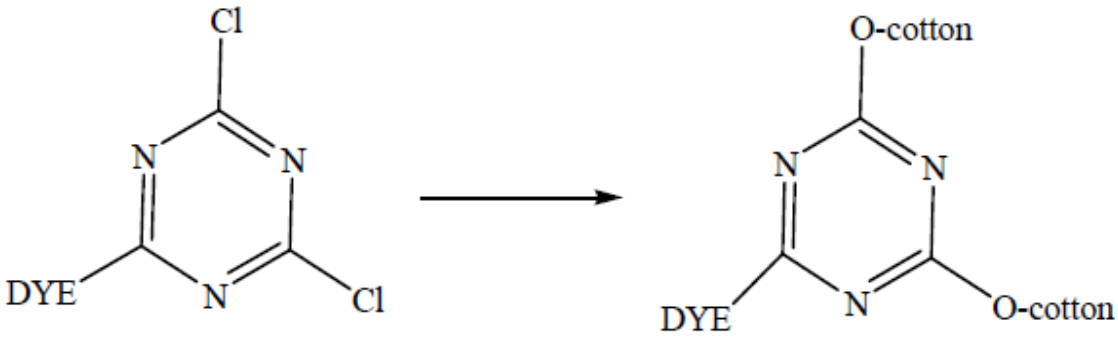

Figure 1.1 - Principle of cotton dyeing with a triazyl reactive dye [250].

1.3.2 Acid dyes

Acid dyes are anionic compounds used in dyeing nitrogen-containing fabrics like wool, polyamide, silk and modified acryl [14, 243]. They bind to the cationic NH_4^+ ions of those fibres. Acid dyes are typically applied to a textile at low pH, infact the term “acid” refers to the pH of the dyebaths. Acid dyes are caractherised by a high fixation degree: 80–95%.

1.3.3 Metal complex dyes

Among acid and reactive dyes, many metal complex dyes can be found. These are strong complexes of one metal atom (usually chromium, copper, cobalt or nickel) and one or two dye molecules, respectively.

1.3.4 Direct dyes

Direct dyes are mostly azo dyes with more than one azo bond or phthalocyanine, stilbene or oxazine compounds [14, 243]. Direct dyes were originally developed for theirs high affinity for cellulose fibres, and are water-insoluble. They can be used to dye polyester, but also nylon, cellulose triacetate, and acrylic fibers. They bind to the fibres through van der Waals forces. The dyes are, usually, finely ground in the presence of a dispersing agent to obtain a paste, or spray-dried to obtain a powder. Sometimes, a dyeing temperature of 130 °C, is required, and a pressurized dyebath is used. The dyeing rate can be influenced by the kind of dispersing agent used during the grinding.

1.3.5 Basic dyes

Most basic dyes are anthraquinone or azo compounds. Basic dyes are water-soluble cationic dyes [14, 244]. They can be used to dye acrylic fibers (they bind to the acid groups of the fibers), wool and silk. Acetic acid can be add to the dyebath to help the dyeing process. Basic dyes are also used in the paper industry.

1.3.6 Mordant dyes

Most mordant dyes are azo, oxazine or triarylmethane compounds. Mordant dyes require a mordant, a chemical that combines with the dye and the fiber. The choice of mordant is very important because different mordants can change the final color significantly.

The most important mordant dyes are the synthetic mordant dyes, or chrome dyes, used for wool. It is important to note that many mordants, particularly those in the heavy metal category, can be hazardous to health and extreme care must be taken in using them [244-248].

1.3.7 Disperse dyes

Disperse dyes are usually small azo or nitro compounds, anthraquinones or metal complex azo compounds. Disperse dyes are generally insoluble dyes. They can be used with synthetic fibers (cellulose acetate, polyester, polyamide, acryl, etc.) [243]. The dye diffusion requires swelling of the fibres, thus high temperatures (> 120 °C) or chemical softners have to be used. Dyeing process takes place in dyebaths with fine disperse solutions of these dyes.

1.3.8 Pigment dyes

Pigment dyes are usually azo or anthraquinones compounds or metal complex phthalocyanines.

Pigment dyes (or organic pigments) are insoluble, non-ionic compounds or insoluble salts. Pigment dyes are used in aqueous solution so a dispersing agent is required. Pigments can be combined with thickeners in print pastes for printing diverse fabrics [1, 14].

1.3.9 Vat dyes

Vat dyes are essentially insoluble in water and incapable of dyeing fibers directly [244]. However, reduction in alkaline liquor produces the water-soluble alkali metal salt of the dye, which, in this leuco form, has an affinity for the textile fibre. Therefore, the soluble leuco vat dyes can impregnate the fabric. Subsequent oxidation reforms the original insoluble dye. The color of denim is due to indigo, the original vat dye. Vat dyes are anthraquinones or indigoids. They are usually used for dyeing cellulose fibers.

1.3.10 Sulphur dyes

Sulphur dyes are complex polymeric aromatics with heterocyclic S-containing rings. They are used to dye cellulose fibres [243].

The fabric is usually heated in a solution of an organic compound (sulfide or polysulfide or nitrophenol derivative) that reacts with the sulphur dye and forms a dark color that bind to the fibers.

1.3.11 Solvent dyes

Lysochromes or “solvent dyes” are nonpolar or weakly polar and they cannot be ionizated. Solvent dyes are not soluble in water but they are soluble in organic solvents, thus they are used to color hydrocarbon fuels, waxes, lubricants, plastics, and other hydrocarbon-based non-polar materials [1, 14].

Solvent dyes are usually diazo compounds, but con also be triarylmethane, anthraquinone and phthalocyanine solvent dyes.

Structures of some organic dyes from different classes are given in Figure 1.2.

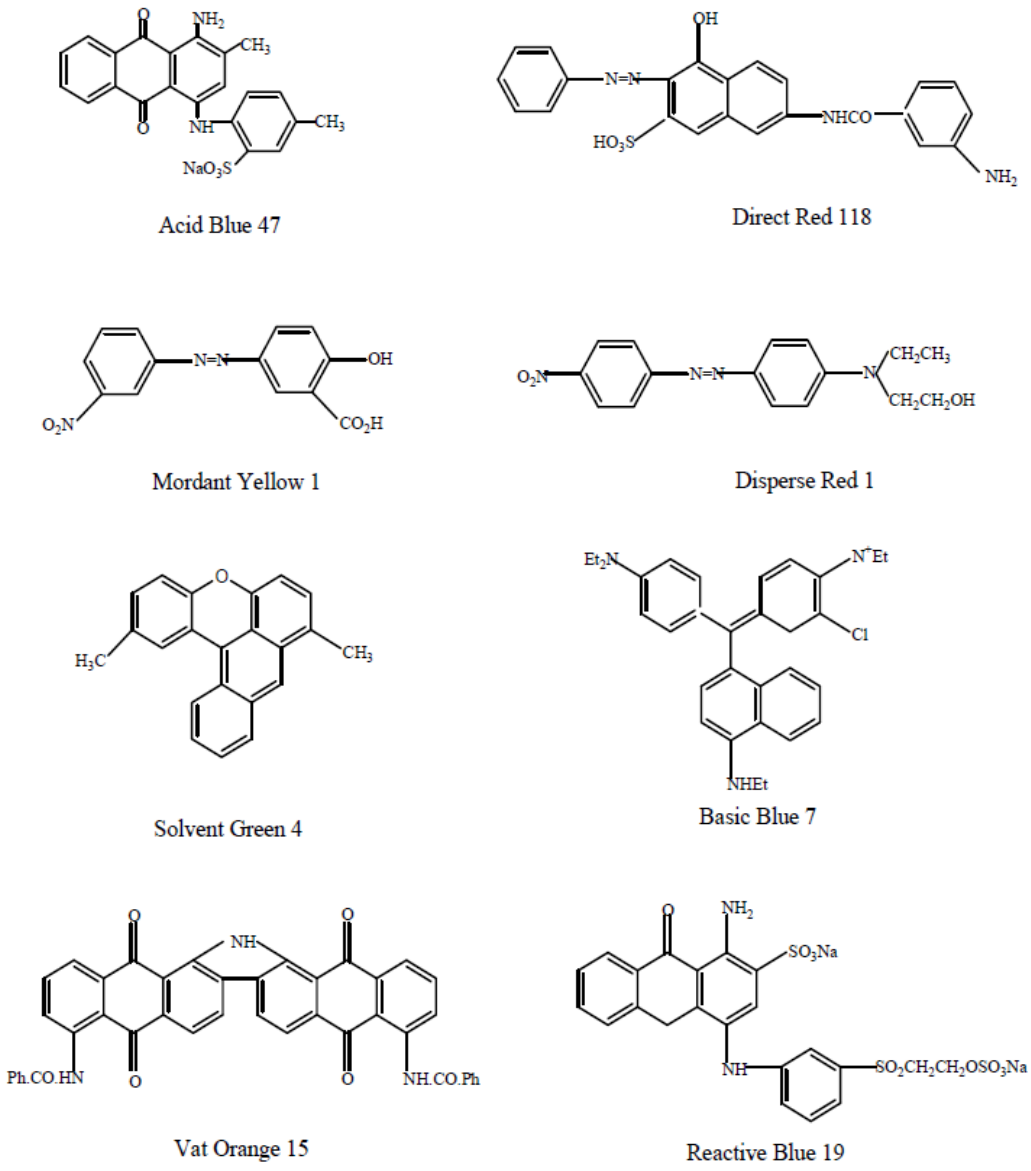

Figure 1.2 – Molecular structure of various organic dyes.

In Table 1.1 the fixation efficiency of some azo-dyes are reported.

Table 1.1- Fixation degree of different dye classes on textile support.

Dye class	Fibre type	Fixation degree (%)	Loss in effluent (%)
Acid	Polyamide	80-95	5-20
Basic	Acrilic	95-100	0-5
Direct	Cellulose	70-95	5-30
Disperse	Polyester	90-100	0-10
Metal complex	Wool	90-98	2-10
Reactive	Cellulose	50-90	10-50
Sulphur	Cellulose	60-90	10-40
Dye-stuff	Cellulose	80-95	5-20

Table 1.1 shows that reactive dyes exhibit a very low degree of fixation on the fiber, typically between 50 and 90%, which results in the release of substantial amounts of the these dyes in the dyeing waters [86, 249] .

1.4 Traditional methods for removal of dyes from wastewater

Due to their synthetic nature and mainly aromatic structure, most of dyes are non-biodegradable, having carcinogenic action or causing allergies, dermatitis, skin irritation or different tissular changes. Moreover, various azo dyes, mainly aromatic compounds, show both acute and chronic toxicity. High potential health risk is caused by adsorption of azo dyes and their breakdown products (toxic amines) [9, 10, 14]. For these reasons, nowdays, government legislation regarding the removal of dyes from industrial effuents, is becoming more and more stringent, especially in developed countries.

This means that effluents must be treated before discharging into watercourses or water bodies in general. The treatment methods can be divided into three categories: chemical, physical and biological.

1.5 Physical methods

One of the most effective and economically advantageous is the adsorption. This process produces a high quality product [15]. Decolorization occurs both by adsorption and ion exchange [16] and it is influenced by many physio-chemical factors, such as dye/adsorbent interaction, sorbent surface area, particle size, temperature, pH, and contact time [17]. There are several types of adsorbent materials.

1.5.1. Activated carbon

Activated carbon is very effective for adsorbing different types of dyes: cationic, mordant, and acid dyes but it is less effective for treating dispersed, direct, vat, pigment and reactive dyes [19, 51]. The effectiveness of the process is strongly influenced by the type of carbon used and the characteristics of the wastewater. Activated carbon is not suitable for all types of liquid effluents, and it is also very expensive.

The activated carbon activity decreases during the time, so it needs to be reactivated. Reactivation, however, results in 10–15% loss of the sorbent.

1.5.2. Peat

Peat is able to adsorb transition metals and polar organic compounds from dye-containing wastewaters. Peat is cheaper than activated carbon, and does not need to be reactivated [20]. Due to its cellular structure, it has a large surface area, and good capacity for adsorption.

1.5.3. Wood chips

Wood chips are able to absorb acid dyes, but adsorption requires long contact time [20]. Moreover, wood chips are not as good as other available sorbents [21-23].

1.5.4. Silica gel

Silica gel is a granular, vitreous, porous form of silicon dioxide made synthetically from sodium silicate. Silica gel contains a nano-porous silica micro-structure, suspended inside a liquid. It is very effective for removing basic dyes, but it is not used commercially [249].

1.5.5. Other materials

Some substrates such as natural clay, corn cobs, rice hulls can be efficiently used for dye removal, especially because of their low cost and high availability. They are cheaper than activated carbon and they have often allowed achieving high removal yields [21-25]. These materials don’t require any regeneration.

1.5.6. Membrane filtration

This method is used to clarify, concentrate and separate dye continuously from effluents [26, 27]. It has better features than some other methods: resistance to temperature, an adverse chemical environment, and microbial attack. After separation, a concentrated residue is obtained; this is difficult to dispose. Some other problems can be represented by the clogging or the replacement of the membrane. Membrane filtration can be successfully employed for water re-cycling within a textile dye plant if the effluent contains low concentration of dyes, but it is not effective to reduce the dissolved solid content, which makes water re-use a difficult task.

1.5.7. Ion exchange

Wastewater passes trough the coloumn that contains the ion exchange resin until the available exchange sites are saturated. Ion exchange is mainly effective for removing anionic and cation dyes from dye-containing effuents. This method is not able for treating other dyes, such as disperse dyes [16, 26]. Ion exchange is very interesting because there is no loss of adsorbent during regeneration, but it remains an expensive method. Organic solvents are expensive, and the ion exchange method is not very effective for disperse dyes.

1.5.8. Irradiation

Organic pollutants, such as dyes contained in wastewaters, can be easly broken down by radiations, but a sufficient quantity of dissolved oxygen is required. Dissolved oxygen is consumed very rapidly; therefore, a constant supply is necessary. For this reason the process is very expensive. This method allowed obtaining high removal yields, at a laboratory scale, in treating some dyes and phenolic molecules [28].

1.5.9. Electro-kinetic coagulation

Electro-kinetic coagulation is an economically feasible method of dye removal. This method requires the addition of ferrous sulphate and ferric chloride. It is very effective for the removal of direct dyes from wastewaters. It is not suitable for treating of acid dyes because of the high cost of the ferrous sulphate and ferric chloride. This process is not commonly used, because the sludge formed as part of the coagulation is very difficult to remove [26].

1.6. Biological treatments

1.6.1. Decolorization by white-rot fungi

White-rot fungi are organisms able to degrade lignin, the structural polymer coming from woody plants [29]. White-rot fungi are also able to degrade dyes using enzymes, such as lignin peroxidases (LiP) or manganese dependent peroxidases (MnP). Other enzymes can be used to degrade dyes: glucose-1-oxidase and glucose-2-oxidase, along with laccase, and a phenoloxidase enzyme [30-32]. Azo dyes, can be successfully degraded by *P. chrysosporium* [33], but other fungi such as, *Hirschioporus larincinus, Inonotus hispidus, Phlebia tremellosa* and *Coriolus versicolor* can also be used [32, 35-37].

1.6.2. Other microbial cultures

The ability of bacteria to metabolise azo dyes were widely investigated. Mixed bacterial cultures from different habitats were able to decolorize the diazolinked chromophore of dye molecules in 15 days [38]. Some researchers [21-23] verified that a mixture of dyes could be decolorized by anaerobic bacteria in 24-30 h, using free growing cells or in the form of biofilms on various support materials. They also verified the use of bacteria for azo dye biodegradation [40]. Anyway, these microbial systems requires a fermentation process and cannot be used for treating large volumes of textile effluents. Azo dyes cannot be immediately metabolised under aerobic conditions, but it was found that *Pseudomonas* strains are able to aerobically degrade some azo dyes [41]. However, the intermediates coming from these degradative steps caused the disruption of metabolic pathways, thus the dyes were not actually mineralised. Under anaerobic conditions, many bacteria reduce azo dyes through the activity of unspecific, soluble, reductases, called azo reductases. These enzymes can cause the production of colorless aromatic amines which are toxic, mutagenic, and carcinogenic to animals.

Further research using mesophilic and thermophilic microbes also showed their ability to degrade and decolorize dyes [21-23, 35-37].

1.6.3. Adsorption by living/dead microbial biomass

Biosorption is the uptake or accumulation of chemicals by microbial mass [17, 42-44]. Dead bacteria, yeasts and fungi, can be used for treating dye-containing effluents. Different results can be obtained by varying the type of dye and biomass. Some dyes have a particular

affinity for binding with microbial species. For example it was observed that biomass derived from the thermotolerant ethanol-producing yeast strains, *K. marxianus IMB3*, showed a relatively high biosorption capacity for dye removal [45]. The biomass can be used especially if the dye-containing effluent is very toxic. Biomass adsorption can be successfully used when decolorization by microbial colture cannot be used [46]. It was demonstrated that bacterial cells are able to adsorb reactive dyes [42, 43]. Actinomyces were employed to adsorb anthroquinone, phalocyanine and azo dyes from wastewaters [47]. Biosorption is very quick: it requires few minutes in algae and few hours in bacteria [42, 43].

1.6.4. Anaerobic textile-dye bioremediation systems

Azo dyes represent almost 60-70% of all textile dyestuffs. These dyes are soluble in solution, and cannot be removed by conventional biological treatments. Reactive dyes, especially, are the most problematic compounds in textile effluents [48-50]. Anaerobic bioremediation is useful to decolorize azo and other water-soluble dyes. The process involves an oxidation-reduction reaction with hydrogen. (In aerobic systems free molecular oxygen is involved). The anaerobic degradation of a textile effluent only involves decolorization of the solution, but the dye molecule is not mineralized.

1.7 Chemical methods

1.7.1 Oxidative process

Oxidative process is the most common chemical method of decolorization. The main oxidising agent is usually hydrogen peroxide (H_2O_2). It needs to be preliminarily activated by ultra-violet light or other sources. Many methods of chemical decolorization can be classified according to the activation mode of H_2O_2 [51]. The chemical oxidation of a dye involves the opening of the aromatic ring of the dye molecule [52].

1.7.2 H_2O_2 + Fe(II) salts

Fenton's reagent can be successfully used for treating textile wastewaters, which are resistant to biological treatment or are toxic to biomass [51]. One of the main drawback of this method is the sludge generation due to flocculation of the reagent and the dye

molecules. The sludge contains the concentrated impurities, so it requires to be disposed of. It can be generally incinerated to produce power, even though this step is not environmentally friendly.

1.7.3 Ozonation

Ozone is a powerful oxidising agent. It has an higher oxidation potential (2.07 V) than chlorine (1.36 V), and H_2O_2 (1.78 V). Ozonation can be used to degrade textile dyes, chlorinated hydrocarbons, phenols, pesticides and aromatic hydrocarbons [53, 27]. The ozone dosage that can be utilised depends on the total color and total organic carbon (TOC) of the dye-containing effluents. Dyes have to be removed with no residue or sludge formation [54] and no toxic metabolites [55]. After ozonation an effuent with no color and low TOC (suitable for discharge into water bodies) is obtained [27]. This method gives good results especially when double-bonded dye molecules [51] are treated. Ozone can be used in its gaseus state so it does not increase the volume of wastewater and sludge.

A drawback of ozonation is its short half-life (about 20 minutes). This time decreases if dyes and salts are present in the treated solution, and it also depends on pH and temperature conditions. For example in alkaline conditions, ozone decomposition goes faster, so it is very important to regulate the effluent pH [51]. Results can be improved using irradiation [57] or with a membrane filtration technique [56]. A weakness of the process is its high cost, actually continuous ozonation is required due to its short half-life [27].

1.7.4 Photochemical

This method is able to degrade the dye molecules using the combined action of UV radiations and hydrogen peroxide [58, 59]. Dye molecules can be completely mineralized and form CO_2 and H_2O. Several literature studies carried out the degradation of commercial dyes by UV/H_2O_2 in aqueous solutions. Enhanced efficiency of UV/H_2O_2 oxidation at alkaline pH region was attributed to hydroxyl radical formation [60, 61]. It was also reported that the decolorization of C. I. Acid Black 1 decreased with increasing solution pH due to decomposition of H_2O_2 into water and oxygen rather than hydroxyl radical formation [62-64]. A suitable H_2O_2 dosage showed enhanced performance of the process to degrade crystal violet [65]. This process produces a high concentration of hydroxyl radicals that quickly degrade dye molecules. The process can be influenced by the intensity of the UV

radiation, pH, type of dye and dye-bath composition [32]. A drawback is the generation of by-products such as halides, metals, inorganic acids, organic aldehydes and organic acids [58]. This method does not generate sludge and it is effective for the odours removal.

1.7.5 Sodium hypochloride

Sodium hypochlorite (NaOCl) is a clear, slightly yellowish solution with a characteristic odour. It is used on a large scale for surface purification, bleaching, odour removal and water disinfection.

When sodium hypochlorite dissolves in water, two products are formed. They play an important role for oxidation and disinfection. These substances are hypochlorous acid (HOCl) and hypochlorite ion (OCl^-). Hypochlorous acid is divided into hydrochloric acid (HCl) and oxygen (O). The oxygen atom is a very strong oxidator. The pH of the water determines how much hypochlorous acid is formed.

Sodium hypochlorite is used on a large scale. For example in agriculture, chemical industries, paint- and lime industries, food industries, glass industries, paper industries, pharmaceutical industries, synthetics industries and waste disposal industries. In the textile industry sodium hypochlorite is used to bleach textiles. It can also be added to industrial wastewater to reduce odours. Hypochlorite neutralizes sulphur hydrogen gas (SH) and ammonia (NH_3) and detoxifies cyanide baths in metal industries. Hypochlorite can be used to prevent algae and shellfish growth in cooling towers. In water treatment, hypochlorite is used to disinfect water. It also is effective against bacteria, viruses and fungi.

The use of chlorides for dye removal is becoming less frequent due to the negative effects it has when released into waterways [51] and the release of aromatic amines which are carcinogenic, or otherwise toxic molecules [35-37].

1.8 New methods for removal of dyes from wastewater: Advanced Oxidation Processes

Traditional methods for treating textile wastewaters are not very effective: biological methods require the use of micro-organisms whose activity is strongly inhibited by the levels of effluent toxicity. Physical methods only transfer dyes from one phase to another, but the problem still remains unsolved. The drawbacks of the chemical processes are the formation of sludge, its disposal and the space needed.

Advanced oxidation processes (AOPs) represent a new promising technology for the treatment of wastewaters containing recalcitrant organic compounds. All AOPs are designed to produce hydroxyl radicals. Hydroxyl radicals, in fact, are very effective to destroy organic compounds. AOPs are able to completely mineralise pollutants by converting them into water and carbon dioxide.

There are different types of AOPs, based on chemical, photochemical, sonochemical, and electrochemical reactions.

1.8.1 The hydroxyl radical

The hydroxyl radical is a powerful oxidant ($HO\cdot + H+ + e- \rightarrow H_2O$). Its oxidation standard potential is $E°$ ($\cdot OH/H_2O$) = 2.8 V/SHE [251]. This radical is able to quickly degrade organic and organometallic pollutants until their complete mineralization into CO_2, H_2O and inorganic ions. The hydroxil radical reacts rapidly with organics (R) mainly by the abstraction of a hydrogen atom (aliphatics) or the addition on an unsaturated bond (aromatics) to initiate a radical oxidation chain:

$$RH + \cdot OH \rightarrow H_2O + \cdot R \quad (1.1)$$

$$\cdot R + O_2 \rightarrow ROO\cdot \quad (1.2)$$

$$ROO\cdot + RH \rightarrow ROOH + \cdot R \quad (1.3)$$

$$ArH + \cdot OH \rightarrow ArH(OH)\cdot \quad (1.4)$$

$$ArH(OH)\cdot + \cdot O_2 \rightarrow [ArH(OH)OO]\cdot \quad (1.5)$$

$$[ArH(OH)OO]\cdot \rightarrow ArH(OH) + HO_2\cdot \quad (1.6)$$

1.8.2 Electrochemical destruction

The electrochemical oxidation is an efficient process for recovery and re-use of textile wastewater [66]. The efficiency of the process was comprovated by many studies: for a dyeing wastewater, a complete removal of the color was found within only 6 minutes of

electrolysis [67]. In conventional electro-oxidation processes, contaminants can be removed by *direct oxidation*, in which the pollutant is oxidized by electron transfer directly to the anode material, or *indirect oxidation*, in which the electron transfer is mediated by an oxidant species [68, 69] such as the hydroxyl radical (·OH) from water discharge. Contaminants may also be oxidized by other oxidants, such as active chlorine (Cl_2, HClO, and ClO^-), $S_2O_8^{2-}$, and $P_2O_8^{4-}$, when chloride, sulphate, and phosphate containing solutions are used, respectively [69]. The process is also influenced by the anode material and electrolysis conditions [71-74].

The electrochemical processes are able to remove the pollutants without adding chemicals. The main drawback of electrochemical processes is the use of electric energy that increases the costs.

The main advantages of this treatment are considered the requirement of simple equipment and operation, low temperature in comparison with other non-electrochemical treatments, no requirement of any additional chemicals, easy control but crucial for pH. Moreover, the electrochemical reactors (with electrolytic cells) are compact, and environmental friendly because all the emissions are minimized and undesired by-products are not generated.

1.8.3 Photocatalysis

In chemistry, photocatalysis is the acceleration of a photoreaction in the presence of a catalyst. Photocatalysis is a potential new method to eliminate recalcitrant organic compounds from wastewaters. It is based on physically and chemically induced processes. Photocatalysis can be homogeneous [60, 61, 64, 65] or heterogeneous [180].

1.8.4 Homogeneous photocatalysis

In homogeneous photocatalysis, the reactants and the photocatalysts exist in the same phase. The most commonly used homogeneous photocatalyst include hydrogen peroxide as it is reported in the paragraph (1.7.4).

1.8.5 Heterogeneous photocatalysis

Heterogeneous photocatalysis has the catalyst in a different phase from the reactants. Physically, heterogeneous photocatalysis involves a 4 - step process:

• transport of the pollutant from bulk of the solution onto the surface of the photocatalyst;
• adsorption;
• photoreaction;
• desorption of final products from the surface to the bulk again.

The photoreaction mechanism can be summarized as follows:

- Photoexcitation: when a photocatalyst absorbs a photon of light having energy greater than its band-gap energy, an electron is promoted from the valence band of the irradiated particle to its conduction band, producing a positively charged hole in the valence band and an electron in the conduction band (Eq. (1.7)). These charges migrate to the particle surface and react with adsorbed species (Eqs. (1.14) and (1.15)). Both oxidation and reduction processes commonly take place on the surface of the photoexcited semiconductor photocatalyst.
- Ionization of water: water molecules can react with photogenerated holes to produce hydroxyl radicals (Figure 1.3). Hydroxyl radicals attack the adsorbed organic molecules or those that are very close to the catalyst surface non-selectively causing them to mineralize (Eq. (1.13)).
- Oxygen ionosorption: while the photogenerated hole reacts with surface bound water or OH^- to produce the hydroxyl radical, the conduction band electron reduces absorbed oxygen to form superoxide radical anion ($O_2^{-\cdot}$) (Eq. (1.10)). This superoxide ion can not only take part in the further oxidation process but also prevents the electron-hole recombination (Eq. (1.8)).
- Protonation of superoxide: the generated superoxide can be protonated forming hydroperoxyl radical ($HO_2^{\cdot}$) (Eq. (1.11)) and then H_2O_2 which further dissociates to highly reactive hydroxyl radicals (·OH) (Eq.(1.12)).

$$\text{photocatalyst} + h\nu \longrightarrow e^-_{CB} + h^+_{VB} \quad (1.7)$$

$$e^-_{CB} + h^+_{VB} \longrightarrow \text{energy (heat)} \quad (1.8)$$

$$h^+_{VB} + H_2O \longrightarrow \cdot OH + H^+ \quad (1.9)$$

$$e^-_{CB} + O_2 \longrightarrow O_2^{-\cdot} \quad (1.10)$$

$$2\ O_2^{-\cdot} + 2\ H_2O \longrightarrow H_2O_2 + 2\ OH^- + O_2 \quad (1.11)$$

$H_2O_2 + e^-_{CB} \longrightarrow OH^- + \cdot OH$ (1.12)

$Dye + \cdot OH \longrightarrow CO_2 + H_2O(\text{dye intermediates})$ (1.13)

$Dye + h^+_{VB} \longrightarrow \text{oxidation products}$ (1.14)

$Dye + e^-_{CB} \longrightarrow \text{reduction products}$ (1.15)

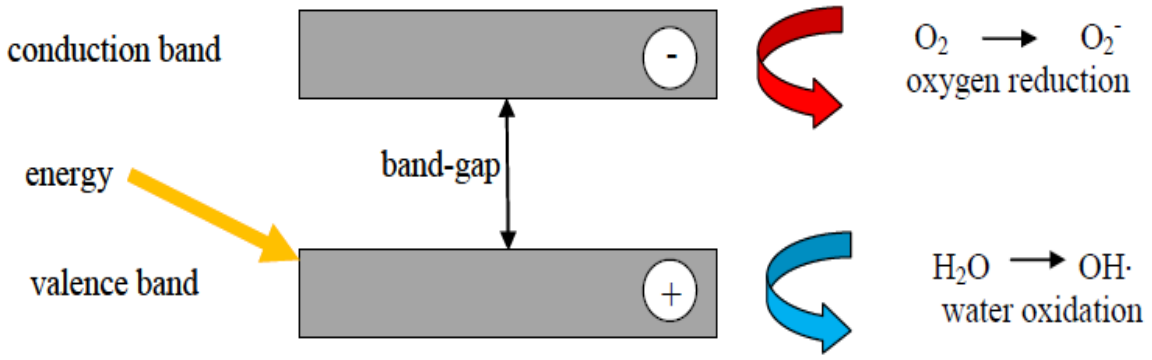

Figure 1.3 - Conduction and valence bands and electron–hole pair generation in a semiconductor.

1.9 Photocatalysts for heterogeneous photocatalysis

The oxidation reaction will occur if the valence band (VB) of the catalyst has a higher oxidation potential than the species that have to be treated. The redox potential of the valence band and the conductance band for several semiconductors ranges between +4.0 and -1.5 Volts versus Normal Hydrogen Electrode (NHE). Therefore, by choosing the suitable catalyst, it is possible to treat different species trough the photocatalytic processes. Metal oxides are semiconductor materials suitable for photocatalysis.

The wavelength of the light, required to activate a catalyst has to be equal or lower than that calculated by the Planck's equation (Eq. 1.16):

$$\lambda = hc / E_{bg} \quad (1.16)$$

where E_{bg} is the semiconductor band-gap energy, h is the Planck's constant and c is the speed of light.

The photocatalysts can be used under dispersed form (powder, aqueous suspension) or in thin film form (fixed catalytic layer) [226].

The dispersed catalysts present several advantages: they are easy to use, they possess an important specific surface, and they can be aerated to prevent the recombining of electron-hole pairs and increase the catalyst efficiency. However, a drawback of the dispersed form is the progressive formation of dark catalytic sludge, that diminishes the efficiency of light irradiation and reduces the photoreactor performances. In contrast, for the catalysts in form of film, there is no need to separate the catalytic particles at the end of the process, but, on the other hand, the catalytic layer has to be very stable and active.

The amount and type of catalyst to be used depend on the irradiation source, the nature and concentration of pollutants to be treated, and the photoreactor. The pH value of the medium have to be optimized according to the type of pollutant and to the type of catalyst.

1.9.1 Titanium dioxide

Titanium dioxide (TiO_2) is a white powder semiconductor having a wide band gap of 3.0–3.2 eV. TiO_2 is one of the most suitable semiconductors for photocatalysis and it can be applied into various photocatalytic reactions [75-85]. This is due to its high reactivity, aivalability, affordability, non-toxicity and photochemical stability. It can be excited by UV light with a wavelength below ca. 430 nm.

In general, titanium exists in three different polymorphic forms (Figure 1.4) including anatase (tetragonal), rutile (tetragonal) and brookite (orthorhombic). Rutile is the most stable phase, but, anatase, is the most commonly polymorphic form used in photocatalysis.

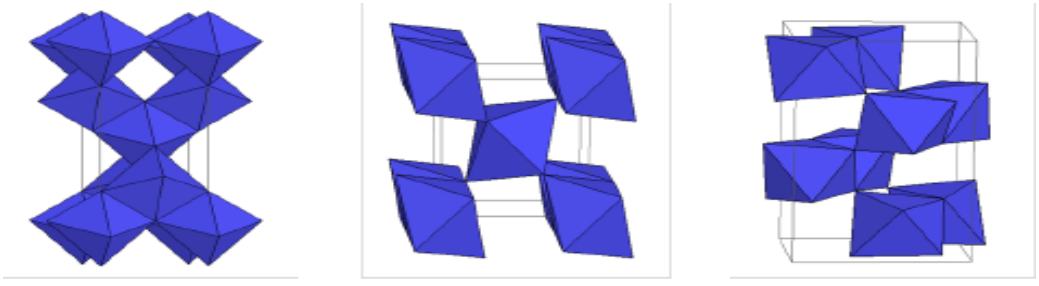

Figure 1.4 - Polymorphic forms of the TiO_2[226].

Anatase phase is often found having particle size of 10 nm or less with a band gap of 3.2 eV corresponding to a UV wavelength of 385 nm. Rutile phase generally exists having particle

size in the order of 50 nm. Moreover, rutile has a smaller band gap of 3.0 eV with excitation wavelengths extending to visible 410 nm range.

TiO_2 nanoparticles are widely available commercially or can be easily prepared using sol-gel method. Heating the anatase phase results in a gradual phase transformation of anatase to rutile, thus, on the base of the method of preparation, mix phase anatase-rutile can be easily prepared or purchased [226].

If the source of irradiation is the UV light, the TiO_2 can be used without any modification, but, to use visible light, TiO_2 needs to be modified by non-metal and/or metal doping, dye sensitization, and coupling semiconductors.

1.9.2 Non-metal doping: N-doped TiO_2

A drawback of TiO_2 for photocatalysis is that its band-gap is rather large, 3.0-3.2 eV, and thus only a small fraction of the solar spectrum (λ < 380 nm, corresponding to the UV region) can be absorbed. To reduce the energy for photoexcitation, the researches focused their attention on doping TiO_2 with both transition metal (such as Fe, Cr, Co, Mo, and V) and non-metal impurities (such as B, C, N, S, and F) [88-100]. Doping with transition metals showed positive and negative effects. Several authors reported that although metal ions doping decreases the photothreshold energy of TiO_2, the metal ions may also serve as recombination centers for electrons and holes, thus reducing the overall activity of the photocatalyst.

Recently, the interest in TiO_2 doping with non-metal ions, especially with nitrogen, grew considerably. N-doping can be obtained by various methods such as sputtering [101], treating of TiO_2 powders in ammonia atmosphere [102], or hydrolysis with urea in the presence of organic or inorganic titanium-based compounds [103, 104].

Besides the preparation procedures, many other aspects must be elucidated about the properties and behaviour of N-doped TiO_2. First of all the chemical nature, the location in the solid, and the involvement in photoactivity of the nitrogen species. Nitrogen can be found in different forms in chemical species, such as NO_x [105-110], substitutional N [111-114], or NH_x [115]. It is important to know if the species are interstitial or substitutional, because their behaviour is very different and might affect the material properties. It is also important to know if the species tend to segregate at the surface of the material or are incorporated in sub-surface or bulk sites, because this can influence the surface reactivity and photocatalytic properties.

Another aspect is the electronic structure of the doped material and the change of the optical gap [116, 117]. According to some authors, the band gap of the solid is reduced due to a rigid valence band shift after doping [118, 119], other authors claim that the absorption of visible light by N-doped TiO_2 is due to the excitation of electrons caused by localized impurity states in the band-gap [120, 121]. Also, the N-doping induced modifications of the electronic structure may be different for the anatase and rutile polymorphs of TiO_2.

Another object of investigation is the interaction between N-impurities and oxygen vacancies. Some authors identified the role played by impurities (dopants, oxygen vacancies, hydroxyl groups) in the photo-activity of N-doped TiO_2 samples. In their opinion, the photocatalytic properties of TiO_2, both in UV and vis-regions, can be largely improved by tailoring the number and type of defects present in the photocatalyst.

The last and probably most important question for photocatalysis is the effect of N-doping on the photocatalytic activity of TiO_2. A large part of the existing literature on N-doped TiO_2 materials agrees that the addition of nitrogen results in an improvement in visible light photocatalytic activity, but this explanation is still controversial [116]. For example, in a recent study on N-doped TiO_2 films obtained by the addition of ammonia during chemical vapour deposition growth of TiO_2 [122], no evidence of photocatalytic activity in the visible was found.

1.9.3 Photosensitization

To extend the photocatalytic activity to the visible region, photocatalysts can be photosensitized by several colored organic and inorganic compounds. The most common method used for TiO_2 photosensitization involves surface modifications.

This route is based on the formation of ionic or covalent bonds between the surface of a semiconductor and chromophores (sensitization mechanism). Several organic dyes, such as erythrosine B, porphyrines [149; 150], phtalocyanines [151; 152]) and metal complexes (with Fe(II) [42], Pt(IV) [153]), can be adsorbed on the TiO_2 surface. These species are able to absorb visible light and therefore promote an electron in the conduction band of the semiconductor. This mechanism is called *photoinduced electron transfer* and can be summarised as follow (Eq. (1.17); (1.18)):

$$TiO_2\text{-----}S + h\nu \rightarrow TiO_2\text{-----}S^* \quad (1.17)$$

$$TiO_2\text{-----}S^* \rightarrow TiO_2(e^-_{CB})\text{-----}S^+ \quad (1.18)$$

If the recombination step is eliminated, the oxidative degradation of the dye can start. Many colored compounds may act as photosensitizers. Recent studies suggest that photosensitized degradation on photocatalyst surfaces can be used for treating colored pollutants such as textile dyes.

1.9.4 Metal doping: Fe-TiO_2

Metal doping is another way to improve the TiO_2 photoefficiency. It consists in the introduction of impurities able to attract one type of the photogenerated charges, e^- or h^+, reducing their recombination probability. Doping of the nanoparticles surface with iron, can be used to achieve this goal.

Fe^{3+} ions can act as shallow trapping sites for both photoinduced CB (conduction-band) electrons and VB (valence band) holes. As a result, the photoinduced charges can be better separated and conserved for a longer time. Consequently, the redox reactions of adsorbed species take place more efficiently. Iron is also considered an optimal doping agent because its radius (0.64 Å) is similar to that of Ti^{4+} (0.68 Å). Therefore, Fe ions can easily be incorporated with the crystal lattice of TiO_2. The band-gap of iron is 2.6 eV, therefore, it reduces the width of the energy gap of TiO_2 and increases the efficiency of absorbing visible light. The material properties of the Fe-doped TiO_2 are strongly dependent on the crystal structure, the size of the nanoparticles, and morphology, which are correlated with the TiO_2 method of synthesis. There are several methods of synthesising Fe doped TiO_2: sol–gel, hydrothermal, wet chemical synthesis, thermal hydrolysis and plasma oxidative pyrolysis. There are also some combined methods, such as combining the sol–gel method with hydrothermal treatment.

Another reason to synthesise Fe-doped TiO_2 is that TiO_2 is not effective for degradation of polymers. In fact, TiO_2 is polar, while organic polymers are non-polar materials. For this reason it is difficult to disperse TiO_2 nanoparticles in the polymers. The nanoparticles of TiO_2 can be well dispersed in organic medium by surface modification with surfactants, [123-125] coupling agents, [126, 127] or polymers, [128, 129], but, these modifications, could also reduce the catalytic activity of nano-catalyst. Although many methods have been proposed to prepare active TiO_2, such as doping with metal ions [130-134] or non-metal elements, [135-137] the surface property of nanoparticles is still polar. It is essential, for nano-TiO_2, to display non-polar surface property as well as good catalytic activity. It was

found that nano-TiO_2 displays better photocatalytic activity for degradation of methyl orange after its surface was modified by complex of $Fe(acac)_3$ [138].
These modifications not only increase the catalytic activity (the ferric complex acts as a photo-sensitizer), but also the surface oleophylicity (the ferric complex also acts as a surfactant). Hence, the modified TiO_2 (Fe-TiO_2) should be a suitable photocatalyst for degradation of both polar and non-polar substances.

1.10 Natural light sources and artificial light sources for photocatalysis

Lamps are artificial sources of visible, UV, or both UV/visible light. Lamps, can generally be divided in:

- Incandescence lamps;
- Electric discharge lamps;
- Fluorescent lamps;
- LED lamps.

Radiations emitted by a natural source of light, such as the solar one, have a varying intensity according to the country, the season and the weather conditions, but have the disadvantage of being unidirectional.

1.10.1 Incandescence lamps

Incandescent lamps are made up of a base and a glass bulb containing a filament. An electric current flows through the filament making it incandescent, therefore it can emit radiant energy including the visible wavelengths. The filament usually contains tungsten, a metal having a very high melting point (3770 K), that can reach very high temperatures (2700-3000 K), ensuring high energy emissions with wavelengths in the visible field. The glass bulb also contains an inert gas, generally Ar or Kr, to limit the sublimation of the tungsten. The color temperature varies from 2700 K to 3000 K. The emissions are mostly in the IR and almost absent in the UV.
Halogen lamps represented a development of the incandescence lamps. They contain a gaseous mixture of halogen gas (generally iodine, bromine or chlorine) to avoid the evaporation of tungsten.

1.10.2 Gas discharge lamps

In discharge lamps, the production of light is caused by the emission of light radiations by a previously excited gas: when an electron returns to its stable orbit, a quantum of light energy is emitted. When an electron is excitated, it is promoted from its stable orbit to a more external one. The electron can be excitated by external energy sources, such as high-energy photons or other electrons accelerated by an electric field. Because of the properties of electronic orbits, the electronic orbits are defined: to a fixed energy correspond a well defined wavelength and a specific color. Gas discharge lamps are made up of a chamber, made of glass or quartz, which contains a gaseous substance at a suitable pressure. Generally, metallic vapours such as sodium, (with emission into the visible spectrum), mercury (with emission into the UV spectrum), xenon and other rare gases, (with emission in the UV spectrum) are used. On the base of the discharge tube pressure, these types of lamps can be divided into high and low pressure lamps. Low pressure mercury usually has an emission spectrum consisting of a pair of lines in the ultraviolet (at 254 and 185 nm.). High pressure mercury has an emission spectrum consisting of a pair of lines in the visible field (blue, green). If pressure is increased, the emission spectrum will become continuos, but the wavelengths corresponding to the red color are absent. Low pressure lamps are only used for scientific applications requiring UV radiations. There are also discharge lamps containing xenon as gaseous substance. Xenon allows obtaining an emission spectrum that reproduces the visible fraction of solar radiation. Xenon also has a strong UV emission, with several bands in the spectral range between 200 and 300 nm.

1.10.3 Fluorescent lamps

Fluorescent lamps use some substances (such as phosphors) able to absorb small wavelength electromagnetic radiations and to re-issue the relative energy in the form of longer wavelength radiations. These lamps exploit the emission of ultraviolet radiation from some gases and vapours (mainly mercury) used in discharge tubes. Here the fluorescence phenomenon is exploited, properties that have some substances (phosphors) to absorb small wavelength electromagnetic radiations and to re-issue the relative energy in the form of longer wavelength radiation. The inner surface of the glass chamber is treated with oxy-sulphides, aluminates, tungstates, phosphates and Ca, Mg, Zn silicate and heavy metals such as copper or antimony. Tubular fluorescent lamps usually contain argon, and a small amount of mercury, to facilitate the discharge start. This type of lamp is not suitable as UV sources.

1.10.4 LED lamps

A LED consists of a “p and n” type semiconductor junction. It is a p–n junction diode that emits light when activated. The p-n junctions in LEDs usually are made up of a mixture of Group III and Group V elements such as gallium arsenide, gallium arsenide phosphide, and gallium phosphide. In this p-n junction, the p-type region is dominated by positive charges and the n-type region is dominated by negative charges. When a suitable voltage is applied across the LED’s electrical contacts, current flows and electrons move across the junction from the n-type semiconductor region into the p-type semiconductor region. Electrons then combine with positive charges. This effect is called electroluminescence, and the color of the light is determined by the energy band gap of the semiconductor.

When a combination occurs, a quantum of electromagnetic energy is released in the form of light. The frequency and, therefore, the apparent color of the emitted photons is characteristic of the semiconductor material. So, different color LEDs can be obtained by changing the semiconductor composition of the chip used.

Recently, LEDs were found to be an alternative for traditional light sources, and they were used in various application including UV curing, disinfection, sensors and photocatalytic applications [139-148]. LEDs generate cold light because of their low operating temperature. In fact, 5 mm LEDs are usually only 10–25 °C warmer than the ambient temperature during operation, whereas incandescent bulbs can be several hundred degrees warmer under similar conditions.

The energy of the photons that leave the diode depends on the material used to make the LEDs. At each wavelength of light corresponds a certain amount of energy. Shorter wavelengths (especially those close to UV) contain more energy. LEDs can produce light of different wavelengths including infrared, UV, and visible light.

1.11 Kinetics

It is very important to determine the reaction rate and the influence of different parameters on it. These parameters are: illumination intensity, catalyst type, oxygen concentration, pH, presence of inorganic ions and the concentration of organic reactants. Several experiments showed that the rate of photocatalytic oxidation of various organic pollutants over illuminated nanocatalysts fits the Langmuir–Hinshelwood (L–H) kinetics model equation [154]. The reaction rate is given by Equation 1.19:

$$r = -dC/dt = k_1 k_2 C/(1+k_2 C) \quad (1.19)$$

where r is the oxidation rate of the dye (mg/L min), C is the bulk reactant concentration (mg/L), t the illumination time, k_1 the reaction rate constant (mg/L min), and k_2 is the equilibrium adsorption constant (L/mg). For low solute concentration, the equation can be simplified to a pseudo first-order equation (Eqs. (1.20) and (1.21)):

$$r = -dC/dt = k_1 k_2 C = \quad (1.20)$$

Or

$$r = k_{app} C \quad (1.21)$$

After a few steps the equation becomes:

$$\Delta C/C = (1 - e^{-t/\tau}) \quad (1.22)$$

where τ is the inverse of the apparent reaction rate constant: $\tau = 1/k_{app}$. τ represents the expected value of time that a dye molecule remains in the solution before being removed. k_{app}, the reaction rate constant, is not a traditional rate-constant. It is a function of external system parameters such as light intensity, pH, catalyst loading, geometry of photoreactor and initial concentration of the pollutant.

Chapter 2

Literary review

2.1 Introduction

Wastewaters, coming from textile industries, contain considerable amounts of dyes that can cause serious damages to the ecosystem [181, 182]. Due their high molecular stability, these dyes can hardly be removed from the effluents by conventional treatment techniques [183]. Heterogeneous photocatalysis is one of the new methods able to degrade these organic pollutants [182, 184, 185].

2.2 Recent Advances in Synthetic Dyes Photocatalytic Decolorization

Recently, studies about photocatalytic treatment of dyes by using traditional light sources were carried out. Zielinska et al. (2003) [155] investigated the photocatalytic activity of two photocatalysts, TiO_2 Tytanpol-A11 and TiO_2 Degussa P-25, from the degradation of Reactive Red 198 (RR198), Acid Black 1 (AB1) and Acid Blue 7 (AB7), under UV-visible light. Dye treatment was carried out in a quartz photoreactor equipped with an external mercury lamp. All experiments were carried out using a constant amount of photocatalyst (0.4 g/L), dye concentration (30 mg/L) and at constant pH (pH = 2). It was found that TiO_2 Degussa P-25 exhibited a better photocatalytic activity than the other catalysts [160].

In 2005 Gonçalves et al. [156] compared the relative efficacy of two photocatalysts: Degussa P-25 and Riedelde-Häen TiO_2 using the Reactive Orange 4 (38 mg/L) as model pollutant. UV-irradiation experiments were carried out using an immersion reactor fitted with a medium pressure 400 W Hg vapour lamp. The experiments were also carried out under sunlight exposure. The influence of various parameters such as pH (5.6 - 10 - 13) and catalyst concentration (0.36 – 1 g/L) was evaluated. It was observed that, when sunlight was used as light source, Degussa P-25 catalyst was more efficient than the Riedel-de-Häen catalyst.

In 2005 Thi Dung et al. [161] used several commercial titania powders (Degussa P-25 and Ishihara Sangyo ST-01) and TiO_2 supported on diatomite to study the degradation of Reactive Red 3BA (RED-3BA) under UV-visible light and under different pH values (4 – 7 – 9). The experiments were carried out in a photocatalytic reactor; a 150 W halogen lamp was positioned inside a cylindrical Pyrex vessel surrounded by a circulating water jacket to cool the lamp. The halogen lamp had a spectral emission ranging from 360 nm to 830 nm. It was observed that the rate constant for Degussa P-25 was higher than that achieved by using Ishihara Sangyo ST-01 (k_{obs} = 3.3 × 10^{-2} min^{-1} for Degussa P-25 and 4 × 10^{-4} min^{-1} for Ishihara Sangyo ST-01). It was also found that the photocatalytic activity of supported TiO_2 was twice smaller than TiO_2 Degussa P-25 ($k_{P\text{-}25}$ = 3.3×10^{-2} min^{-1}; $k_{P25/diatomite}$ = 1.6×10^{-2} min^{-1}). Therefore, Degussa P-25 was the best catalyst for dyes degradation, but TiO_2/diatomite could be separated more easily from the treated solution. Moreover, pH = 4 was identified as the optimal pH value able to favour both adsorption and the consequent degradation rate.

In 2007 Chatterjee et al. [157] studied the decolorization of different dyes such as Reactive Red 11, Reactive Red 2, Reactive Orange 84, Reactive Orange 16 and Reactive Black 5. The experiments were carried out in a flat-surfaced glass reactor illuminated with a 150 W xenon lamp. A filter solution containing sodium nitrite, copper sulphate and ammonium hydroxide, was used as a UV-filter to eliminate light < 420 nm. TiO_2 nanoparticles were used as catalysts. The influence of the initial dye concentration (10 – 100 mg/L) on the process was evaluated. The results demonstrated the capability of visible light/TiO_2 photocatalytic system to decolorize the triazine and vinylsulfone reactive dyes. Furthermore, the efficacy of the photodegradation depends on the susceptibility of the dyes as well as the intermediates formed.

In the same year, Rupa et al. [158] used Reactive Yellow-17 (RY-17) as model pollutant to test the photocatalytic efficiency of Ag-TiO_2 nanoparticles (synthesized by sol–gel technique) under UV and visible light. A 200 W halogen lamp and a 125W mercury lamp were used as visible and UV sources, respectively. 200 mL of the dye solution with 1.5 g/L of the photocatalyst were taken in a photoreactor made up of pyrex glass. The influence of different parameters, (such as dye concentration, amount of hydrogen peroxide and pH) on the photocatalytic process, was evaluated. The photocatalytic efficiency of nano-TiO_2 (synthesized by sol–gel technique), nano-commercial TiO_2 (Degussa P-25) and Ag-TiO_2 was evaluated. An increase of the rate dyes degradation was found by using Ag-TiO_2 .

In 2008 Chung et Chen [159] studied the photocatalytic degradation of Reactive Violet 5 dye using TiO_2 as catalyst. The experiments were carried out in a quartz beaker. 0.08 g/L of TiO_2 were added to 300 ml of the dye solution (that had a concentration of 10 mg/L). Reactor was equipped with four Xenon 254 nm lamps. The effect of different variables (such as initial dye concentration (10 – 50 mg/L), pH (2 – 12), photo catalyst amount (0 – 100 mg/L), UV light intensity) on the photocatalysis efficiency, was evaluated. Due to the short degradation times (20 minutes for 90% decolorization), it was concluded that TiO_2 photocatalysis could be used as an easy and efficient method to remove azo dyes from wastewaters.

In 2011 Souza et al. [160] used Blue 5 G dye as a model pollutant to test some cerium-titania-alumina-based nanocatalysts, modified with Ag and Fe, for photocatalytic application. They observed that decolorization with the mixed oxide photocatalyst CeO_2-TiO_2-Al_2O_3 gave a result similar to that of TiO_2 (96 % and 100 % respectively). They found that the addition of Ag and Fe to the mixed oxide increased the decolorization and reaction rates of Reactive blue 5G dyes. The experiments were carried out in cylindrical Pyrex cell having a volume of 500 mL. The solution containing 70 ppm of Blue 5G dye was treated using 2 g/L of catalyst. An oxygen stream was bubbled into the suspension. A 125 W medium pressure mercury lamp was used for irradiation. To avoid the heating of the solution, the vessel was equipped with a cooling jacket.

In the same year, Kavitha and Palanisamy [162] studied the sonophotocatalytic degradation of Reactive Red (RR) 120 dye under visible light using dye sensitized TiO_2 activated by ultrasound. An immersion well photochemical reactor made of Pyrex glass, equipped with a water-circulating jacket and an opening for supply of oxygen, was used. Irradiations were carried out using a 50 W halogen lamp. A comparative study of photocatalysis and sonophotocatalysis using TiO_2, Hombikat UV-100 and ZnO was carried. ZnO was identified as the best catalyst. The order of activity of the tested photocatalysts was ZnO > TiO_2 P-25 > UV-100.

Saggioro et al. (2011) [163] studied the photocatalytic degradation of two commercial azo dyes: Reactive Black 5 and Reactive Red 239. TiO_2 Degussa P-25 was used as catalyst. Photodegradation was carried out in a 100 mL aqueous solution irradiated with a 125 W mercury vapour lamp. The effects of the catalyst concentration (0.001 – 1 g/L), UV-light irradiation time (0 – 120 min), pH of the solution (2 – 10), initial concentration of the dyes (30 – 150 mg/L) and addition of different concentrations of hydrogen peroxide (0 – $6 \cdot 10^{-2}$

mol/L) were investigated. Results showed that the optimal amount of catalyst was 0.1 g/L. It was observed that the increase in the initial dye concentration lead to a decrease in photodegradation. It was also demonstrated that RR5 and RR293 photodegradation was favored in acidic solution. The photodegradation of the mixture of the two dyes was also analysed. The results confirmed that TiO_2 had the same photocatalytic activity both in reaction with mono-component solutions and in reaction with bi-component solutions.

In 2013, Cabansag et al. [164] studied the degradation of Reactive Violet 5 dye under UV light with bulk zinc oxide (ZnO) slurry as photocatalyst. A 10 W UV lamp, having UV emission peak at 365 nm, was used. A 1 L reaction vessel, immersed in a water bath with an inlet and outlet water pump system to maintain the desired temperature, was used. The effects of varying amounts of zinc oxide (0.65 – 5 g/L), dye concentration (15 – 60 mg/L), exposure time (0 – 3 h), pH (3 – 10), temperature (30 – 70 °C) and lamp intensity (20 – 10 W) on degradation efficiency, were evaluated. For low dye concentration (15 mg/L) results showed that UV enhanced the dye degradation of about 90% immediately after 30 minutes of irradiation. Moreover, the rate of dye degradation increased as the amount of zinc oxide increased until optimum loading was achieved.

Many authors evaluated the difference between visible/UV illumination and solar light illumination on the photocatalytic process efficiency. In 2002 Saquib et Muneer [165] investigated the photocatalytic degradation of Remazol Brilliant Blue B under sunlight and compared the results to those obtained by using an artificial light source. An immersion well photochemical reactor made of Pyrex glass was used. 250 mL of the desired solution was filled into the reactor and the required amount of photocatalyst was added. A 125 W medium pressure mercury lamp was used as light source. IR radiation and short wavelength UV radiation were eliminated by a water jacket. When sunlight was used as light source, the experiments were performed from 9.00 a.m. to 2.30 p.m. (during the winter season in India). The experiments were carried out in roundbottom flasks (250 mL) made of Pyrex glass. Three different commercially available photocatalysts were tested: Degussa P-25, Hombikat UV-100 and PC-500. The effect of the pH (3 - 11), the initial dye concentration (80 – 330 mg/L) and the catalyst concentration (0.5 – 5 g/L), on the process efficiency, was evaluated. It was found that Degussa P-25 worked better under UV light, and Hombikat UV-100 worked better under sunlight than other photocatalysts.

In 2005 Liu et al. [166] studied the photocatalytic degradation of three azo dyes, Acid Orange 7 (AO7), Procion Red MX-5B (MX-5B) and Reactive Black 5 (RB5) using nitrogen-doped TiO_2 nanocrystals prepared by a sol–gel method. Solar light and UV

radiations were used as energy sources. The UV light source was a 150 W high-pressure mercury lamp. Experiments were carried out in Petri dishes with 10 cm diameter. Each Petri dish contained 15 ml of dye and TiO_2 suspension. The experiments were carried out to compare the photocatalytic activity of N-doped TiO_2 to Degussa P-25 under exposure to UV radiations and solar light. Results showed that the N-doped TiO_2 exhibited substantial photocatalytic activity under sunlight irradiation (70% of color removal was found after 1 hour and complete decolorization was achieved within 3 hours), whereas Degussa P-25 and pure TiO_2 nanoparticles did not give good results as the N-doped TiO_2.

In 2013 Chatzysmeon et al. [167] examined the photocatalytic treatment of two synthetic textile dyehouse effluents. The first one (SE1) was a Remazol Black B aqueous solution (159 mg/L of dye) and the second one (SE2) was an aqueous mixture of sixteen dyes and auxiliary chemicals, usually employed in the textile industry. TiO_2 (Degussa P-25) was used as catalyst. Different light sources were employed to evaluate the influence of the type of radiation on the photocatalytic process. Radiation was provided by:

- a 9 W UVA lamp;
- a 400 W high pressure mercury lamp;
- a 150 W solar simulator system.

It was found that UVA radiation was better than the solar one. This was due to the fact that TiO_2 could be activated at wavelengths below about 385 nm (in the UV region of the electromagnetic spectrum). Solar radiation consists of only about 5% of UVA radiation, while the rest illuminates in the visible region of the electromagnetic spectrum. It was also found that increasing the catalyst concentration in the range 0.5 - 4 g/L, generally enhanced the decolorization and mineralization of SE1 and SE2 because more active sites on the photocatalyst surface were available for reactions.

In 2014 Khanna and Shetti [168] synthesized Ag core–TiO_2 shell (Ag@TiO_2) structured nanoparticles with Ag to TiO_2 molar ratio of 1:1.7. The photocatalytic activity of Ag@TiO_2 photocatalyst was compared to those of other catalysts such as TiO_2 and Ag-doped TiO_2 based on the degradation of Reactive Blue 220 dye. A 50 mg/L solution at pH 3 was treated under exposure to UV and solar light irradiations. A 250 mL capacity borosilicate glass beaker was used as reactor. It was equipped with two 18 W UV lamps (wavelength, λ = 365 nm), which were placed vertically, specified to radiate 80% UVA and 20% UVB light. Solar experiments were carried out in an open terrace. A photocatalyst concentration of 1 g/L was

used. It was found that Ag@TiO_2 exhibited better photocatalytic activity than Degussa P-25 TiO_2, synthesized TiO_2, and Ag-doped TiO_2 photocatalysts.

In 2015 Samsudin et al. [169] studied the photocatalytic degradation of Reactive Blue 4 (RB4), using pure anatase nano titanium (IV) oxide (TiO_2). The experiments were carried out in a 750 mL borosilicate-glass cylindrical photochemical reactor. The RB4 solution (100 mL) containing the appropriate quantity of TiO_2 was irradiated by a mercury lamp (25, 70, 125 and 400 W), a visible lamp (400 W) and natural sunlight. The effect of the pH (3 - 13), the initial dye concentration (20 – 100 mg/L), the catalyst concentration (0.25 – 1.25 g/L), the hydrogen peroxide concentration (0 – 1 g/L) and the light intensity on the process efficiency, was evaluated. Results showed that the dye could be completely degraded and the addition of hydrogen peroxide enhanced the photodegradation efficiency.

In 2017 Thamaraiselvi and Sivakumar [170] synthesized three types of catalysts: $SrTiO_3$ nanocube, three dimensional, mesoporous, BiOBr catalysts, and $SrTiO_3$/BiOBr heterojunction catalysts, respectively, by sol-gel, precipitation, and impregnation methods. $SrTiO_3$/BiOBr heterojunction catalysts were synthesized by using different weight percentages (5, 10, 30, 50 70%) of $SrTiO_3$. The catalysts were used for the degradation of Reactive Blue 198, Reactive Black 5 and Reactive Yellow 145 in the presence of visible and solar light. The photocatalytic degradation of the three dyes was carried out in an immersion type visible reactor equipped with a 500 W tungsten lamp (420 nm), and a water circulation system to avoid the thermal decolourization. The experiments under solar light were performed in an open terrace. Among the catalysts, the one containing a $SrTiO_3$ weight percentage of 10%, gave the best results. It was also observed that solar light was better than visible light due to the presence of 4% of UV light in the solar radiation.

Other authors used only the solar light: Neppolian et al. (2002) [171] investigated the mineralization of an aqueous solution containing Reactive Blue 4 by using TiO_2 as photocatalyst. A cylindrical photochemical reactor, with an internal volume of 200 mL, made up of borosilicate glass was used. Solar light was used as the energy source for catalyst excitation. Experiments were performed at ambient temperature. The effect of the initial concentration of dye on the reaction rate was analysed by varying the initial dye concentration from 64 to 320 mg/L with constant catalyst loading (2 g/L). A series of experiments were carried out to find the influence of other parameters, such as catalyst loading (1–4 g/L), pH (3–13), concentration of hydrogen peroxide ($4.4 \cdot 10^{-3}$–$2.6 \cdot 10^{-2}$), potassium persulphate (0.25–2 g/L), sodium carbonate (0.25–2 g/L), and sodium chloride (0.25–2 g/L) on the process efficiency. It was found that the dye molecules were completely

degraded to CO_2, SO_4^{2-} , NO_3 , NH_4^+ and H_2O under solar irradiation. Results showed that the addition of hydrogen peroxide and potassium persulphate influenced the photodegradation efficiency: a faster photodegradation of dye intermediates was observed in the presence of hydrogen peroxide. The auxiliary chemicals such as sodium carbonate and sodium chloride also influenced the photodegradation efficiency.

In 2006 Muruganandham et al. [211] studied the photocatalytic oxidative degradation of Reactive Black 5 (RB 5) using TiO_2 P25 as photocatalyst in slurry form and sunlight as irradiation source. The experiments were carried out from 11 a.m. to 2 p.m. in the months of May–June. An open borosilicate glass tube of 50 mL capacity, 40 cm height and 20 mm diameter, was used as the reaction vessel. Irradiation was carried out in the open air. The solution was continuously aerated by a pump to provide oxygen and ensure the complete mixing of the reaction solution. The degradation was carried out at different experimental conditions to optimize the parameters such as amount of catalyst (1–3 g/L), initial concentration of dye (71.5–214–357–500-634) and pH (3–5–7– 9). Different types of photocatalysts (ZnO, SnO_2, CdS, Fe_2O_3, ZnS, TiO_2 P25) were tested. This study revealed that RB5 could be completely degraded by in the presence of TiO_2 Degussa P-25 and under exposure to solar light irradiation. Results showed that the optimal concentration of the catalyst was 2 g/L. It was found that the complete degradation of the 357 mg/L dye solution under solar irradiation required 3.5 h. Finally, the photochemical degradation in the presence of hydrogen peroxide resulted in the partial removal of the dye.

In 2012 Giwa et al. [172] studied the photocatalytic degradation of Reactive Yellow 81 (RY81) and Reactive Violet 1 (RV1) in the presence of TiO_2 Degussa P-25 and sunlight irradiation. A 100 mL solution of each dye was prepared and transferred into a 500 mL Pyrex beaker for solar irradiation. Before the solar irradiation, the catalyst was added to the solution. The effects of various parameters such as catalyst loading (0.5–2 g/L), pH (3–11), and initial concentration of the dye (10–100 mg/L) on the photocatalytic efficiency were evaluated. The effects of various photocatalysts such as TiO_2 Degussa P-25, TiO_2 (anatase), and ZnO on decolorization were also investigated. It was found that TiO_2-P25 and ZnO are more efficient than TiO_2 (anatase). In the presence of Degussa P- 25 decolorization yields of 92% and 85%, for Reactive Yellow 81 and Reactive Violet 1, respectively, were obtained in 20 minutes.

In 2013 Subash et al. [212] prepared different wt % of Zr-codoped Ag−ZnO catalysts by a simple precipitation−thermal decomposition method. The catalyst were used for the degradation of Reactive Red 120 (RR 120) under natural sunlight. The photocatalytic

activity of 4 wt % Zr-codoped Ag−ZnO was compared to that of other single-metal-doped, undoped, and commercial catalysts. The influence of operational parameters such as the amount of photocatalyst (2–6 g/L), dye concentration, and initial pH (3–5–7–9–11) on the photocatalytic process was evaluated. The experiments were carried out on sunny days between 11 a.m. and 2 p.m. An open borosilicate glass tube of 50 mL capacity, 40 cm height, and 20 mm diameter, was used as reaction vessel. 50 mL of RR 120 (294 mg/L) were used. Reaction mixture was continuously aerated by a pump to provide oxygen and to ensure complete mixing of the solution. Results showed that Zr−Ag−ZnO was more efficient in RR 120 degradation than the other catalysts. The photocatalytic efficiency of Zr−Ag−ZnO was also tested with other dyes such as Reactive Orange 4 (RO 4) and Reactive Yellow 84 (RY 84), and good results were obtained.

In the same year, Badawy et al. [173] prepared pure and silver doped ZnO thin films over a glass substrate using a sol–gel spincoating method. Prepared films were calcined at different temperatures. Photocatalytic efficiency of the prepared films was evaluated by the decolorization of three azo reactive dyes, Reactive Red 195, Reactive yellow 145 and Reactive orange 122, under solar light irradiation. Various operational parameters such as pH of the solution (3–11) and initial concentration of the dye (10–25 ppm) were investigated. 75 mL of 10 ppm dye solution was placed in a glass Petri dish. A catalyst of rectangular geometry 1.2 · 2.6 cm was immersed in the dye solution. It was found that Ag-doped-ZnO (6 % wt. Ag) showed the highest photocatalytic activity. The optimal pH value was the natural pH of the studied dyes.

Chen et al. [140] published in 2005 the first article regarding the use of UV-LEDs. They used the UV-LEDs as alternative sources of light for the oxidation of perchloroethylene (PCE). Then, many articles about the use of UV and visible LEDs in the photocatalytic processes to treat aqueous organic dyes such as methylene blue (MB), rhodamine B (RhB), malachite green (MG), reactive red 22 (RR-22), methyl orange (MO), congo red (CR), and Reactive Black 5 (RB-5), were published. Here, the studies about the photocatalytic degradation of different dyes under UV and visible LEDs irradiation were summarized.

Wang et al. (2006) [173] successfully used UV-LEDs for the photocatalytic mineralization of Reactive Red 22. TiO_2 was used as photocatalyst. A rectangular planar fixed-film reactor in recirculation mode was used. Various operative conditions such as initial dye concentration (10- 100 mg/L), and different TiO_2 coating arrangements were investigated. It was found that Reactive Red 22 could be treated, with good results, trough photocatalytic process.

Many researchers used methylene blue as model pollutant in water to test the photocatalytic activity of commercial and synthesized catalysts under UV-LEDs irradiation [175-177, 141-148].

In 2009, Tayade et al. [175,145,146] realized a simple photocatalytic set up using five UV-LEDs for the decolorization and mineralization of Methylene Blue and Rhodamine B. The photocatalyst (Degussa P-25) nanoparticles were suspended in the dye solution and irradiated with UV-LEDs. It was also investigated The effects of operational parameters such as the amount of the photocatalyst, the dye concentration, the pH, and the amount of hydrogen peroxide on the decolorization and mineralization of methylene blue was evaluated. It was used A methylene blue concentration of $3.12 \cdot 10^{-5}$ mol/L and a rhodamine B concentration of $2.08 \cdot 10^{-5}$ mol/L were used for the experiments. Results showed that for the methylene blue the optimal conditions were the following:

- 1.2 g/L of catalyst;
- 3.12×10^{-5}mol/L of dye;

for the rhodamine B the optimal condition were:

- 1.6 g/L;
- 6.26×10^{-5} mol/L;
- pH = 3.05.

Sacco et al. [104] used white and blue LEDs as visible light irradiation sources for the photocatalytic degradation of methylene blue and methyl orange in aqueous solution. N-doped TiO_2 nanoparticles (having a bandgap varying between 2.6 eV and 3.3 eV) were synthesized by the direct hydrolysis of titanium alkoxide with ammonia, and used as photocatalysts. The photoreactor was equipped with a strip composed of 30 white light LEDs (wavelength of emission: 400 – 800 nm) with a nominal power of 6 W. A strip of 30 blue light LEDs (wavelength of emission: 400–550 nm) having a nominal power of 6 W was also used. The LEDs strips were covered on the outside of the reactor to ensure uniform light exposure of the reaction mixture. The N-doped TiO_2 showed high photocatalytic activity, therefore it was also used to treat methyl orange. Results confirmed the high photocatalytic efficiency of the N-doped TiO_2 [145, 146].

Dai et al. [143, 148, 178] also used methylene blue to test a plasmonic Ag/AgBr heterostructure as photocatalytic material. A LED device (wavelength: 450 nm) was used as light source. A vessel containing 100 mL of methylene blue (10 mg/L) and 0.05 g of the photocatalyst was used as photoreactor. Experiments were carried out at room temperature. The distance between the LED light source and the reactor was 1 cm; the reaction mixture

was stirred continuously during the photocatalysis. It was observed a 95% methylene blue dye decomposition over 240 min [143].

Repo et al. [142] synthesized CdS microspheres by a hydrothermal method. The catalyst was used for the photocatalytic treatment of some dyes under LEDs light irradiation. Methylene blue, phenol red, and methyl red were exposed to different LEDs lights (wavelengths: 405 and 450 nm). The nominal power of the near-UV LEDs was 24 W and it was 17.5 W for the blue LED. A dye concentration of 3–5 mg/L was used. Results showed the complete decolorization of each dyes occurred within 3 hours.

Repo et al. also tested the photocatalytic activity of other CdS nanoparticles having different sizes. The photocatalytic decolorization of methylene blue dye in the presence of blue LEDs (3 W) and solar light was investigated. It was found that smaller nanostructures enhanced photocatalytic efficiency. The photocatalytic activity of CdS was compared to that of commercial TiO_2 (under exposure to blue LEDs light). It was found that CdS was more efficient than TiO_2.

Eskandari et al. (2013) [177] used cadmium sulphide nanostructures synthesized via chemical precipitation method by using MEA as capping agent. The photocatalytic activities of the samples were investigated for degradation of methylene blue (MB) under blue LEDs (3 W) and solar light irradiation. For comparison purposes, TiO_2 Degussa P-25 was used as the reference photocatalyst. The reaction experiments were carried out in 100 mL roundbottom flask. The reaction mixture was prepared by adding 1 g/L of the CdS nanopowder to 50 mL of a MB aqueous solution (15 mg/L). It was found that under blue LEDs irradiation, the CdS exhibited higher photocatalytic efficiency than the commercial Degussa P-25 TiO_2.

Kuo et al. (2010) [179] used nitrogen-modified TiO_2 photocatalyst (N-doped TiO_2) obtained by a simple hydrolysis method for the photodecolorization of methyl blue (MB) and direct blue 86 (DB-86) under various visible light sources: fluorescent lamp and blue LEDs lamp. TiO_2 was used as the reference photocatalyst. Each test, was carried out the in the presence of 1 g/L of photocatalyst added to 200 mL of a dye aqueous solution (10 mg/L). Results showed that the fluorescent lamp/N-doped TiO_2 system was more efficient than the blue LEDs lamp/TiO_2 one. The effect of the pH on the process efficiency was also evaluated. High decolorization yields were achieved at pH 5 and 7.

Jo et al. (2014) [242] used blue and ultraviolet LEDs for the degradation of malachite green (MG) dye. A slurry type spiral-shaped photocatalytic reactor and Degussa P-25 TiO_2 photocatalyst were employed. The influence of operational parameters such as catalyst

concentration (0.2–0.7 g/L), initial concentration of dye (10–40 mg/L), and pH (3–9) of the medium was evaluated to optimize MG dye degradation.
Results showed that the photocatalytic degradation of malachite green dye under separate irradiation by blue and by ultraviolet LED was nearly the same (~76%). It was also observed that the adsorption of malachite green dye on TiO_2 surface enhanced photocatalytic degradation under blue LED irradiation.

The photocatalytic processes in the presence of the traditional UV sources (such as mercury lamps) were largely investigated, and TiO_2 was often used as catalyst. Most recently, studies on the use of other sources of light, less expensive than the UV one, were carried out. Anyway, these light sources necessitate to be used with opportunely modified photocatalysts, therefore, researches focused on the development of new photocatalysts. The efficiency of these catalyst was tested using industrial dyes as model pollutants. Many studies showed that visible light LEDs can successfully be used for the photocatalytic decomposition of various dyes such as methilene blue, malachite green, Direct Blue 86, by employing photocatalysts with a bandgap in the range of 2.0–3.1 eV. Anyway there are few papers regarding the photocatalysis of reactive dyes under exposure to visible LEDs.

2.3 Parameters affecting photocatalytic process

The analysis regarding the state of art of the photocatalytic processes also evidenced that this type of treatments could be influenced by a lot of parameters such as type of dye, dye concentration, catalyst loading, light sources, pH, amount of hydrogen peroxide and aeration.

2.3.1 Influence of Dye Type on the Photocatalytic Process

The chemical structure of the organic dyes has a considerable effect on the reactivity of dyes on photodegradation system [186]. This effect was investigated by different researchers. For example, Khataee and Kasiri (2010) [187] found that the COD removal rate of Reactive Yellow 17 was higher than Reactive Red 2 and Reactive Blue 4 dyes. This results was attributed to the particular structures of the three molecules of dyes. Reactive Yellow 17 and Reactive Red 2 are provided with an azo group (–N=N–) which makes these dyes easy to

degrade, while in RB4 there is the anthraquinonic group that makes this dye more resistant to photodegradation.

TiO_2 photocatalisys can be successfully used to treat Reactive Orange 16, Reactive Black 5 and Reactive Blue 4. The reaction rate follows the subsequent order: RO16 > RB4 > RB5. The reason can depend on the different chemical structure of dyes that implies different adsorption characteristics and propensity to photodegradation [188 - 191]. In fact, Reactive Black 5 has a more complex structure than Reactive Orange 16 and Reactive Blue 4 that makes it more difficult to treat. Moreover, Reactive Black 5 tends to absorbe light photons causing a decrease of photons useful for the generation of hydroxyl radicals: dye molecules adsorb light and photons cannot reach the photocatalyst surface; thus, the photodegradation efficiency decreases. Moreover, it can be observed that different dyes can follow different degradation pathways; it is due to their different chemical structures and functional groups. For example, an ·OH radical who attacks an aromatic ring (of a dye molecule) can generate a hydrogen atom [192 - 196]. In the case of hydroxy azo dyes (Acid Orange 7 and Acid Orange 8) a competition between an oxygen atom in the azo form or in the hydrazone form and ·OH radical occurs. Oxygen tends to abstract a hydrogen atom from the dye molecules, whereas ·OH radical tends to add it-self on a phenyl or naphtyl nucleous [197].

A dye can have different functional groups such as nitrite group, alkyl side chain, chloro group, carboxylic group, sulfonic substituent, and also hydroxyl group [187], thus the catalyst necessitate to be chosen on the base of the characteristic group of the dye [198-201]. There are some groups, such as the alkyl side chain, that could reduce the water solubility of the molecules causing a slowing down of the photodegradation process. This explains because the rate of decomposition decreases with increasing length of the side chain and, consequently, with increasing hydrophobicity of the dye molecule.

This is the case of the Reactive Blue 19 [198-202], in fact ·OH radical, that should degrade the dye chromophore, could react with the hydrogen atoms of the side chains; therefore the absorbance doesn’t decrease.

A considerable decrease of the photocatalytic decolorization rate was observed when two or three chloro substituents were present on the phenyl ring of a pyrazolone dye [203, 204]. The comparison of Acid Yellow 17 and Acid Yellow 23 decolorization rates suggests that the difficulty of the dye to be degraded directly depends on the number of electron withdrawing chloro groups in the molecule.

Another efficient withdrawing group is the $–SO_3^-$ one. The difficulty to degrade Orange G and Aizarin S depends on the presence of this group in the two dyes molecules [205],

whereas the high decolorization yields achieved by Methyl Red photocatalysis is due to the presence of the carboxylic group. Dyes containing more sulfonic substituents are less reactive in a photocatalytic process, while hydroxyl group intensifies the electron resonance in the molecule and the degradation rate of the dye [206]. Finally, photocatalytic decolorization of monoazo dyes is easier than anthraquinone degradation.

2.3.2 Dye concentration

The initial dye concentration can influence the photodegradation process based upon two main aspects.

In Table 2.1 the effect of the initial concentration of dye on the degradation (%) of Reactive Blue 4, is shown [171].

Table 2.1 – Influence of the concentration of the dye on the Reactive Blue 4 degradation. Catalyst loading (2 g/L), energy source: solar light [171].

Concentration of the dye (mg/L)	Degradation (%)
64	98
127	98
191	82
255	71
319	32

Table 2.1 shows that the percentage degradation decreases as the initial concentration of the dye increases. One of the reasons is that in high dye concentrations, more active sites of the catalyst may be covered with dye ions. Therefore, the water molecules cannot react with the hole generated on the catalyst surface and this may lead to the decrease in the production of ·OH radicals on the catalyst surface. Furthermore, the path length of the photons entering the solution decreases as the initial concentration of dye increases. This is due to the "shadow effect": the dye molecules hinder the penetration of light radiation through the solution, and therefore, the production of HO· radicals, which are the most reactive species, decreases [170, 156, 169, 177].

Several studies reported the heterogeneous photocatalysis of reactive dyes; generally, the concentration of the treated dye was varied from 20 mg/L to 100 mg/L. In these studies the optimal dye concentration to avoid the shadow effect was found to be about 50 mg/L [154, 155, 157, 161, 170, 171, 172, 204].

2.3.3 Catalyst loading

The amount of catalyst to be used is one of the main factors to evaluate, it's also important to keep the treatment expenses low for industrial use. To avoid using an excessive amount of catalyst, its optimal concentration has to be determined.

The amount of catalysts required depends on the configuration of the reactor, light intensity, type of the targeted dye and type, as well as particle morphology, of the catalyst. Because of these many contributing factors, there are inconsistencies in the optimum catalyst concentration used by different researchers.

Kaur and Singha (2007) [235] reported that in all of the optimized conditions of efficiency, the catalyst dose for maximum photocatalytic degradation of Reactive Red 198 was 0.3 g/L. However, in another study, the optimized condition for TiO_2 consumption was stated to be 0.5 g/L [239]. Also, Muruganandham et al. (2004) [229] reported that an increase of catalyst weight from 1.0 to 4.0 g/L increases the dye decolourization sharply from 69.27% to 95.23% at 60 minutes and dye degradation from 74.54% to 97.29% at 150 minutes.

Other authors [207, 208] studied the variation of the reaction rate by varying the catalyst concentration: in all cases, the total active surface area increased with increasing catalyst dosage, but, for catalyst concentrations higher than the optimal value, both steric encumbrance problems and problems related to the penetration of light through the solution, took over. As a result, the photoactivated volume of suspension decreased.

It can be said that for dye concentrations higher than 100 mg/L the catalyst concentration to be used varies from 1 to 4 g/L. For dye concentrations lower than 100 mg/L the catalyst concentration is comprised between 0.25 and 1-1.5 g/L.

2.3.4 pH

The wastewater from textile industries usually has a wide range of pH values. It is important to study the influence of pH on the degradation of dye. The pH can influence dye adsorption onto the catalyst surface [230] because the semiconductor surface charge depends on the pH

of the given solution. Zhu et al. [234] demonstrated that pH effect could be explained on the basis of point of zero charge (PZC) of the used catalyst. The point of zero charge for TiO_2 particles is pH_{pzc} 6.8. At pH values lower than pH_{pzc} (pH < 6.8) or at acidic conditions, the surface of the catalyst is positively charged and at pH values greater than 6.8 the surface of TiO_2 is negatively charged according to the equations:

$$TiOH_{(surface)} + H^+ \rightarrow TiOH_{2(surface)}^+ \quad (2.1)$$

$$TiOH_{(surface)} + OH^- \rightarrow TiO_{2(surface)}^- + H_2O \quad (2.2)$$

The equations (2.1) and (2.2) show that, when pH is lower than the PZC value, the adsorbent surface is positively charged and the surface becomes anions attracting/cations repelling. Above PZC the surface is negatively charged and it is cations attracting/anions repelling. Zhu et al. (2000) [234] found that highest yield of decolorization of methyl orange was at pH 2. They attributed this result to the electrostatic attraction between the positively charged catalyst surface and methyl orange anions, which increased the degree of adsorption and led to 97% photodecolorization. However, the dye treatment results cannot be explained only on the base of dye adsorption strength on the catalyst surface, because there are many other parameters operating at the same time. For example, Muruganandham et al. (2004) [229] found that increasing pH from 1 to 9 increased decolourization rates for Reactive Orange 4 (an anionic dye) from 25.27% to 90.49% after only 40 minutes. Moreover, the faster rate of color removal was observed at alkaline pH. In contrast, the degradation studies of some azo dyes showed conflicting results [215]. For example, for the Acid Yellow 17 (an anionic dye) the highest degradation value was obtained at pH 3, whereas, for the Orange II (anionic dye) and Amido Black 10 B (anionic dye) the maximum degradation yields were found at pH 9 [236].

For a 200 mL solution containing 318 mg/L of Reactive Blue 4, treated using 2.5 g/L of TiO_2 and exposed to sunlight, the optimal pH was found to be comprised between 5 and 10 [155]. For the same dye, Zhou et al. (2008) [214] found that the optimal pH was 11, but they used a different dye concentration (20 ppm), a different catalyst (ZnO and N-doped Zn) and a different catalyst loading (0.1 g/L). In other studies, it was found that the optimal pH was that corresponding to the isoelectric point of the catalyst [154, 155, 158, 161, 166, 170, 171, 172, 173, 207]. In other studies, the experiments were carried out at acidic conditions [82, 157, 161, 162, 168, 171, 179]. (For example, for a solution containing 30 mg/L of

Reactive Red 198 treated by using Tytanpol-A11 and Degussa P-25 under UV-visible light, the optimal pH was about 2; therefore the TiO_2 surface was positively charged and more reactive to the anionic dye [238]).

Therefore, to evaluate the influence of pH on a photocatalytic process it is necessary to test different pH values, but it is also important to consider which characteristics of the dye and of the catalyst should be employed.

2.3.5 Concentration of hydrogen peroxide

The photoassisted degradation of organic substrates can be significantly improved in the presence of hydrogen peroxide. Since reactive hydroxyl radicals are easily generated by the breakdown of hydrogen peroxide, the presence of hydrogen peroxide in the reaction mixture will play a key role in the photocatalytic process [209]. It was widely reported that the addition of small amount of hydrogen peroxide greatly enhanced the oxidation of organic pollutants mediated by TiO_2 catalyst [209].

Hydrogen peroxide can react directly with the electrons present in the conduction band of the catalyst, to form the radical ·OH (Eq. (2.1)), but also with the superoxide radical anion, producing hydroxyl radicals indirectly (Eq. (2.2)) [210]). It can also dimerize (Eq. (2.3)) and form others hydroxyl radicals.

$$H_2O_2 + e^- \rightarrow \bullet OH + OH^- \quad (2.1)$$

$$H_2O_2 + O2^{-\bullet} \rightarrow \bullet OH + OH^- + O_2 \quad (2.2)$$

$$H_2O_2 \rightarrow 2 \bullet OH \quad (2.3)$$

When the concentration of hydrogen peroxide is too high, reactions involving HO• radicals could occur. These reactions could compete with those of degradation of the dye (Equations (2.4), (2.5) and (2.6)) and could reduce the colour degradation yields.

$$H_2O_2 + \bullet OH \rightarrow HO_2\bullet + H_2O \quad (2.5)$$

$$HO_2^{\bullet} + \bullet OH \rightarrow H_2O + O_2 \quad (2.6)$$

2.3.6 Aeration

Aeration can influence a photocatalytic process. In fact, different studies regarding the effect of UV-vis illumination and simultaneous UV-vis illumination and aeration on the decolorization of a dye solution, were reported in literature. Figure 2.2 shows the influence of the aeration on the photolysis of Reactive Red 198, Acid Black 1 and Acid Blue 7.

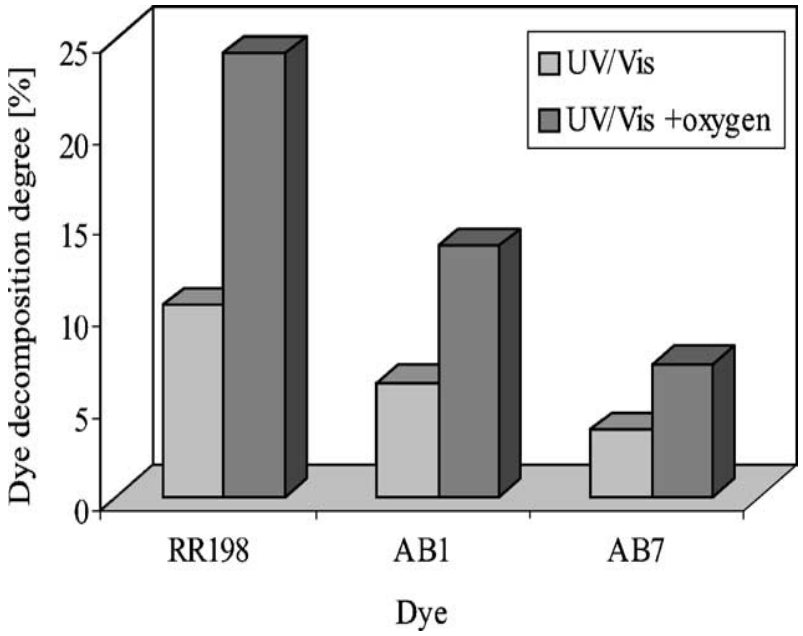

Figure 2.1 - Photocatalytic decomposition of RR198, AB1 and AB7 under UV/Vis illumination and under illumination and simultaneous aeration at pH = 2 [82].

Figure 2.2 shows that simultaneous irradiation and aeration caused an increase of the degree of the dye decomposition indicating a possible role of an active oxygen species. After 40 min of UV/Vis illumination and aeration, dyes decomposition degrees were 24.2% for RR198, 13.7% for AB1 and 7.2% for AB7, respectively.

In a photocatalytic system continuous aeration of the dye solution can be ensured by a pump. Aeration is also useful to ensure the complete mixing of the reaction solution. [154, 155, 165, 170, 204, 207].

2.3.7 Type of light source: LEDs vs. conventional UV irradiation sources

The light source that must be used it is very important. Conventional irradiation sources, such as mercury UV lamps, sunlight, or new irradiation sources such as LED lamps can be

employed. Conventional mercury UV lamps are delicate, contain mercury, have a short working life-span of about 100–1000 hours and tend to lose gas. Moreover, lamp-blasts are possible in medium and high pressure lamps. Another disadvantage is that the operating temperature of medium/high pressure UV lamps is between 600 and 900 °C and they need to be cooled during the reaction. This increases the energy consumption.

LEDs (both UV and visible) are robust, safe, compact, cool, non-toxic, inexpensive, environmentally friendly and have a long life-span of around 100000 h. Moreover, LEDs can emit light at different wavelengths. This depends on the composition and condition of the semiconducting materials [139].

2.3.7.1 Advantages of LEDs

LEDs don't require cooling, they are small, and can be used in different types of photocatalytic reactor set-ups. Furthermore, LEDs irradiation is unidirectional, so the loss of light is lower than that of traditional UV light lamps (reactors employing traditional UV irradiation sources can waste up to 80% of the light that they produce). Conversely, LEDs emit light at specific wavelengths, and the light emitted is completely used. Based on the available literature, it is clear that increasing the number and the power of the available LEDs will ensure a better photocatalytic degradation of dyes in shorter reaction time.

Chapter 3

Photocatalytic degradation of Reactive dyes under visible light

3.1 Introduction

The aim of this work is the study of the photocatalytic decolorization of a reactive dye under exposure to visible light. Reactive Blue 4, Reactive Red 120 and Reactive Violet 5, which are dyes with high structural complexity, were used as model pollutants. The photocatalytic process was carried out in a cylindrical photoreactor. The solution, containing the catalyst as an aqueous suspension, was irradiated under visible blue LEDs.

Before using Reactive Violet 5, the photodecolorization of Reactive Blue 4 and Reactive Red 120 was examined.

At first, Reactive Blue 4 and Reactive Red 120 dyes were used as model pollutants. However results obtained with Reactive Blue 4 showed the same colour removal yields in the presence and in the absence of photocatalysts. Reactive Red 120 showed a high resistance not only to the photolysis, but also to the photocatalytic treatments.

Therefore, Reactive Violet 5 dye was selected to carry out the experiments. Results showed that it couldn't be treated only by photolysis, but also trough a photocatalytic process. To find the most suitable catalytic system, different catalysts, were tested. Then, the effect of various operational parameters like catalyst loading, pH and addition of hydrogen peroxide, was studied to find the optimized conditions for maximum decolorization.

The existence of an optimal catalyst concentration, an optimum pH, and H_2O_2 dosage, was observed. Under the optimal conditions, complete decolorization of the Reactive Violet 5 dye was achieved in less than 2 hours.

3.2 Chemicals and Reagents

Chemicals used in this research work include:

- Reactive Blue 4 (35%), provided by Gamma Color S.A.S, (Italy);
- Reactive Red 120 (70 %) provided by Zaitex S.p.A., (Italy);
- Reactive Violet 5 (150%) provided by Gamma Color S.A.S, (Italy);
- Hydrogen peroxide 30%, provided by Sigma Aldrich S.r.l (Milano, Italy);
- TiO_2, N-doped TiO_2, Fe-TiO_2 (10 mg Fe), Fe-TiO_2 (50 mg Fe), Fe-TiO_2 (100 mg Fe), provided by University of Salerno (Italy);
- P-25 Degussa provided by Sigma Aldrich S.r.l, (Italy);
- KH_2PO_4 (>99%), provided by Sigma Aldrich S.r.l, (Italy);
- NaOH in pellets (>97%), provided by Sigma Aldrich S.r.l, (Italy);
- $NaHCO_3$ (>99.7%), provided by Sigma Aldrich S.r.l, (Italy);
- Na_2HPO_4 (>99%), provided by Sigma Aldrich S.r.l, (Italy);
- CH_3COOH (1 N), provided by Sigma Aldrich S.r.l (Milano, Italy);
- CH_3COONa (>99%), provided by Sigma Aldrich S.r.l (Milano, Italy).

All the reagents were used were used without further purification.

3.2.1 Dyes specifications

In Table 3.1 the dyes specifications are shown.

Table 3.1 – Dyes specifications

Specifications	Reactive Blue 4	Reactive Red 120	Reactive Violet 5
Linear formula	$C_{23}H_{14}C_{l2}N_6O_8S_2$	$C_{44}H_{24}C_{l2}N_{14}O_{20}S_6Na_6$	$C_{20}H_{16}N_3Na_3O_{15}S_4$
Molecular Weight	637.43 g/mol	1469.98 g/mol	735.58 g/mol
Absorption maxima	595 nm	510 nm	559 nm
Purity	35%	70%	150%

Figures 3.1, 3.2 and 3.3 show the chemical structure of the used dyes.

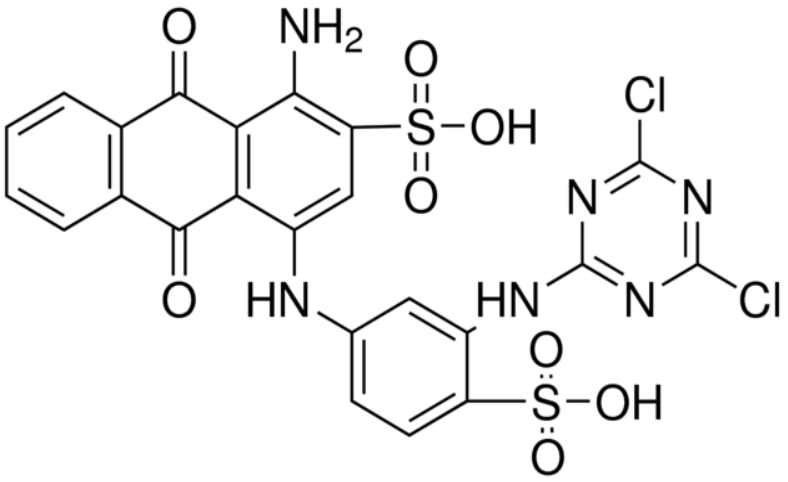

Figure 3.1 – Molecular structure of Reactive Blue 4 dye.

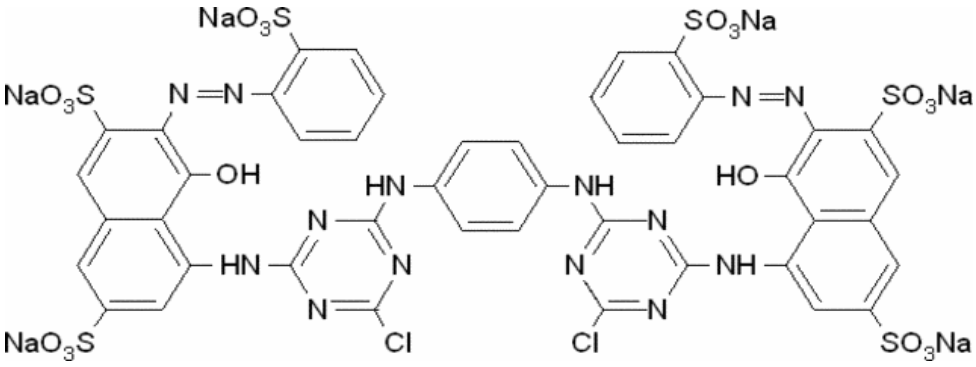

Figure 3.2 – Molecular structure of Reactive Red 120 dye.

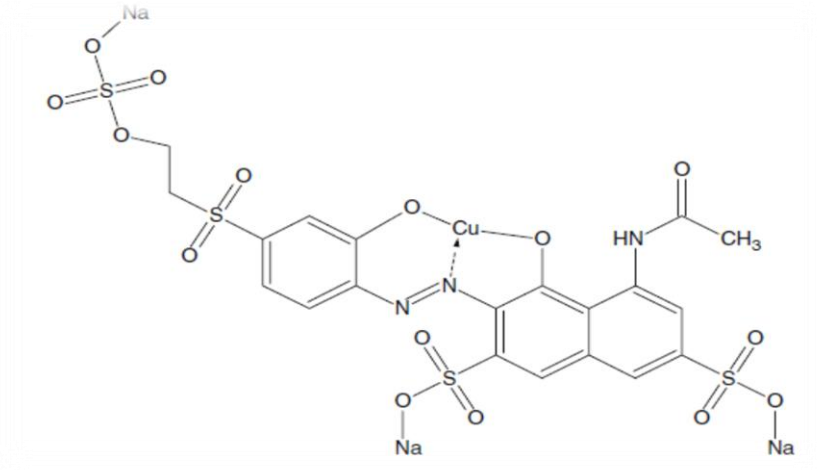

Figure 3.3 – Molecular structure of Reactive Violet 5 dye.

3.2.2 Catalysts specifications

In Table 3.2 the specifications of the employed catalysts are shown.

Table 3.2 – Catalysts specifications.

Catalysts	**TiO_2**	**Degussa P-25**	**N-doped TiO_2**	**Fe-TiO_2 (10 mg Fe)**	**Fe-TiO_2 (50 mg Fe)**	**Fe-TiO_2 (100 mg Fe)**
Molar ratio Fe/Ti	0	0	0	0.00033	0.0017	0.0033
Molar ratio N/Ti	0	0	18.6	0	0	0
Band gap (eV)	3.2	3.2	2.5	3.12	2.9	2.63

Table 3.2 shows that the typical band gap of undoped TiO_2 is 3.2 eV. This value decreases to 2.5 eV for the N-doped TiO_2 due to the presence of nitrogen in the crystal structure phase. The band gap energies of Fe-TiO_2 (10 mg Fe), Fe-TiO_2 (50 mg Fe) and Fe-TiO_2 (100 mg Fe) are 3.12, 2.9 and 2.63 eV, respectively. As the iron content increases, the band gap decreases, and the catalyst becomes able to absorb the visible light.

XRD analysis (not reported) [104, 154] revealed that for the undoped TiO_2, the N-TiO_2 and the Fe-TiO_2 samples, the only crystalline phase is the anatase and it did not change after the doping process.

The crystallites average size is reported in Table 3.3.

Table 3.3 – Crystallites average sizes.

Catalysts	**Crystallite average size (nm)**
TiO_2	8.4
Degussa P-25	21
N-doped TiO_2	15
Fe-TiO_2 (10 mg Fe)	8.3
Fe-TiO_2 (50 mg Fe)	7.9
Fe-TiO_2 (100 mg Fe)	7.9

Table 3.3 shows that the crystallites average size of the Fe-doped samples is similar to that of undoped TiO_2 (8.4 nm). The N-doped TiO_2 crystallites size is 15 nm and it is 21 nm for Degussa P-25.

The XRD analysis are confirmed by Raman spectra (not reported), since the band positions (at 141, 194, 394, 515 and 636 cm^{-1}) are in complete accordance with those reported in previous studies for anatase powder [252, 253].

3.3 Equipment

Equipment used in this study includes:

- a photocatalytic reactor provided by Vetroscientifica S.r.l. (Italy);
- a strip composed by 90 blue visible LEDs, provided by LEDTECH SHOP (Germany), having a nominal power of 24 W, and a wavelength emission in the range 465 - 470 nm;
- syringe filters GMF (pore size 0.45 μm) provided by Sigma-Aldrich S.r.l.(Italy);
- an air distributor device (Q_{air} max 300 l/h) provided by Ecopolis S.r.l. (Italy);
- a UV-vis spectrophotometer, model UV/2700, provided by Shimadzu Italia S.r.l.

3.3.1 UV/VIS Spectroscopy

The UV/Vis spectrophotometer is used to measure the absorbance of light of a chemical at a given wavelength. The value of the absorbance is proportional to the chemical concentration (Beer Lambert law), so concentrations may be measured through absorbance measurements and a calibration curve.

The spectrophotometer is composed of a light source, which can be an incandescent bulb (visible wavelength) or a deuterium lamp (UV regions), a holder for the sample (which is contained inside a 3.5 mL cuvette), a diffracting grating to separate light in its different wavelengths and a detector. The sample is contained in a transparent cuvette, generally of a 1 cm width and 3.5 mL capacity. Cuvettes can be made of plastic, glass or quartz, which are the highest quality ones. The plastic and glass cuvettes are common if used in visible wavelengths, but are not suitable for the UV analysis, as they absorb in that region.

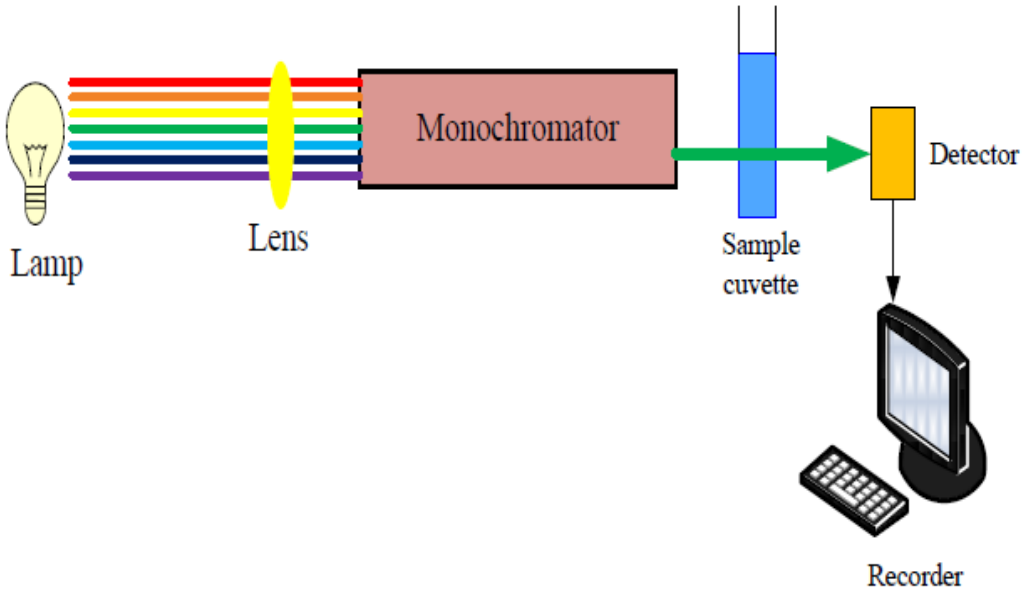

Figure 3.4 – Schematic UV-vis spectroscopy.

The container dimension and the solute concentration are related to the absorbance through the Beer-Lambert law (Eq. 3.1):

$$A = \varepsilon l C \tag{3.1}$$

where ε is the molar extinction coefficient, l is cell path length (the dimension of the container, which was 1 cm) and C is the solute concentration.

During the experiments, the absorbance of the treated solution was monitored. The absorbance values were measured at the wavelengths of 595 nm, 510 nm and 559 nm, for the Reactive Blue 4, the Reactive Red 120 and the Reactive Violet 5, respectively.

The absorbance values obtained were used to calculate the corresponding concentrations through calibration curves obtained from solutions having known concentrations.

In Figures 3.5, 3.6 and 3.7, the concentrations of the calibration solutions and the corresponding absorbances are reported for each dye.

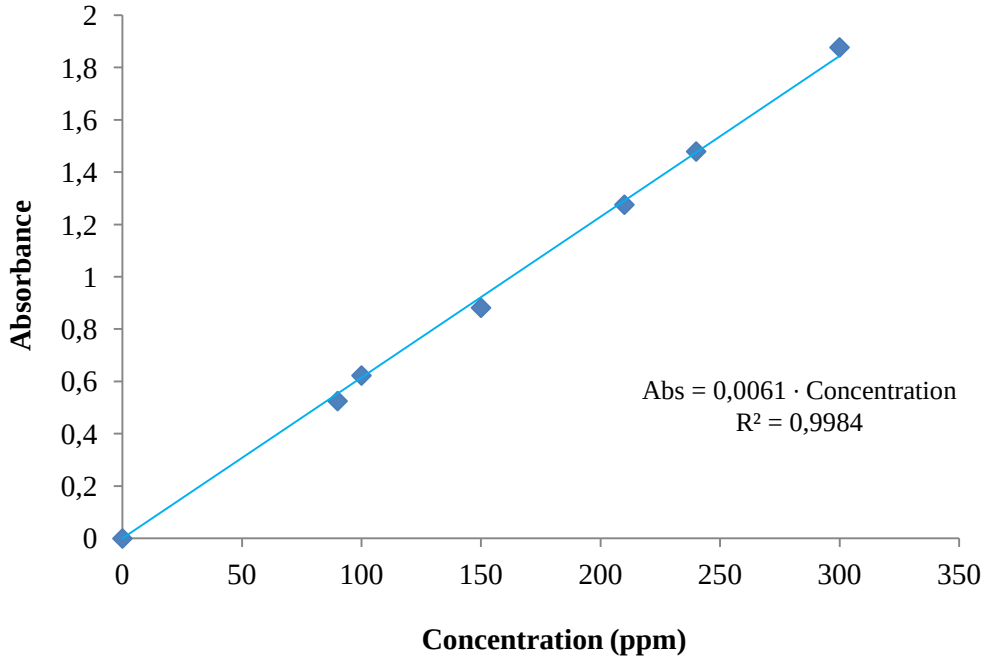

Figure 3.5 –Reactive Blue 4 calibration curve.

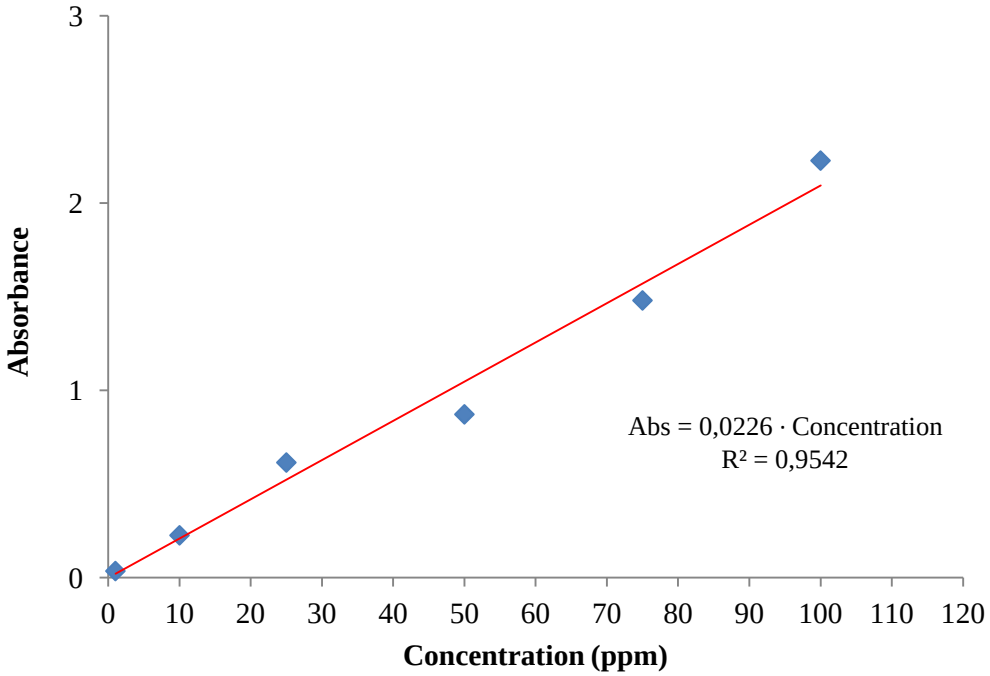

Figure 3.6 – Reactive Red 120 calibration curve.

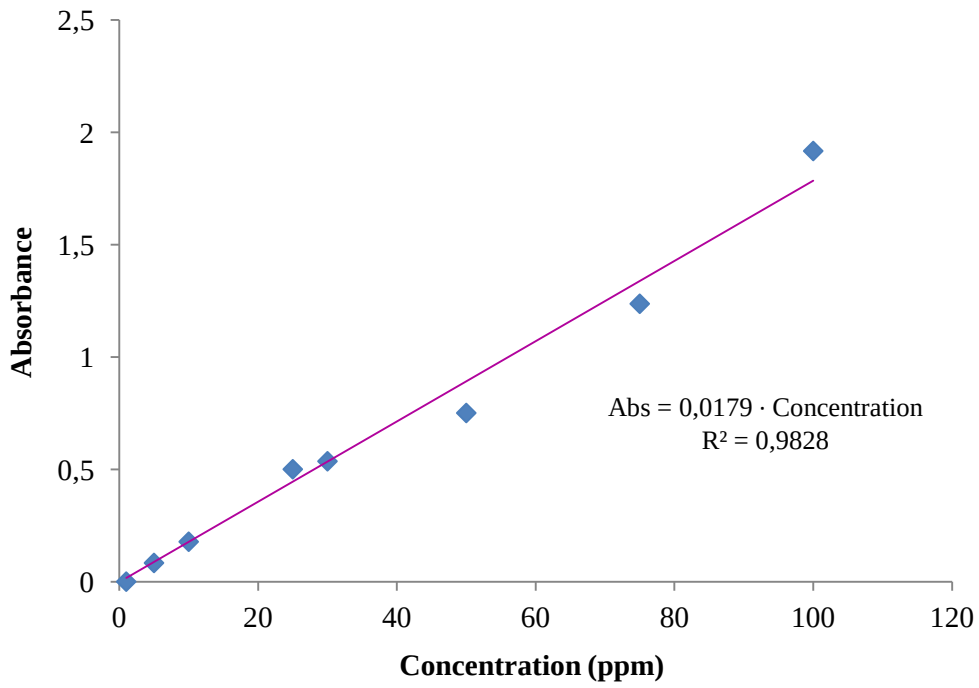

Figure 3.7 –Reactive Violet 5 calibration curve.

Figures 3.5, 3.6 and 3.7 show that the relationships between absorbance and concentration are linear in a wide range of values: [0 – 300] ppm for the Reactive Blue 4; [0 – 100] for the Reactive Red 120 and the Reactive Violet 5. Therefore, the concentration of dye solutions were obtained as follows:

- RB4 concentration = Abs/0.0061; (3.2)
- RR120 concentration = Abs/0.0226; (3.3)
- RV5 concentration = Abs/0.0179. (3.4)

3.4 Experimental procedure

The experiments were carried out using a borosilicate glass cylindrical photoreactor (ID = 3 cm, H = 18 cm) equipped with an air distributor device (Qair = 15 l/h (NTP)) and a magnetic stirrer to maintain the photocatalyst suspended in the aqueous solution. The photoreactor was irradiated with a strip composed of 90 blue LEDs with wavelength emission in the range 465-470 nm (LEDTECH SHOP, Germany). The light source was positioned around the external surface of the photoreactor.

In a typical photocatalytic test, a fixed catalyst concentration, was suspended in 50 mL solution. The system was left in the dark for 1 hour to reach the dye adsorption equilibrium on the catalyst surface, and then the reactor was irradiated with visible light. Liquid samples were taken during the experiments and filtered to remove catalyst powders from the aqueous solution. The reaction was monitored in time, collecting the UV/vis spectra every 60 minutes. 2.5 mL of the reagent solution was transferred inside a quartz 3 mL cuvette.
The natural pH:

- of Reactive Blue 4 solution was 6.5;
- of Reactive Red 120 solution was 6.8;
- of Reactive Violet 5 solution was 7.22.

At first pH was not modified. Then, to evaluate the effect of pH on decolorization rate, buffer solutions were used to keep the pH constant during the experiments.

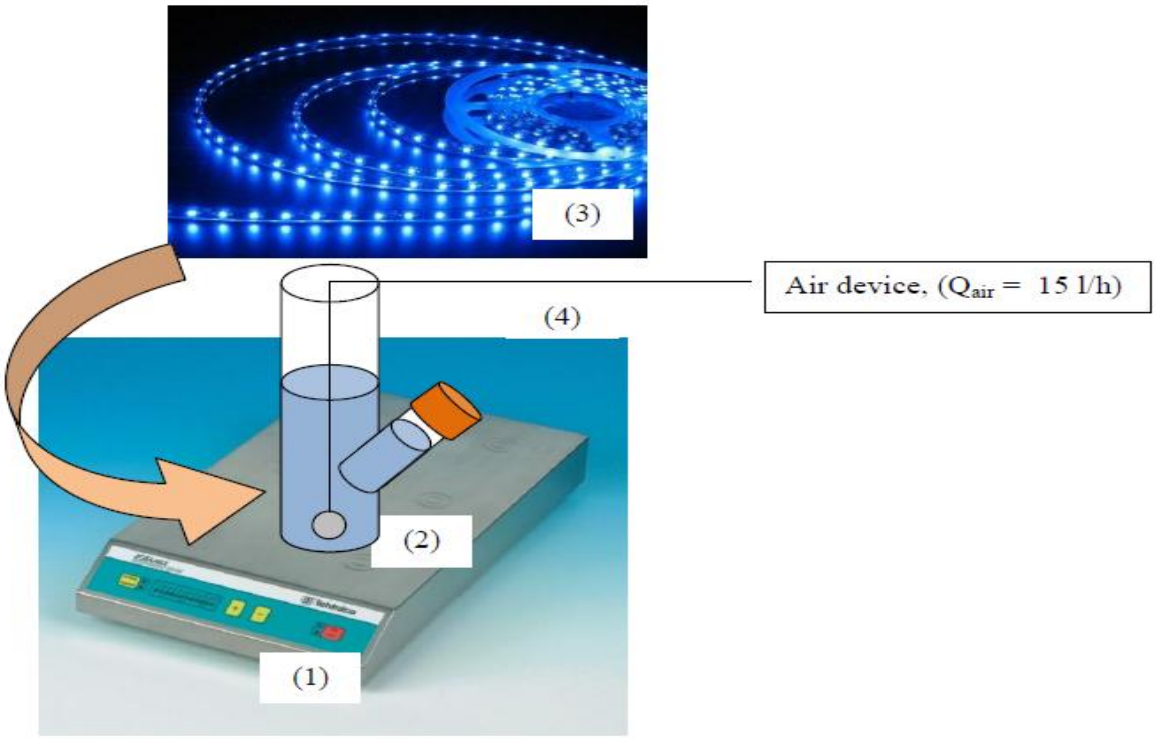

Figure 3.8 – Experimental apparatus for photocatalytic tests: (1) magnetic stirrer; (2) photoreactor; (3) blue LEDs strip; (4) air device.

3.5 Kinetic modelling: Initial Rates Method

The initial rates method (IRM) can be used to estimate the initial rate of a reaction. Initial rates, like all reaction rates, are defined as a change in concentration per unit time. If only two data points are available, the initial rate can be calculated using the formula below:

$$initial\ rate = (C_2 - C_1)/(t_2 - t_1) \quad (3.5)$$

C_2 and C_1 represent the concentrations (of a dye solution) corresponding to the times t_1 and t_2, respectively.

When more data points are available, the initial rate can be determined more accurately from a graph of concentration vs. time:

$$slope = \Delta(concentration)/\Delta(time) \quad (3.6)$$

Since rate is defined as change in concentration per unit time, the initial rate can be defined as the absolute value of the slope of the earliest, reasonably-linear section of a concentration vs. time plot.

3.6 Results and discussion

3.6.1 Photolysis of Reactive Blue 4

50 mL of a 100 ppm Reactive Blue 4 dye solution were irradiated with the blue LEDs strip in the absence of catalyst for 3 hours. In Figure 3.9, the dye removal efficiency as a function of the irradiation time is showed.

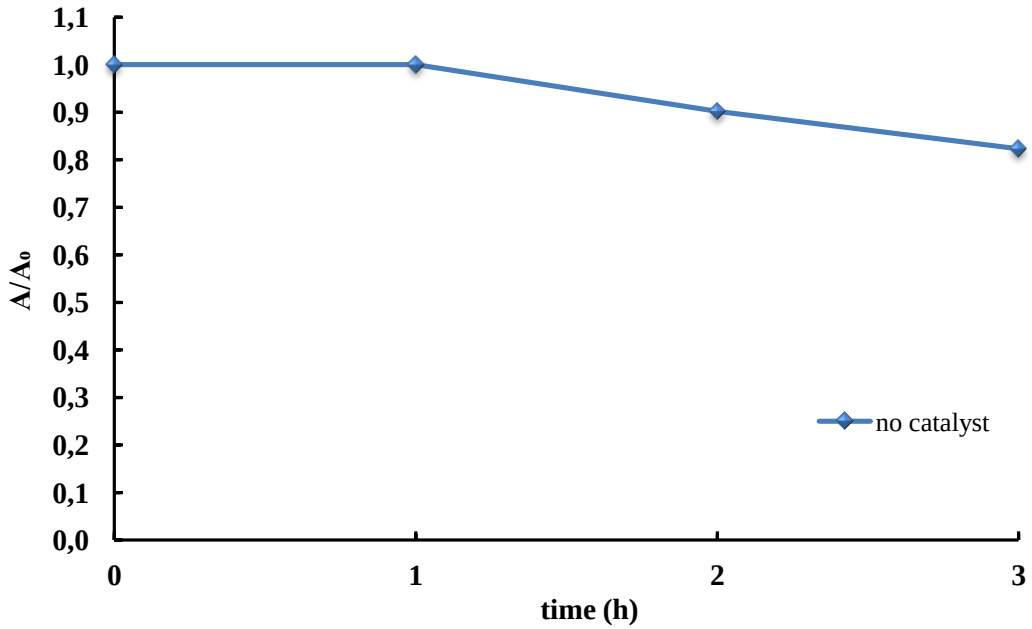

Figure 3.9 – Effect of blue LEDs on the Reactive Blue 4 decolorization, expressed as absorbance change at 595 nm (C_{RB4} = 100 ppm).

During the first hour of irradiation, no colour removal was observed. Since the second hour of exposure to light LEDs, the A/A_0 ratio decreased linearly as a function of time. It was observed that after 180 minutes of photolysis the degradation of dye was almost 17 % . Therefore, it was possible to decolorize a solution containing the Reactive Blue 4 dye by means of a photolytic process, but to increase the colour degradation yields, a photocatalytic process is required.

3.6.2 Photocatalyst selection

To find the catalyst suitable to increase the Reactive Blue 4 colour removal, the decolorization of a Reactive Blue 4 100 ppm solution was examined using different photocatalysts including TiO_2, N-doped TiO_2, Fe-TiO_2 (10 mg Fe), Fe-TiO_2 (50 mg Fe) and Fe-TiO_2 (100 mg Fe). 1 g/L of catalyst was used in each test. After adding the catalyst, the

solution was left in the dark for 60 minutes to promote the adsorption of the molecules of dye on the surface of the catalyst nanoparticles.

The decolorization efficiency, expressed as a function of the different catalysts and the irradiation time, is shown in Figure 3.10 and in Table 3.3, the colour removal values are reported.

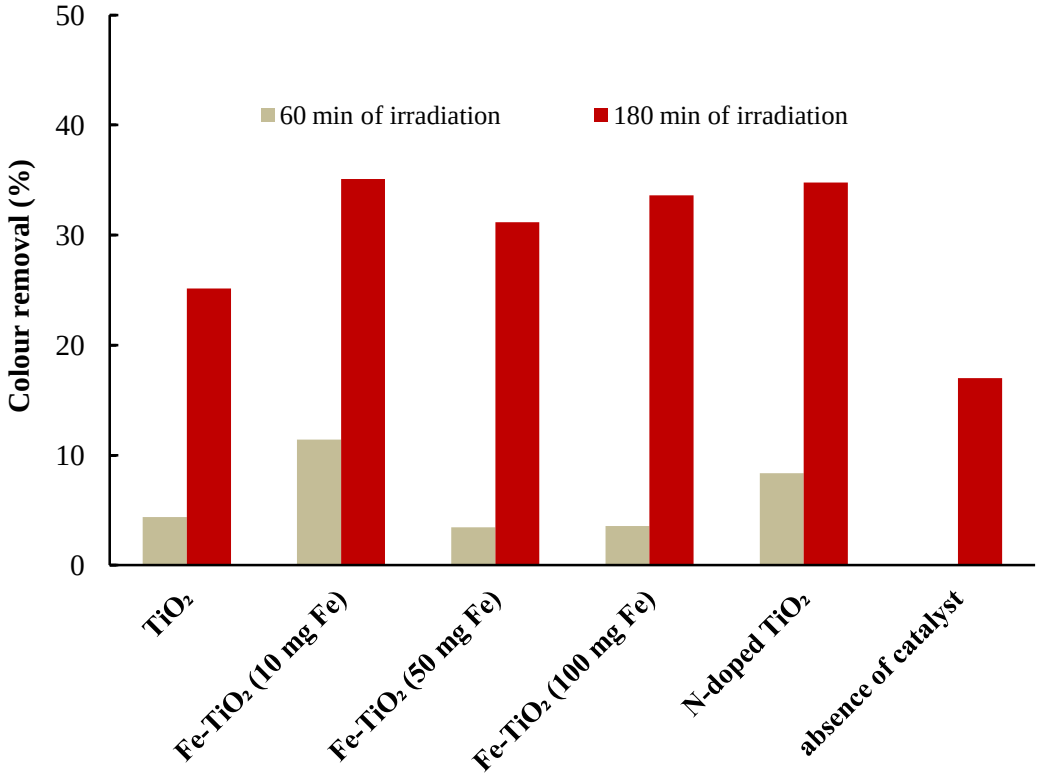

Figure 3.10 – Influence of BL and BL/catalyst on the Reactive Blue 4 decolorization, evaluated at 60 and 180 minutes of irradiation (C_{RB4} = 100 ppm; $C_{catalyst}$: 1 g/L).

Table 3.4 – Reactive Blue 4 decolorization percentages evaluated at 60 and 180 minutes of irradiation by BL, in absence and in presence of catalyst (C_{RB4} = 100 ppm; $C_{catalyst}$ = 1 g/L).

systems	**Colour removal (%)**	
blue LEDs +	**60 min of irradiation**	**180 min of irradiation**
TiO_2	4.37	25.16
Fe-TiO_2 (10 mg Fe)	11.41	35.10
Fe-TiO_2 (50 mg Fe)	3.45	31.16
Fe-TiO_2 (100 mg Fe)	3.57	33.62
N-doped TiO_2	8.35	34.78
absence of catalyst	0	17

Figure 3.10 evidences that the colour removal increased as a function of time, in the absence and in the presence of catalysts. This could mean that the light source contributed to the Reactive Blue 4 decolorization. Figure 3.10 also shows that the colour removal increased when doped catalysts were used. In fact, the purpose of the doping is enhancing the photoefficiency of the catalyst.

Figure 3.10 and Table 3.3 show that the complete colour removal was never achieved. It was also observed that, for TiO_2/LEDs system, the colour removal yields were about 4% and 25% after 60 and 180 minutes of irradiation, respectively. These results are very different from those found by Samsudin et al. (2015) [169]. They treated a Reactive Blue 4 100 ppm dye solution using 1 g/L of pure anatase nano-TiO_2 as catalyst and a 125 W UV light source. They found that the complete dye decolourization was achieved in 60 minutes. Using the TiO_2/LEDs system the colour removal was only 4% after one hour. These different results could be due to the different light sources used in the two cases.

Table 3.4 and Figure 3.10 also evidences that the highest colour removal percentage was about 35% and it was achieved in 180 minutes. This result was achieved in the presence of Fe-TiO_2 (10 mg Fe)/LEDs and N-doped TiO_2/LEDs systems, respectively. At 60 minutes the colour removal percentage was slightly higher for the Fe-TiO_2 (10 mg Fe)/LEDs system than the N-doped TiO_2/LEDs one (11.41% and 8.35% respectively). For these reasons, Fe-TiO_2 (10 mg Fe) could be the most suitable catalyst to treat the Reactive Blue 4 dye, therefore it was selected to carry out this study.

3.6.3 Effect of pH on Reactive Blue 4 decolorization

The effect of pH, on the Reactive Blue 4 photocatalysis with Fe-TiO_2 (10 mg Fe), was evaluated.

At first, the pH was adjusted to the desired value by addition of small amounts of NaOH and H_2SO_4. However, as pH did not remain unchanged during the experiments, buffer solutions at pH 4, 6, 8, 10, and 12 were used.

In Figure 3.11 the colour removal efficiency (evaluated after 3 hours of exposure to the blue LEDs) is shown as a function of pH.

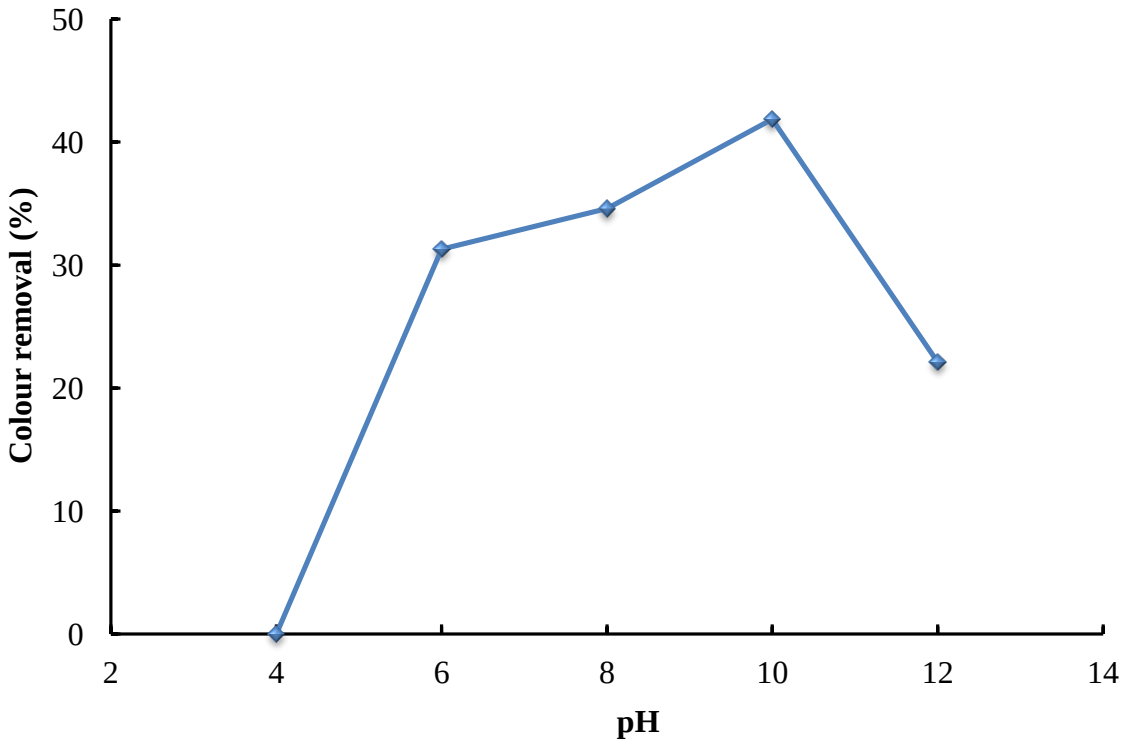

Figure 3.11 – Effect of pH on the Reactive Blue 4 colour removal evaluated at 180 minutes of irradiation (C_{RB4} = 100 ppm; Fe-TiO_2 (10 mg Fe) = 1 g/L; light source = BL).

Figure 3.11 shows that as the pH was increased from 4 to 10, the colour removal also increased, whereas when the pH was increased from 10 to 12, the colour removal efficiency decreased. At pH 10 the colour removal percentage was the highest.

In Table 3.5 the colour removal percentages, achieved in 180 minutes of irradiation, are reported as a function of pH.

Table 3.5 – Reactive Blue 4 decolorization percentages, evaluated at 180 minutes of irradiation, as a function of pH (C_{RB4} = 100 ppm; Fe-TiO_2(10 mg Fe) = 1 g/L; light source = BL).

pH	Colour removal (%) after 180 min of irradiation
4	0
6	31.3
8	34.6
10	41.8
12	22.1
unmodified	35.1

Table 3.5 shows that in each case the colour removal percentage was lower than 35.1 %, and only at pH 10 it was higher (about 42 %).

Zhou et al. (2008) [214] observed a trend similar to the one shown in Figure 3.11 using the Reactive Blue 4 dye (Figure 3.12). They used Nd- doped ZnO as catalyst and an UV lamp as light source and examined the effect of pH in the range 3-13.

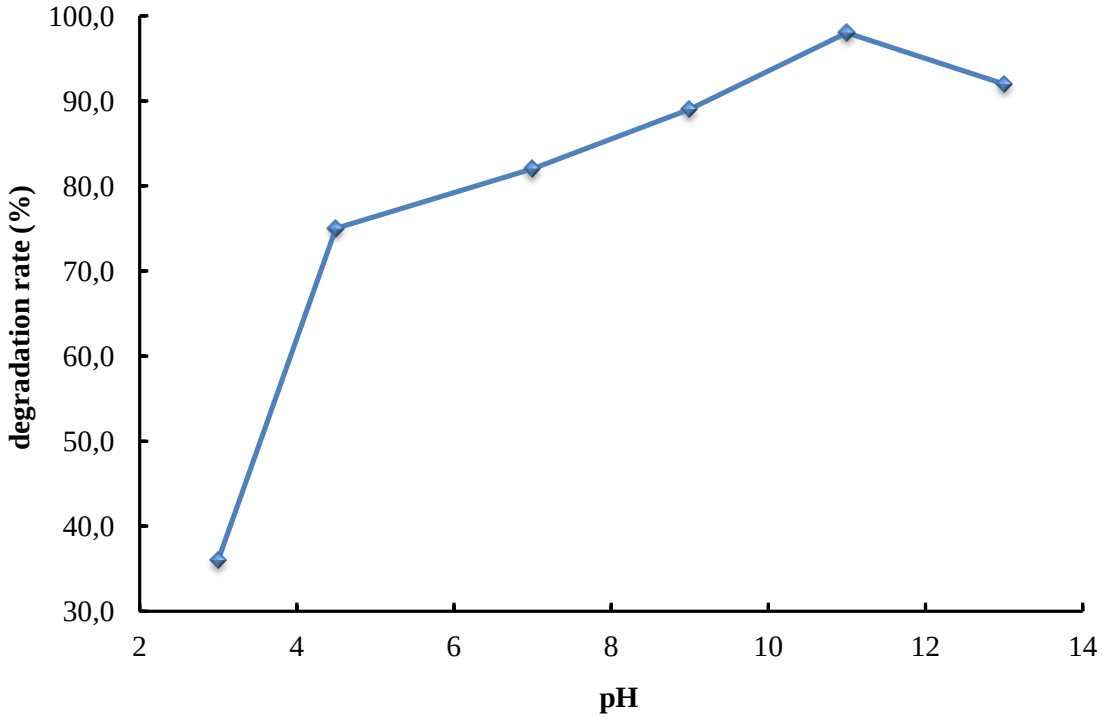

Figure 3.12 - Reactive Blue 4 degradation rate under different solution pHs (C_{RB4} = 20 ppm, V_s = 100 mL; $C_{catalyst}$ = 0.1 g/L) [214].

Figure 3.12 shows that the rate of degradation increases rapidly as the solution pH increases up to 5 and increases gradually above the solution pH of 7, and reaches a maximum value approximately at pH 11. The photocatalytic degradation of Reactive Blue 4 is strongly favoured in alkaline pH. According to Zhou et al. (2008) [214] the zero point charge of ZnO is about 9 and, above this value, the surface is negatively charged due to adsorbed OH^- ions. The presence of large quantities of adsorbed OH^- ions on the particle surface favours the formation of ·OH radicals, which are the primary oxidizing species responsible for degradation. The decrease in the rate of degradation, above pH 11, is due to a decrease in the adsorption Reactive Blue 4 molecules. In fact, the catalyst surface may adsorb OH^- ions and thus it becomes negatively charged. Since Reactive Blue 4 is not protonated at high pH values, there is an electrostatic repulsion between the catalyst nanoparticles and the dye molecules; consequently, the degradation rate decreases. The decrease in the photocatalytic

degradation in the acidic medium is due to a high adsorption of Reactive Blue 4 molecules that fully cover the catalyst surface, reducing absorption of light, which is very important for the photocatalytic process.

A similar trend was also found by Sakhtivel et al. (2003) [215] who investigated the effect of the pH on the Acid Brown 14 photocatalysis. They used ZnO as catalyst and solar light as energy source. They examined the effect of pH in the range 3-11, using a dye concentration of 311 g/L and a catalyst amount of 2.5 g/L. Their results are shown in Figure 3.13.

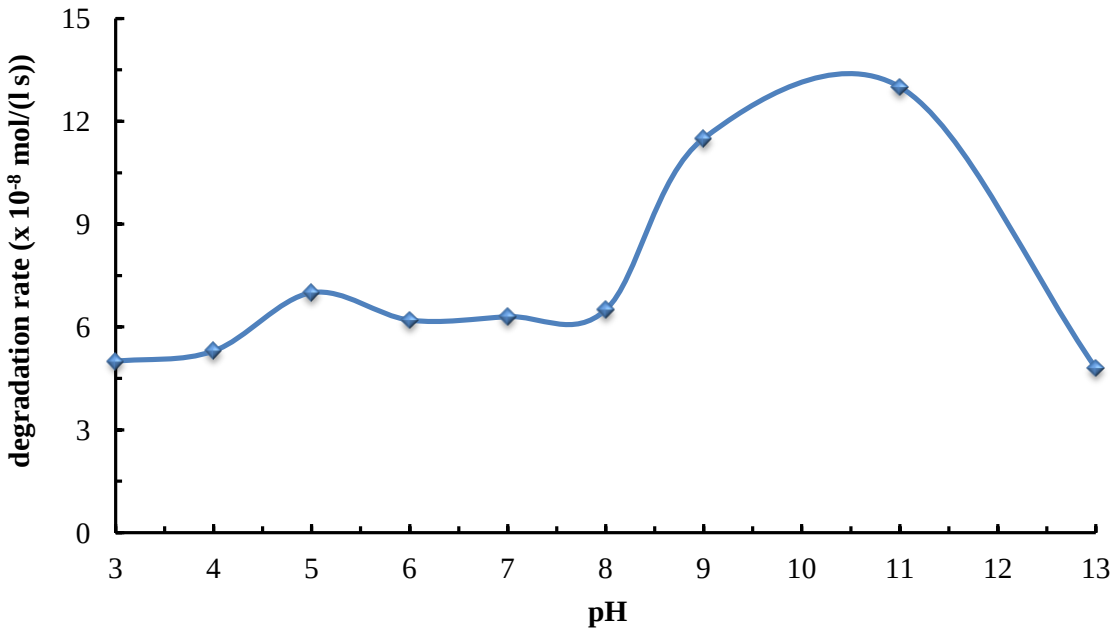

Figure 3.13 - Influence of pH on the rate of degradation of Acid Brown 14 (C_{AB14} = 311 g/L; $C_{catalyst}$ = 2.5 g/L [215]).

They observed that the rate of degradation of the Acid Brown 14 increased with increase in pH, and found the maximum rate of degradation at pH 10. They explained that at low pH range, electrostatic interactions between the positive catalyst surface and dye anions lead to strong adsorption of the dye on the metal oxide support. They also observed that the photocatalytic degradation efficiency of ZnO was higher at alkaline pH range even though the adsorption of the dye molecules is low at alkaline pH. In their opinion, alkaline pH range enhances the formation of more ·OH due to the presence of a large amount of OH^- ions in the alkaline medium, which significantly increases the photocatalytic degradation of dye.

Figure 3.11 shows that the Reactive Blue 4 decolorization increases rapidly as the solution pH increases up to 6 and more gradually above the solution pH of 6. The maximum value is achieved at pH 10. Therefore, the photocatalytic degradation of Reactive Blue 4 is strongly favored in alkaline pH, as it was already reported by Zhou et al. (2008) [214]. The high

colour removal at pH 10 can be explained on the base of the zero point charge of the Fe-TiO_2 catalyst. The zero point charge of Fe-TiO_2 species is comprised between 7.4 and 8.1 (Di Paola et al. (2001)) [216] and, above this value, the surface of the catalyst nanoparticles is negatively charged due to adsorbed OH^- ions. The presence of large quantities of adsorbed OH^- ions on the particles surface favours the formation of ·OH radicals, (OH^- ions react with free electron-hole pairs and produce hydroxyl radicals) which are responsible for dye decolorization.

On the other hand, a decrease in the colour removal at pH 12 is observed as is shown in Figure 3.11. This is due to a decrease in the adsorption of the Reactive Blue 4 molecules on the catalyst surface. At pH 12, the catalyst surface can absorb a lot of OH^- ions and thus it becomes negatively charged. Because the Reactive Blue 4 is not protonated at pH 12, there is a strong electrostatic repulsion between the surface charges on the adsorbent and the adsorbate, that hinders the adsorption of the dye molecules; so the colour removal percentage decreases at pH 12.

Moreover, according to Rys & Zollinger (1992) [217] and Neppolian et al. (1998) [171], in the chemical structure of the Reactive Blue 4 dye, substituents of an electron-donating group such as $–NH_2$ (in the α-positions of the carbonyl group) are able to form intramolecular hydrogen bonds at high pH values: this makes the dye structure chemically stable at high pH ranges. The chromophores of the dye remain intact after light irradiation and hence, the degradation of the dye is reduced (Tusi and Chu, 2001) [218].

At pH 8, the solution pH is near the zero point charge of the catalyst. The catalyst surface is not electrically charged and the molecules of dye cannot be adsorbed on it. Dye molecules are probably oxidised only by hydroxyl radicals, and the direct oxidation by positive holes (h_{VB}^+) and direct reduction by conduction band electrons (e_{CB}^-), proposed by Gotzman (2009) [219] as mechanisms for dyes degradation, don't occur.

At pH 6, the surface of the catalyst nanoparticles is positively charged because the solution pH is below the zero point charge of the catalyst. As the catalyst surface is almost fully covered by Reactive Blue 4 molecules, the absorption of visible radiation on the catalyst surface decreases, and the colour removal efficiency also decreases.

In Figure 3.14 the spectra of the treated solution at pH 4 as a function of the running time are reported.

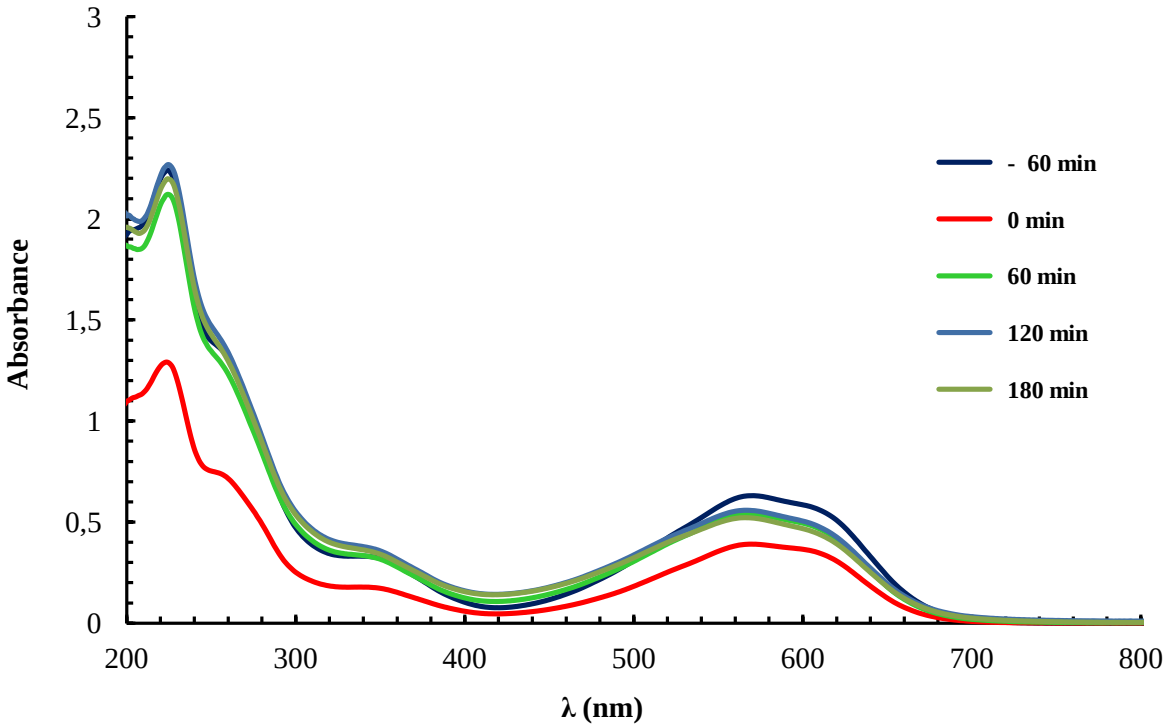

Figure 3.14 – Absorption spectra of Reactive Blue 4 expressed as a function of the time (C_{RB4} = 100 ppm; Fe-TiO_2(10 mg Fe) = 1 g/L; pH = 4; light source = BL).

Figure 3.14 shows that, when the solution was left in the dark (to improve the adsorption of the molecules of dye on the surface of the nanoparticles), the absorbance decreases (curve "0 min") because a strong adsorption occurs. Then, after LEDs irradiation, a part of the molecules of dye desorbs from the surface of the catalyst and returns in solution (curve "60 min"). The photocatalytic reaction didn't occur, in fact the curves " 60 min", "120 min" and "180 min" are overlying. This suggests that in acidic solution (pH 4) the photocatalyst is probably deactivated by the too low pH.

This result is in agreement with the one obtained by Rupa et al. 2007 [158] that studied the effect of the pH on the photocatalysis of Reactive Yellow 17 using Ag-deposited TiO_2 nanoparticles. They observed that at low pH there was a decrease in the photodegradation of Reactive Yellow 17 and concluded that it could be due to the dissolution of TiO_2 at highly acidic conditions.

Similar results were also reported in the photocatalysed degradation of azo dyes [220–222].

At pH 10 the highest colour removal was obtained, therefore this pH value was selected to carry out the following experiments.

3.6.4 Comparison of photocatalytic efficiency of Fe-TiO_2 (10 mg Fe) and TiO_2

The photocatalytic activity of Fe-TiO_2 (10 mg Fe) powder was investigated and compared with that of TiO_2. Laboratory experiments were carried out using 50 mL of a 100 ppm Reactive Blue 4 solution at pH 10. Blue LEDs were used as light sources. The reaction time was 10 hours, included the first hour of adsorption in the dark. At the end of the 10 hours the reaction was expired. The trend of the absorbance peak at 595 nm, expressed as a function of the irradiation time, is shown in Figure 3.15.

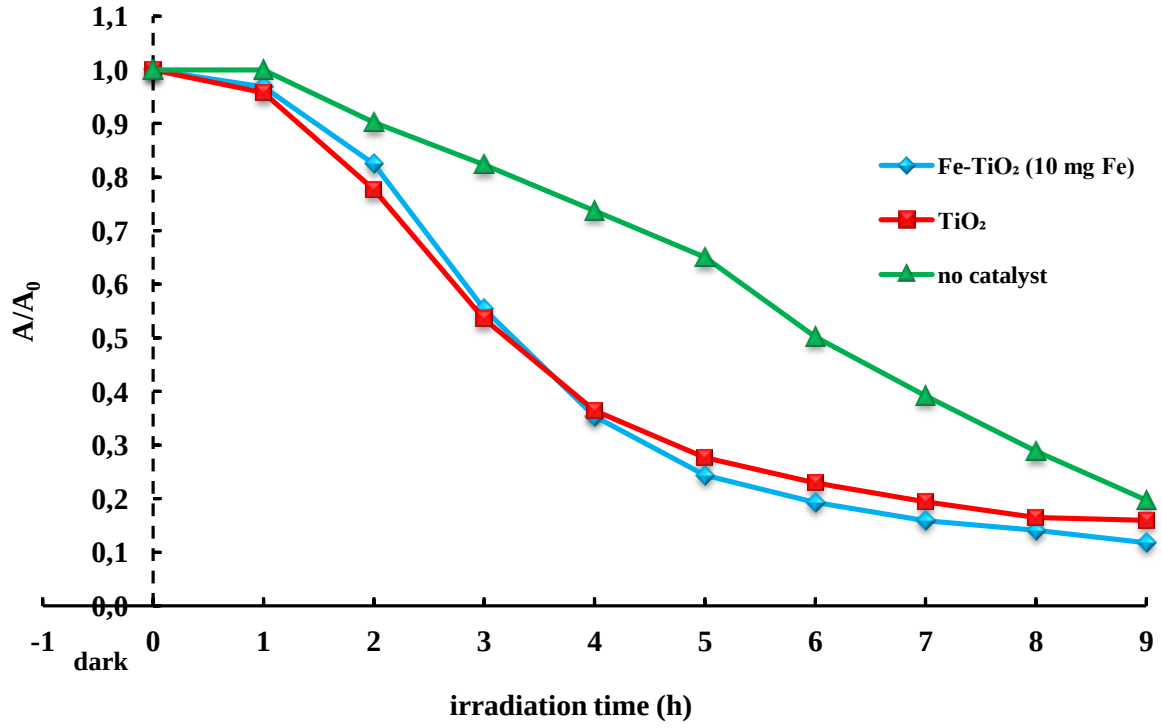

Figure 3.15 – Effect of BL and BL/catalyst on the Reactive Blue 4 decolorization, as a function of the irradiation time (C_{RB4} = 100 ppm; $C_{catalyst}$ = 1 g/L; light source = BL).

Figure 3.15 shows that, after 9 hours, the decrease in absorbance, in the presence of TiO_2 or Fe-TiO_2, and in the absence of catalysts, was the same.

Moreover, the trends of the curves describing the TiO_2/LEDs and Fe-TiO_2 (10 mg Fe)/LEDs systems were identical, whereas the trend of the curve describing the system in the absence of catalyst was linear.

In Table 3.6 the colour removal percentages evaluated at 9 hours of irradiation for each system are reported.

Table 3.6 – Reactive Blue 4 decolorization percentages achieved at 9 hours of irradiation (C_{RB4} = 100 ppm; $C_{catalyst}$ = 1 g/L; pH = 10; light source = BL).

blue LED +	Colour removal (%) after 9 hours of irradiation
Fe-TiO_2 (10 mg Fe)	89
TiO_2	84
no catalyst	81

The results shown in Table 3.6 suggest that Reactive Blue 4 dye is highly unstable under exposure to blue LEDs irradiation and the presence of photocatalysts is not necessary for the degradation of this dye.

To confirm these results, the behaviour of a 300 ppm Reactive Blue 4 solution, at pH 10, was explored under exposure to blue LEDs both in the absence of catalyst and in the presence of 3 g/L of Fe-TiO_2 (10 mg Fe). The reaction time was 6 hours, including the first hour of adsorption in the dark. The results are shown in Figure 3.16.

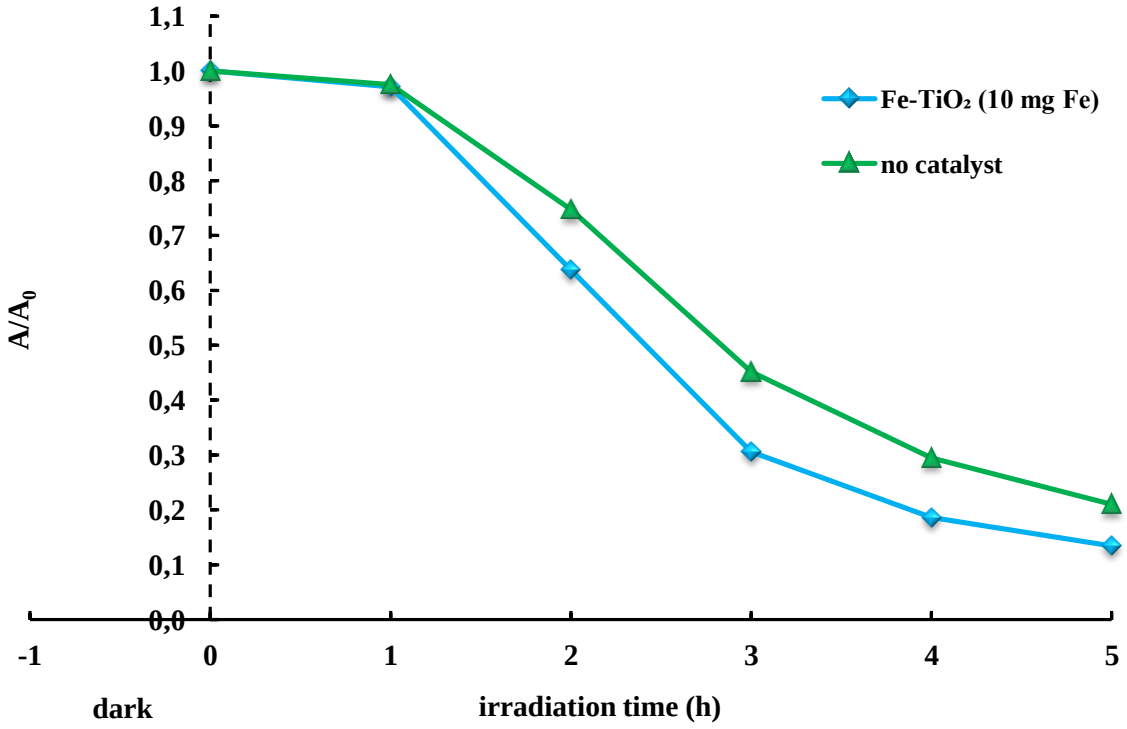

Figure 3.16 – Effect of BL and BL/catalyst on the Reactive Blue 4 decolorization, as a function of the irradiation time (C_{RB4} = 300 ppm; Fe-TiO_2(10 mg Fe) = 3 g/L; pH = 10; light source = BL).

Figure 3.16 shows that the trends of the curves describing the absorbance decrease, are similar, and that the solution could be almost totally decoloured in 5 hours of irradiation.

In Table. 3.7 the colour removal percentages, evaluated after 5 hours of exposure to LEDs, are shown.

Table 3.7 – Reactive Blue 4 removal percentages calculated after 5 hours of irradiation. (C_{RB4} = 300 ppm; pH = 10, Fe-TiO_2(10 mg Fe) = 3 g/L; light source = BL).

LEDs light +	Colour removal (%) after 5 hours of irradiation
Fe-TiO_2 (10 mg Fe)	87
no catalyst	79

Table 3.7 shows that the colour removal percentages are almost the same for both systems. This could mean that the Reactive Blue 4 dye was not stable under irradiation with blue light LEDs. However, as Jo et al. (2014) [242] reported, *some dyes are degraded by exposure to light in the absence of any catalyst*. Moreover, there could also be a strong relationship between the light LEDs and the dye, that are both blue. The dye could absorb all the light emitted by the LEDs, therefore the light photons cannot excite the catalyst nanoparticles, and cannot start the separation of the electron-hole pairs and all the other reactions.

Since this study concerns the treatment of reactive dyes by photocatalysis, another dye was chosen to carry out the experiments, although, for this dye, further investigations would be necessary.

3.7 Reactive Red 120

3.7.1 Photodecolorizaton of Reactive Red 120: preliminary experiments

The other reactive dye used to carry out the experiments, was the Reactive Red 120. 50 mL of a 100 ppm Reactive Red 120 solution at pH 10 were used in each test.

Dye solution was treated by irradiation with blue LEDs, in the following conditions:

- in the absence of catalyst;
- in the presence 1 g/L of Fe-TiO_2 (10 mg Fe);
- and in the presence of TiO_2 nanoparticles (1 g/L).

The reaction was stopped after 2 hours of exposure to blue LEDs irradiation for the photocatalytic systems, and it was stopped at 5 hours for the system without catalysts. The results are shown in Figure 3.17.

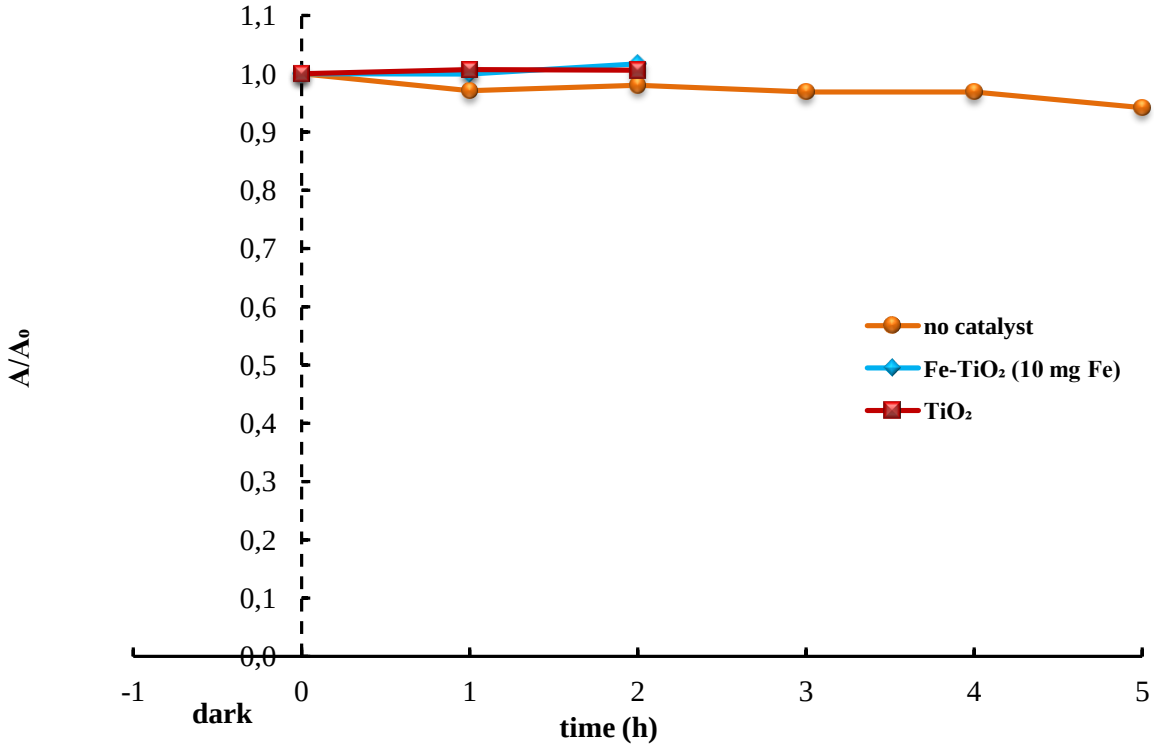

Figure 3.17 – Effect of photolysis and photocatalysis on Reactive Red 120 decolorization. (C_{RR120} = 100 ppm; pH = 10; Fe-TiO_2(10 mg Fe) = 1 g/L; TiO_2 = 1 g/L; light source = BL).

Results show that:

- in the absence of catalyst the LEDs light is not able to decolorize the dye, the absorbance remains the same even after 5 hours of irradiation;
- the dye cannot be decolorized even in the presence of catalysts and, as result, after 2 hours of irradiation, the absorbance remains unchanged.

In the same conditions, the Reactive Blue 4 dye decolorization was 20% in the presence of catalyst, and 10% without catalyst, as shown in Figure 3.18.

The decolorization of Reactive Red 120 was studied also by Kavitha and Palanisamy (2011) [162]. They treated 100 ppm of Reactive Red 120 solution at pH 4.1 using 2.5 g/L of TiO_2 and a 50 W halogen lamp as source of visible light. They found no degradation in the presence of visible light only, but in the presence of both catalyst and visible light, a high dye degradation was observed. Their results are different from those reported in Figure 3.17.

One possible explanation could be the different type of light source (LEDs strip vs. halogen lamp), the different power of the light sources (24 W vs. 50 W), the pH of the treated solution (10 vs. 4) and the catalyst concentration (1 g/L vs. 2.5 g/L). However, because the results in Figure 3.17 show that the Reactive Red 120 dye cannot be treated merely by direct irradiation and cannot be decolorized even in the presence of photocatalysts, a different dye was chosen to carry out this study.

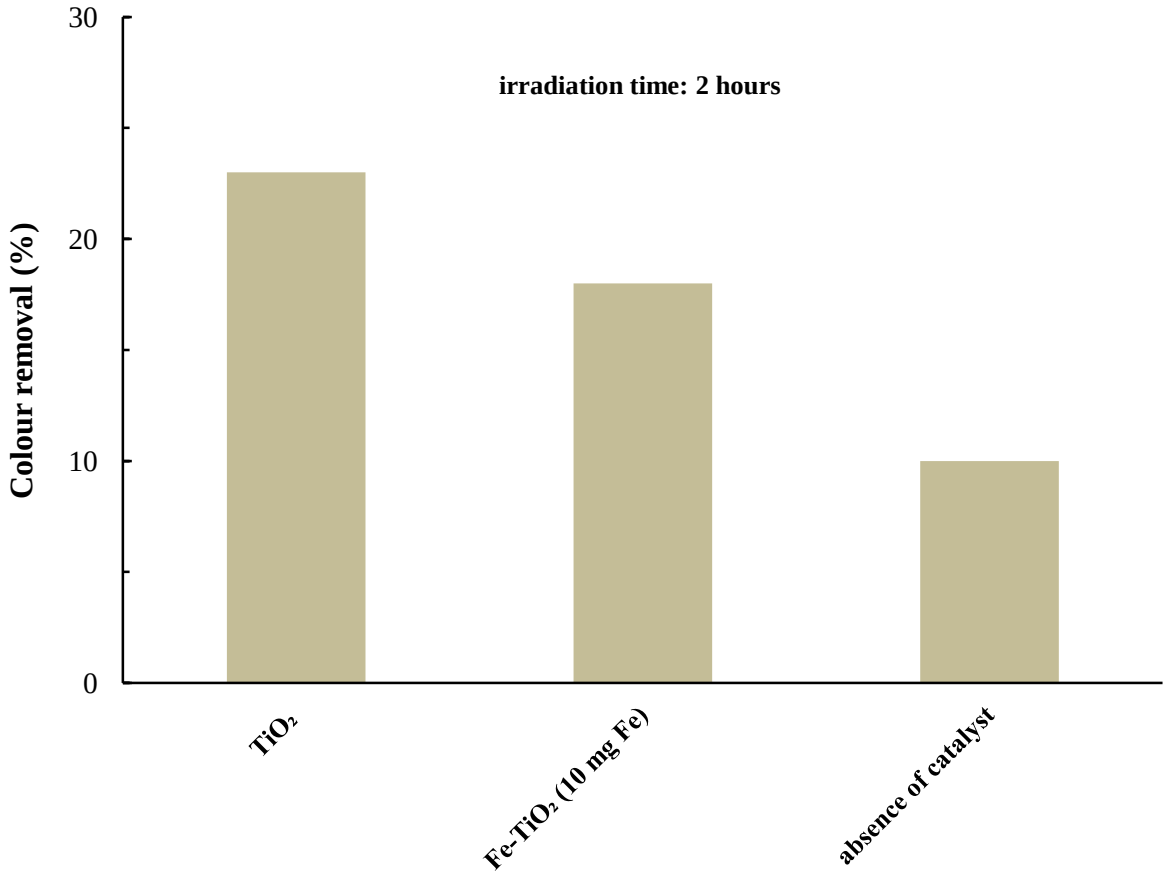

Figure 3.18 – Effect of BL and BL/catalyst on the Reactive Blue 4 decolorization (C_{RB4} = 100 ppm; pH = 10; $C_{catalyst}$ = 1 g/L).

3.8 Reactive Violet 5

3.8.1 Photodecolorization of Reactive Violet 5: preliminary tests

To evaluate the photodegradability of Reactive Violet 5, preliminary experiments were conducted. 50 mL of a 100 ppm Reactive Violet 5 solution, at pH 10, were treated trough photolysis and photocatalysis.

For the photocatalytic decolorization tests, 3 g/L of Fe-TiO_2 (10 mg Fe) were used. The experiments were stopped after 2 hours of irradiation.

The results are shown in Figure 3.19.

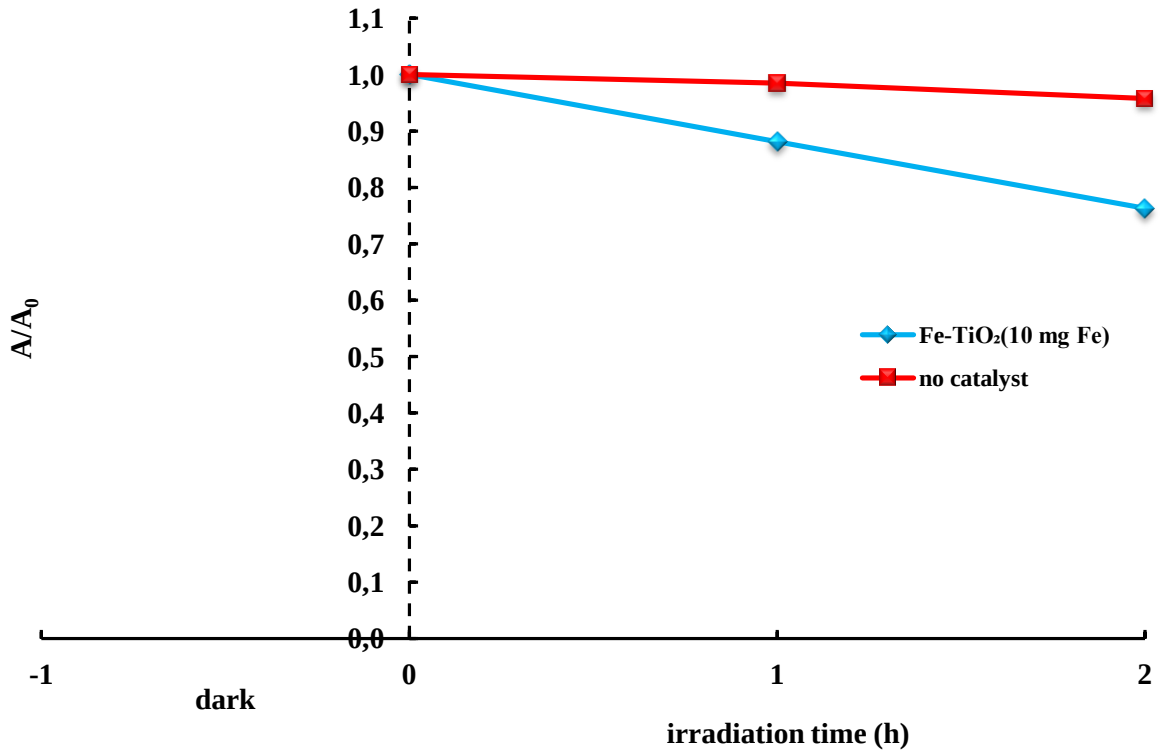

Figure 3.19 – Effect of BL and BL/catalyst on Reactive Violet 5 decolorization (C_{RV5} = 100 ppm; pH = 10; $C_{catalyst}$ = 3 g/L).

The experimental data presented in Figure 3.19 indicate that blue LEDs alone had not appreciable effects on the removal of Reactive Violet 5. In contrast, significant dye decolorization was observed when blue LEDs and catalyst were used simultaneously.
Moreover it can be seen that:

- in the absence of catalyst, the absorbance peak (at 559 nm) decreases very slowly as a function of irradiation time, and only about 5% of dye decolorization was obtained after 2 hours of exposure to LEDs light;
- in the presence of catalyst and LEDs light, the absorbance peak decreases linearly as a function of irradiation time. About 24% of decolorization was achieved after 2 hours of irradiation.

For the Reactive Violet 5 solution the difference between the color removal yields in the presence and in the absence of the catalyst, is about 20%.

In the same conditions, for the Reactive Blue 4 dye, the difference between the color removal yields in the presence and in the absence of the catalyst, was only 8%.

These findings suggest that Reactive Violet 5 cannot be treated merely by direct irradiation, as it occurred for Reactive Blue 4, and that it requires a suitable catalyst. The UV/vis spectra, reported in Figure 3.20, clearly show the decrease in concentration of the Reactive Violet 5 solution.

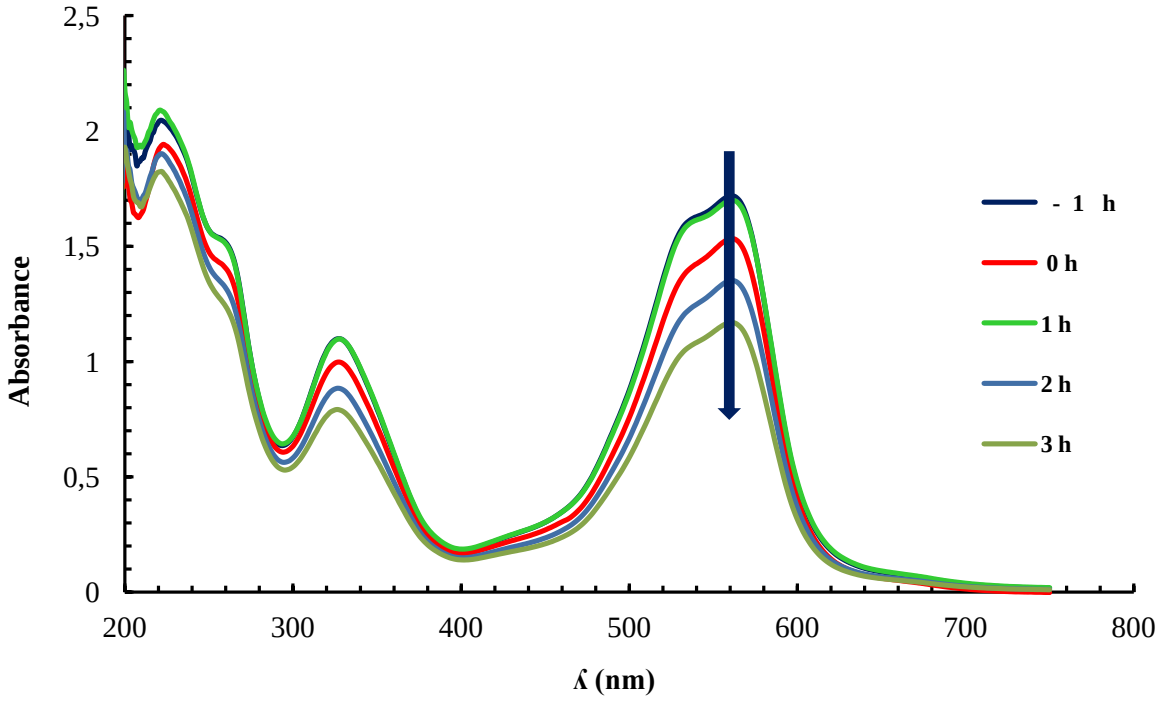

Figure 3.20 – Absorption spectra of Reactive Violet 5 (C_{RV5} = 100 ppm; pH = 10; Fe-TiO_2(10 mg Fe) = 3 g/L; light source = BL).

The spectra in Figure 3.20 show that there was no formation of by-products during the photocatalytic treatment. The decolorization of the Reactive Violet 5 may be due to the initial electrophilic cleavage of its chromophoric azo (-N=N-) bond. The azo bonds are more reactive in azo dyes and can be oxidized by the positive holes or the hydroxyl radicals; they can also be reduced by the electrons in the conduction band of the catalyst (Ganesh el at., 1994) [223].

3.8.2 Catalyst to dye concentration ratio of 10

The photodegradability of Reactive Violet 5 was also studied using a dye of initial concentration of 100 ppm, in the presence of blue LEDs irradiation and:

- in the absence of catalyst;
- in the presence of TiO_2 photocatalyst (1 g/L);
- in the presence of Fe-TiO_2(10 mg Fe) photocatalyst (1 g/L).

In each test the temperature was maintained at ambient conditions and the pH was left unmodified. The UV/vis spectra were monitored for ten hours (including the hour of adsorption in the dark), to observe the trends of absorbances as a function of time. The trend of the characteristic Reactive Violet 5 peak (at 559 nm), expressed as a function of irradiation time, is shown in Figure 3.21.

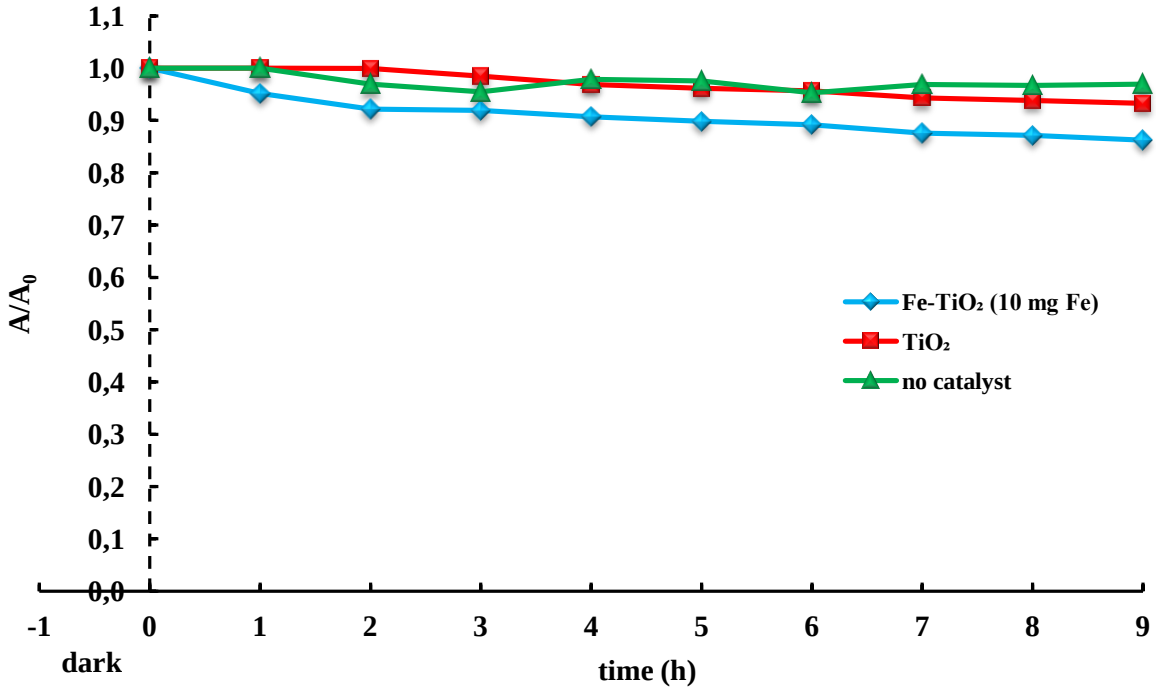

Figure 3.21 – Effect of BL and BL/catalyst on the Reactive Violet 5 decolorization (C_{RV5} = 100 ppm; Ccatalyst = 1 g/L; light source = BL).

Figure 3.21 shows that:

- under blue LEDs irradiation and in the absence of catalysts, the Reactive Violet 5 solution cannot be decolorized, even after 9 hours;
- in the presence of TiO_2 and under blue LEDs irradiation, the Reactive Violet 5 solution can be decolorized, but the reaction is slow;
- in the presence of Fe-TiO_2 and blue LEDs irradiation, the decolorization occurs at a faster rate.

In Table 3.8 the colour removal yields, evaluated after 9 hours of exposure to blue LEDs irradiation, are shown for each system.

Table 3.8 – Reactive Violet 5 decolorization values, evaluated at 9 hours of irradiation, in the absence and in the presence of catalysts. (C_{RV5} = 100 ppm; $C_{catalysts}$ = 1 g/L; light source = BL).

blue LEDs +	Colour removal (%) (irradiation time 9 hours)
TiO_2	7
Fe-TiO_2 (10 mg Fe)	14
no catalyst	0

The results reported in Table 3.8 confirm that the decolorization of Reactive Violet 5 is due to the photocatalytic reactions that can successfully decolorize and degrade this dye. However, after 9 hours of irradiation the color removal was (7% and 14% with TiO_2 and Fe-TiO_2 (10 mg Fe), respectively), even changing catalyst. Therefore another "catalyst concentration/dye concentration" ratio was chosen to carry out this study.

3.8.3 Catalyst to dye concentration ratio of 100

Experiments were carried out using a Reactive Violet 5 dye concentration of 30 ppm and a catalyst concentration of 3 g/L. 50 mL of dye solution were used in each test.

3.8.3.1 Photocatalyst selection

To find out the catalyst for highest photocatalytic decolorization, different types of catalyst including TiO_2, N-doped TiO_2, Fe-TiO_2(10 mg Fe), Fe-TiO_2 (50 mg Fe), Fe-TiO_2 (100 mg Fe), an Degussa P-25 were employed.

The concentration of Reactive Violet 5 (30 ppm) and the catalyst concentration (3 g/L) were maintained constant in all experiments. The pH was unmodified. The reaction time was fixed at 10 hours, including the adsorption time in the dark.

In Figure 3.22 the results of the experiments are shown.

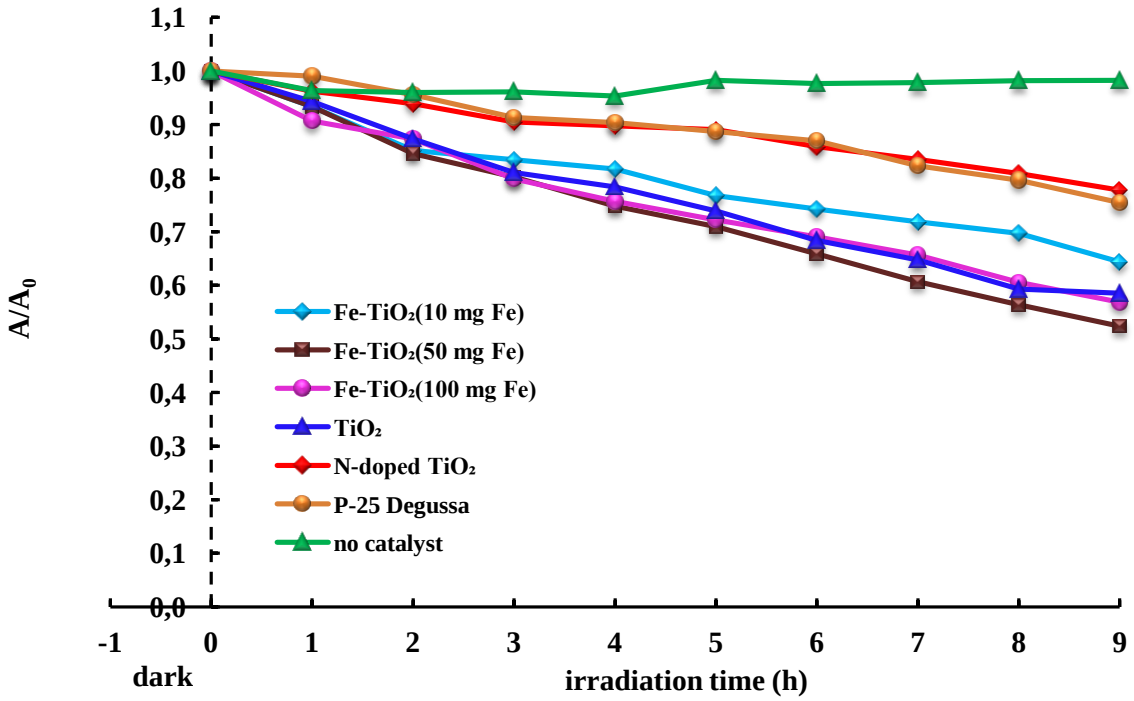

Figure 3.22 - Reactive Violet 5) photolysis and photocatalytic degradation in the presence of different catalysts (C_{RV5} = 30 ppm; $C_{catalyst}$ = 3 g/L; light source = BL).

Figure 3.22 shows that in the presence of 3 g/L of catalyst the 30 ppm Reactive Violet 5 dye solution can be decolorized and that the absorbance decreases as a function of irradiation time almost linearly.

In Table 3.9 the colour removal yields evaluated after 9 hours of blue LEDs irradiation, in the absence and in the presence of catalysts, are reported.

Table 3.9 – Reactive Violet 5 decolorization, evaluated after 9 hours of irradiation, in the absence and in the presence of catalysts (C_{RV5} = 30 ppm; $C_{catalyst}$ = 3 g/L; light source = BL).

blue LEDs +	Colour removal (%) at 9 hours of irradiation
TiO_2	41
P-25 Degussa	25
N-doped TiO_2	22
Fe-TiO_2 (10 mg Fe)	36
Fe-TiO_2 (50 mg Fe)	48
Fe-TiO_2 (100 mg Fe)	43
no catalyst	2

Table 3.9 shows that:

- the photolysis alone is not able to decolorize the dye: the colour removal is only 2% after 9 hours;
- the photocatalytic decolorization efficiency is similar for the N-doped TiO_2 and P-25 Degussa/ blue LEDs systems (22% and 25%, respectively);
- the Fe-TiO_2 (50 mg Fe)/ blue LEDs system is the most efficient in decolorizing Reactive Violet 5 (dye removal 48%);
- the Fe-TiO_2 (100 mg Fe)/ blue LEDs also has high efficiency in Reactive Violet 5 decolorization (43%);
- for each system the colour removal is never higher than 50%.

These results can be motivated as follows. Although the band gap energy of the Fe-TiO_2 (100 mg Fe) is smaller than that of the Fe-TiO_2 (50 mg Fe) (2.63 and 2.90 eV, respectively), the first one seems to have a lower photocatalytic activity. This could be due to the high content of Fe(III) ions which can act as recombination centers for the photo-generated hole-electron pairs [224, 225].

Fe-TiO_2 (10 mg Fe) and TiO_2 have similar band gap energies (3.12 and 3.17 eV, respectively), this could explain the similar colour removal percentages obtained, though TiO_2 exhibits a slightly higher photocatalytic activity.

Commercial Degussa P-25 and N-doped TiO_2, although they have different band gap energies (3.17 and 2.5 eV, respectively), gave almost identical results. Probably, the nitrogen content of the N-doped TiO_2 was too high (N/Ti molar ratio was 18.6), thus the nitrogen ions enhanced the recombination of photogenerated electrons and holes and did not allow reactions to proceed with any noticeable effect under visible light [226]. Moreover, the colour removal yields obtained with N-doped TiO_2 were lower than that of undoped TiO_2; also in this case, the reason could depend on the doping sites which could also work as recombination centers for the photogenerated electron–hole pairs as it was reported by Irie et al. (2003) [227].

Generally, the addition of nitrogen results in an improvement in visible light photocatalytic activity as it was reported in literature [104, 154], but contrasting findings were also reported [116, 122]. For example, in a recent study, N-doped TiO_2 films were obtained by the addition of ammonia during chemical vapour deposition growth of TiO_2, and, despite the presence of N impurities at substitutional sites, none visible light-induced photocatalytic

activity was observed. According to the authors, the presence of N impurities at substitutional sites couldn't be cited as a means of inducing visible light activity in TiO_2 films [122]. Selvaraj et al. (2013) [228] studied the photocatalytic degradation of some reactive triazine dyes including Reactive Red 120 and Reactive Blue 160 on N-doped TiO_2 anatase and Degussa P-25 in the presence of natural sunlight. They reported that Degussa P-25 showed higher photocatalytic activity compared to the N-doped TiO_2 for the degradation of Reactive Red 120 and Reactive Blue 160, but the high photocatalytic activity found for the Degussa P-25 was not explained.

Figure 3.23 and Table 3.9 show that for the Reactive Violet 5 decolorization, Fe-TiO_2 (50 mg Fe) is the most suitable catalyst. It could be due to its ions content, that allows maintaining the hole-electron pairs effectively separated, enhancing the colour removal yields. These results are different from those obtained for the Reactive Blue 4 decolorization, suggesting that the nature of the dye, the solutions concentration, the concentration of doping agents and the catalyst loading could widely influence the photocatalytic processes.

The UV/vis spectra obtained for the Reactive Violet 5 photodecolorization in the presence of Fe-TiO_2 (50 mg Fe) are shown in Figure 3.23.

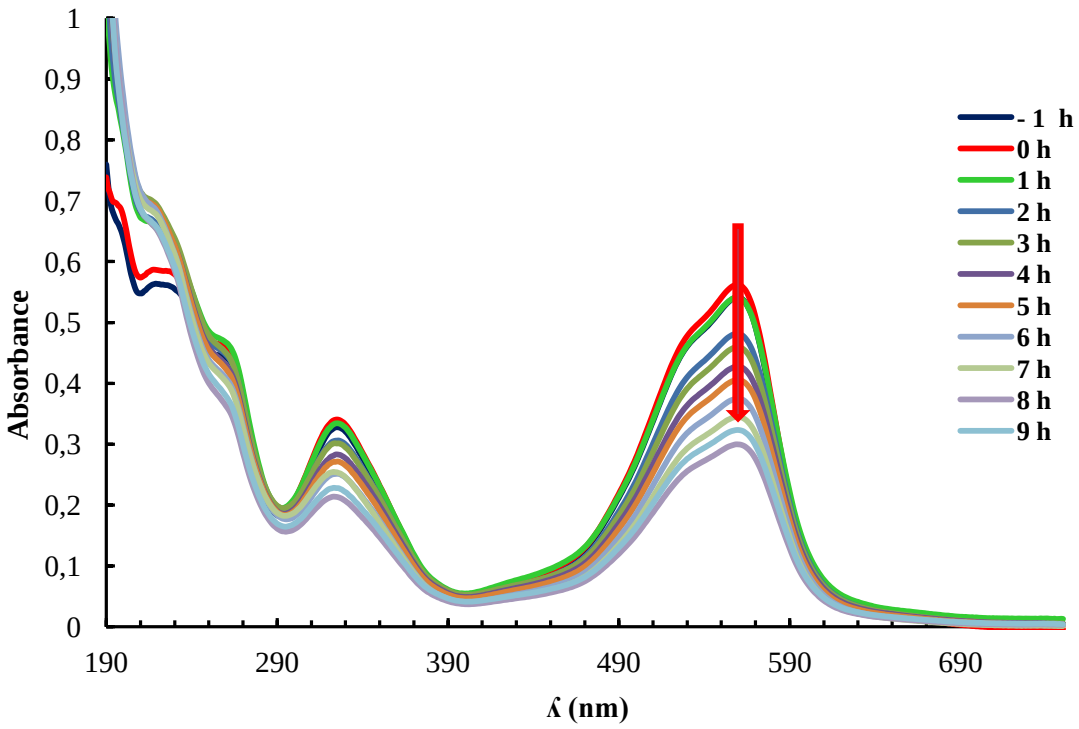

Figure 3.23 – Absorption spectra of Reactive Violet 5 solution (C_{RV5} = 30 ppm; Fe-TiO_2(50 mg Fe) = 3 g/L; light source = BL).

As it can be observed from the spectra obtained before the irradiation, Reactive Violet 5 exhibits two main bands, one in the UV region (λ_{max} 221 nm), and the other in the visible region (λ_{max} 559 nm). The 559 nm band is due to the azo bonds (–N=N–), which are responsible for the violet color, whereas the 221 nm band observed in the UV region can be attributed to the aromatic rings present in the azo dye structure. It can be observed that, during the treatment, the intensities of both bands decreased suggesting that decolorization was accompanied by at least partial degradation of the aromatic ring structures.

3.8.3.2 Effect of pH

pH is one of the significant parameters for the photocatalytic dye degradation. In order to find out the optimal pH for the decolorization of Reactive Violet 5 dye, the pH of the reaction mixture was varied from 4 to 12 by keeping the dye concentration (30 ppm) and the catalyst amount (3 g/L) constant in all experiments. To keep the pH constant during each experiment, buffer solutions were used. After the adsorption in the dark, which required 1 hour, the solution was exposed to blue LEDs irradiation for 9 hours.

Results are reported in Figure 3.24.

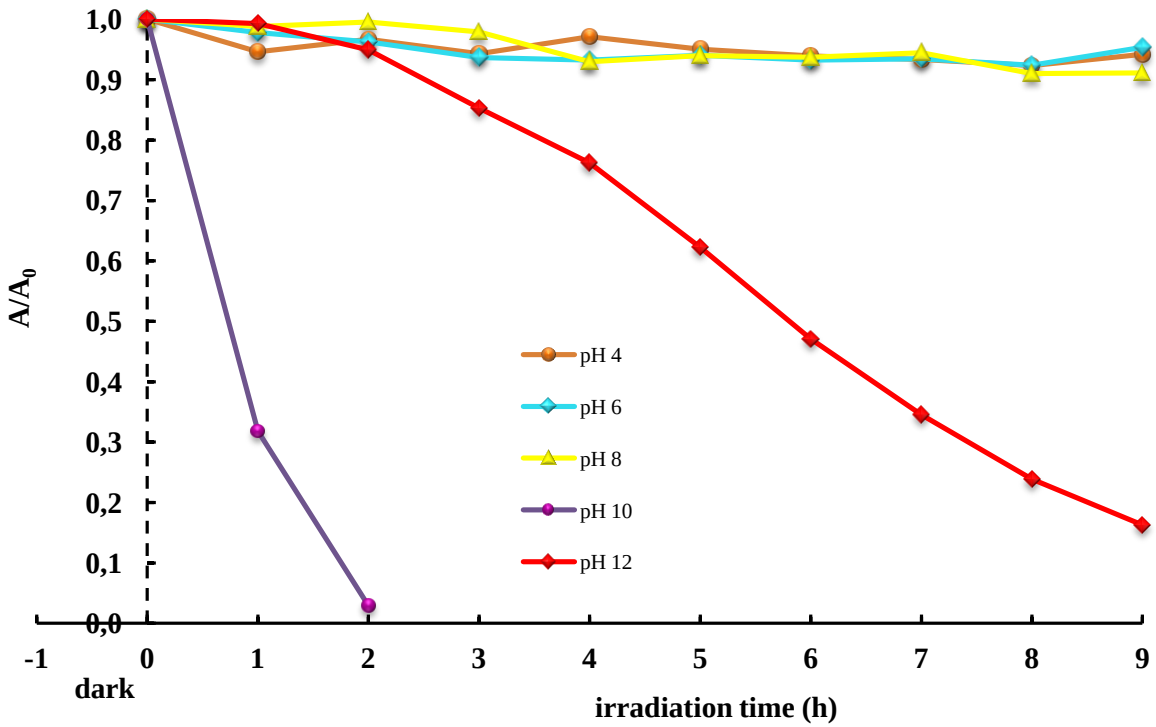

Figure 3.24 – Effect of pH on the Reactive Violet 5 photocatalysis (C_{RV5} = 30 ppm; Fe-TiO_2(50 mg Fe) = 3 g/L; pH = (4 – 12); light source = BL).

It can be observed that at pH 4, 6 and 8 the decrease in the absorbance peak is not appreciable, whereas at pH 12 and 10, a significant decrease in the absorbance peak is achieved. It can also be observed that at pH 10 the solution is totally decolourized after only 2 hours of irradiation.

The absorbance decreases almost linearly as a function of time, both at pH 10 and at pH 12. For the solution at pH 12, the absorbance decrease is about 80% after 9 hours of irradiation, whereas the solution at pH 10 can be totally decolorized after only 2 hours of exposure to blue LEDs.

In Figure 3.25 the trend of the colour removal as a function of pH is shown.

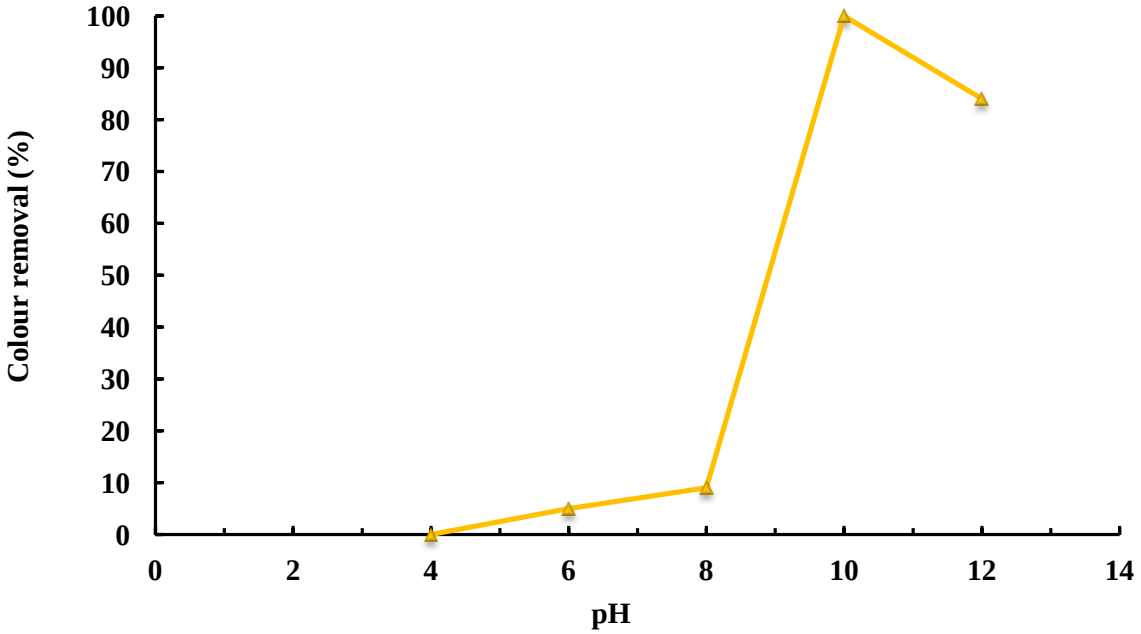

Figure 3.25 - Effect of pH on the Reactive Violet 5 decolorization evaluated after 9 hours of irradiation (C_{RV5} = 30 ppm; Fe-TiO_2(50 mg Fe) = 3 g/L; light source = BL).

Figure 3.25 shows that the Reactive Violet 5 decolorization trend, as a function of pH, is similar to those obtained for the Reactive Blue 4 dye.

As reported in Figure 3.25, the colour removal percentage slightly increases as the solution pH increases from 4 to 8 and reaches a maximum at pH 10. When pH increases from 10 to 12, the colour removal decreases.

The high colour removal at pH 10 can be due to the generation of hydroxyl radicals, which are largely responsible for oxidation processes, in alkaline solutions. (These radicals play an essential role in the breaking of the N=N conjugated system in azo dyes). According many authors high pH can enhance the dyes decolorization; Murugarandham et al. (2004) [229] found that increasing pH from 1 to 9 increased decolourization rates for Reactive Orange 4

(an anionic dye) from 25.27% to 90.49% after only 40 minutes. They also observed (2006) [84] that Reactive Black 5 decolorization rates increased with pH. Also in this case, the results were attributed to a more efficient generation of hydroxyl radicals due to the increase of the hydroxide ions concentration.

Figure 3.25 shows a decrease in the colour removal at pH 12. This could be due to a decrease in the adsorption of the Reactive Violet 5 molecules on the catalyst surface. Probably, at pH 12 the OH^- ions adsorption on the catalyst is too high, and its surface becomes negatively charged. The negative charges on the catalyst are expected repel the Reactive Violet 5 dye molecules, so a decrease in photodegradation efficiency can be observed.

At pH 8 the Reactive Violet 5 removal was only 9%. This result suggests that, decreasing the pH of only two units with respect to its optimal value (pH 10) can cause a noticeable decrease of the OH^- ions in solution. This results in a strong decrease of the ·OH radicals and in a decrease of the solution decolorization.

At pH 6, the surface of the catalyst nanoparticles is positively charged because the solution pH is lower than the zero point charge of the catalyst. The positively charged catalyst surface favours the attraction of Reactive Violet 5 molecules which covers all the active sites of the catalyst. As a result, the absorption of the photons on the catalyst surface decreases and so does the colour removal efficiency.

In Figure 3.26 the UV/vis spectra of the solution at pH 4 are shown.

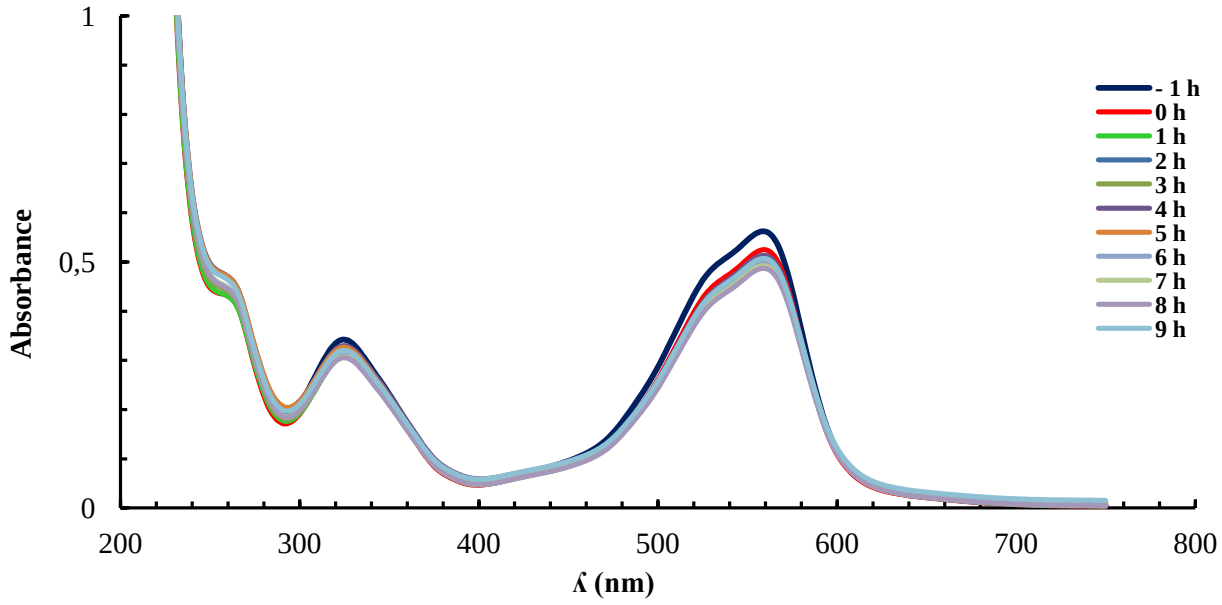

Figure 3.26 - UV/vis spectra of Reactive Violet 5 solution (C_{RV5} = 30 ppm; pH = 4; Fe-TiO_2(50 mg Fe) = 3 g/L; light source = BL).

Figure 3.26 shows that, at pH 4, there is a little adsorption in dark (curve “0 h”). When the LEDs are on, the absorbance values seem to increase, this may be due to dye desorption phenomena from the catalyst surface probably induced by heating the solution. It is clear that there are no degradation phenomena, because the spectra remain qualitatively the same. This suggests that the catalyst could be deactivated in acidic conditions. The loss of photocatalytic activity could be also due to the fact that, in acidic conditions, the particles that tend to agglomerate, this may reduce the surface area of the catalyst for the maximum dye adsorption as well as the photon absorption [230].

As the Fe-TiO_2 (50 mg Fe) showed its highest photocatalytic activity at pH 10, this value of pH was selected to carry out this study.

3.8.3.3 Effect of catalyst concentration

The catalyst concentration is another important parameter, which has strong influence on the degradation kinetics of dye solution. To avoid the use of a catalyst excess, it is necessary to identify the optimum loading for an efficient removal of dye. So it is necessary to optimize the amount of catalyst with respect to the highest photocatalytic activity.

In order to determine the optimal catalyst concentration, a series of experiments were carried out using different concentrations of the Fe-TiO_2(50 mg Fe) catalyst varying from 0 to 6 g/L, at optimized pH of 10 with 30 ppm dye solution. The results of the experiments are shown in Figure 3.27.

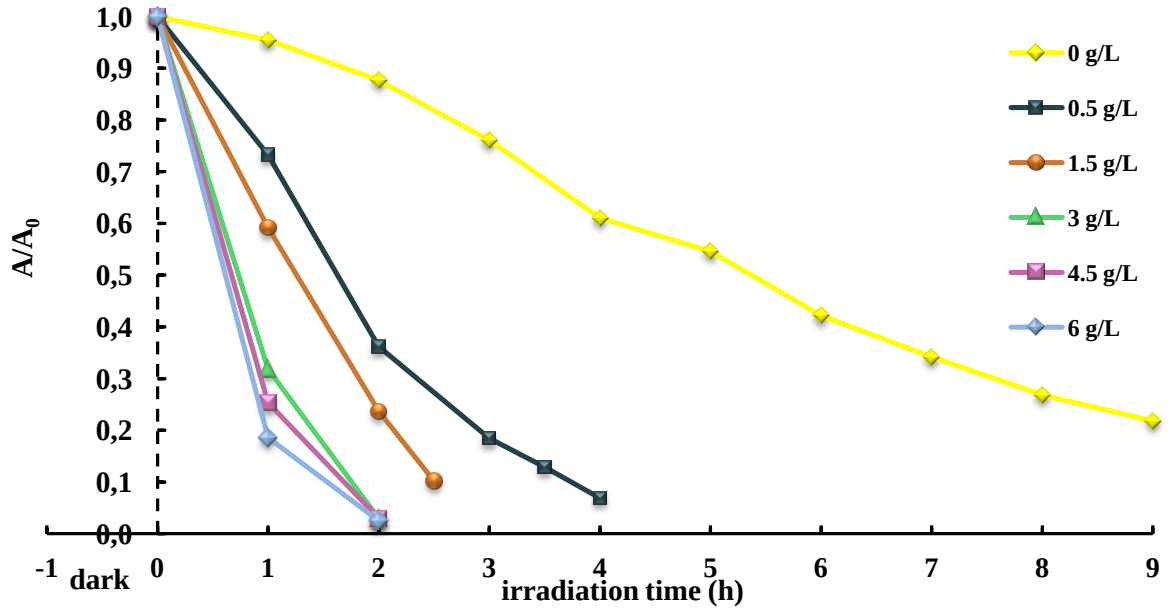

Figure 3.27 – Effect of the catalyst concentrations on the Reactive Violet 5 decolorization (C_{RV5} = 30 ppm; pH = 10; Fe-TiO_2(50 mg Fe) = (0 – 6 g/L); light source = BL).

Figure 3.27 shows that the absorbance of the treated solution decreases as a function of time, both in the absence and in the presence of Fe-TiO_2 (50 mg Fe). In the absence of catalyst, the solution can be decolorized, but the photolysis requires a longer time, and cannot be completed even after 9 hours (the decrease in absorbance is about 80%).

In the presence of 0.5 g/L of catalyst, the reactions proceed rapidly, and the complete decolorization can be achieved in 4 hours, whereas, in the presence of 1.5 g/L of catalyst, the complete decolorization requires 2.5 hours. For catalyst concentration of 3 g/L, 4.5 g/L and 6 g/L, the decolorization of the solution was completed in 2 hours; this because the absorbance of the solution was measured at t = 2 h. However, the trend of the curves at 3, 4.5 and 6 g/L of catalysts, suggests that the decolorization was completed in less than 2 hours. Therefore the values of the rate constants of reaction, k, (shown in Figure 3.28) are not reliable because they overlook that the decolorization was completed in less than 2 hours.

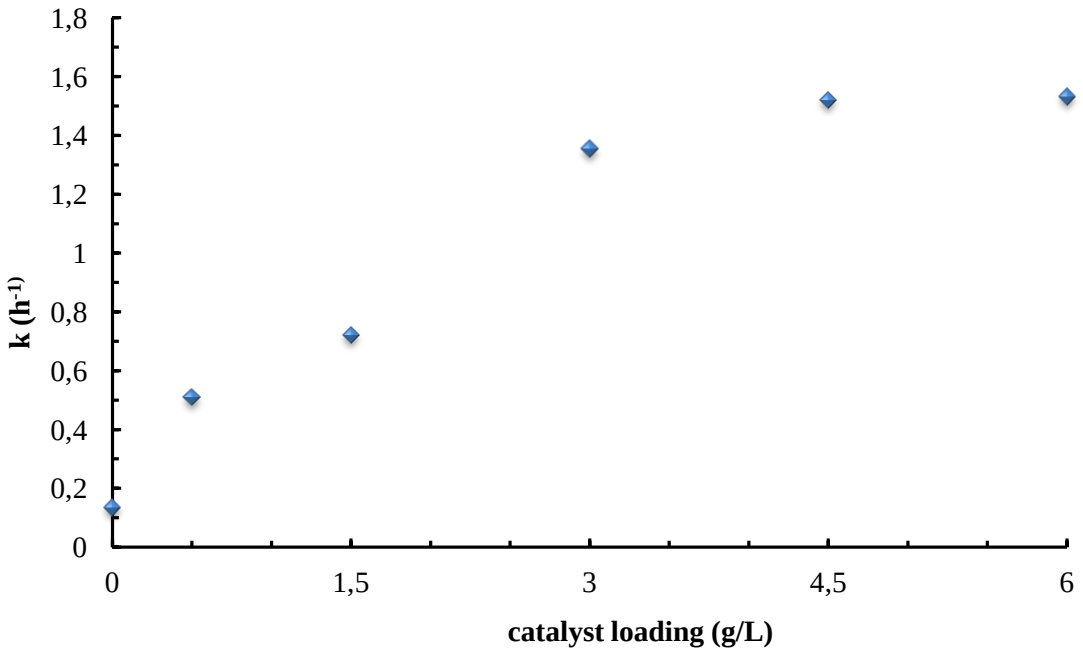

Figure 3.28 – Rate constants evaluated for each catalyst concentration (C_{RV5} = 30 ppm; pH = 10; Fe-TiO_2(50 mg Fe) = (0 – 6 g/L); light source = BL).

For these reasons, the initial rate of each reaction, as a function of the catalyst concentration, was evaluated. The Initial Rate Method was used for this purpose. As unit of time, the first hour of irradiation was chosen. The trend of the initial rate of reaction (m), is shown in Figure 3.29.

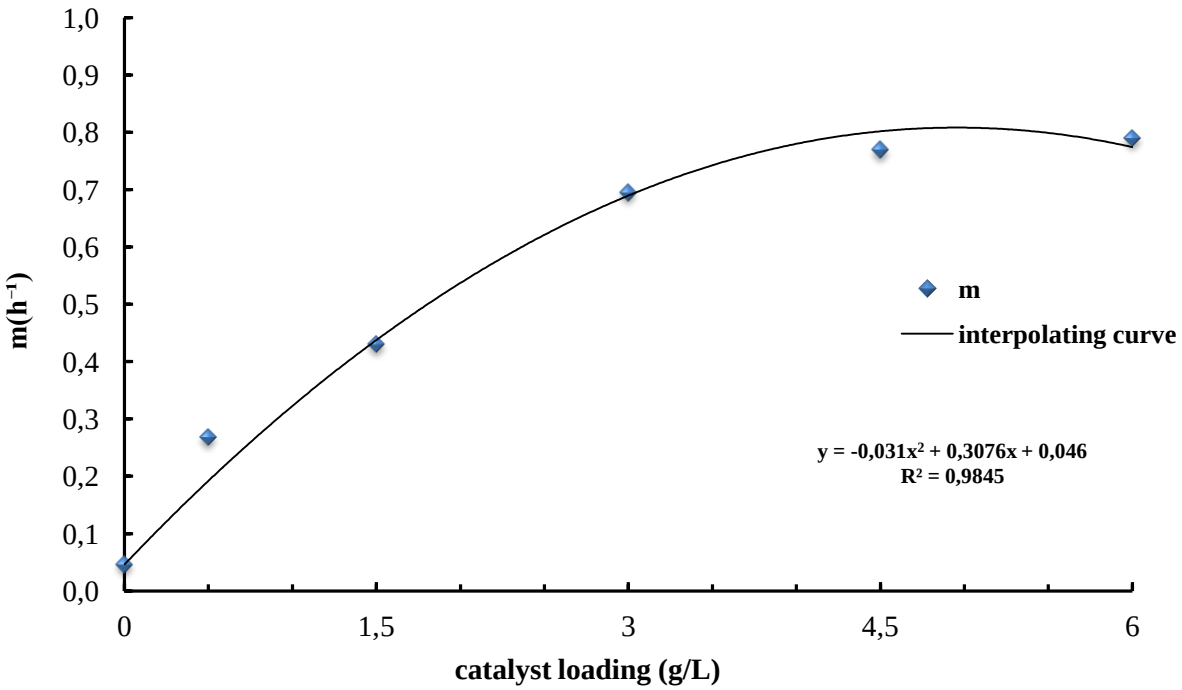

Figure 3.29 – Trend of the initial rate (m) of reaction as a function of the catalyst concentration (C_{RV5} = 30 ppm; Fe-TiO_2(50 mg Fe) = (0 – 6) g/L; pH = 10; light source = BL).

Figure 3.29 shows that the photocatalytic decolorization rate increases with increasing the amounts of Fe-TiO_2 (50 mg Fe). When the amount of Fe-TiO_2 (50 mg Fe) is increased from 0 up to 3 g/L, the initial reaction rate, greatly increases. Over 3 g/L, the increase of the initial reaction rate isn't significative, so 3 g/L was selected as the optimal catalyst concentration.

The results showed in Figure 3.27 and 3.29 suggest that as the catalyst concentration increases, the surface area for the photocatalytic reaction also increases so the incident light absorbed by Fe-TiO_2 (50 mg Fe) progressively increases because a larger amount of photons are adsorbed [159]. Moreover, more active sites may be covered with dye ions, but, when all the dye molecules are adsorbed on the catalyst surface, adding more catalyst doesn't enhance the decolorization. When the catalyst is overdosed, the opacity of the suspension increases and the light reflectance also increases. Additionally, agglomeration and sedimentation of nanocatalyst particles could occur. It makes a significant fraction of catalyst inaccessible to absorbing both the dye molecules and the radiations. Generally, lower values of catalyst concentration may be inadequate to achieve rapid reaction while high levels may be inhibitory. The presence of a maximum in the catalyst concentration

dependence of the inital rate of reaction, is more likely the result of different competing effects. Similar observations were reported in earlier works for degradation of dyes such as malachite green [242], methilene blue [104; 142; 175; 177], phenol red and methilene red [142], rodhamine B [146], Reactive Blue 4 [169; 171; 214], Reactive Orange 4 [156; 212], Reactive Red 120 [162; 212], Reactive Black 5 [84, 170], Reactive Blue 19 [165], Reactive Yellow 81 and Reactive Violet 1 [172], Reactive Blue 198 and Reactive Yellow 145 [170], and drugs such as spyramicine [154].

3.8.3.4 Effect of H_2O_2

The photoassisted decolorization of organic dyes can be significantly improved in the presence of hydrogen peroxide. In order to evaluate this effect, hydrogen peroxide was added in 50 mL of a Reactive Violet 5 solution (30 ppm) buffered at pH 10, in a concentration range of 10-100 mM. The results of the experiments are shown in Figure 3.30.

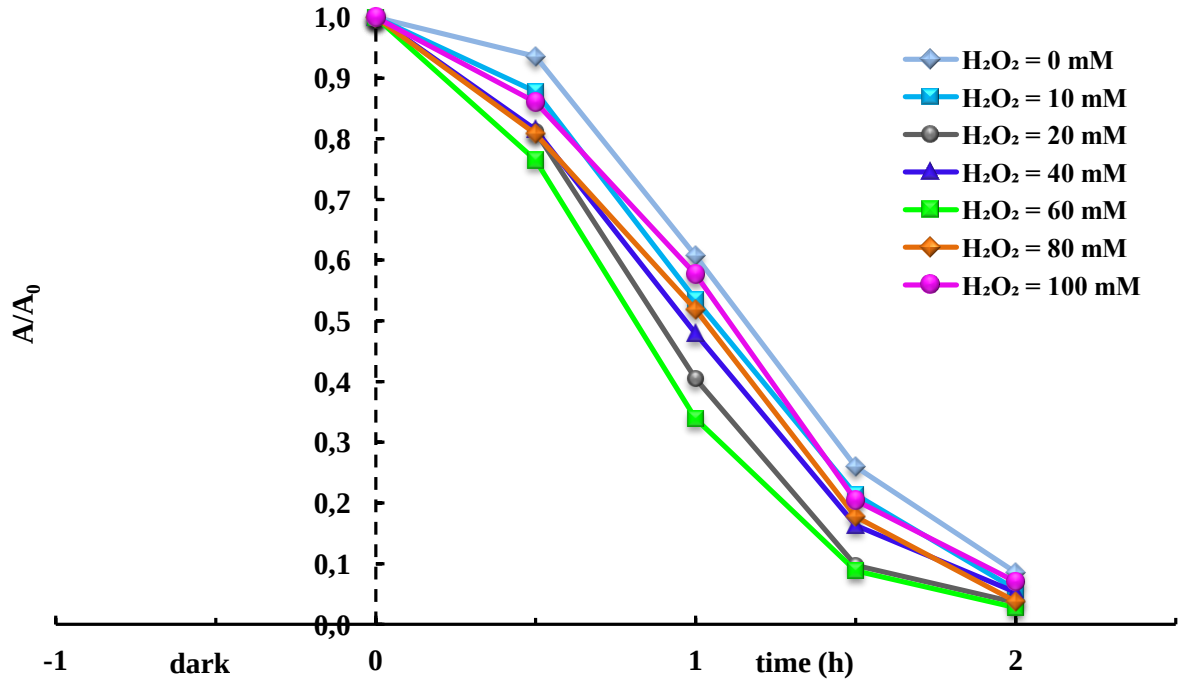

Figure 3.30 – Effect of H_2O_2 concentration on the Reactive Violet 5 decolorization, expressed as a function of irradiation time (C_{RV5} = 30 ppm; Fe-TiO_2(50 mg Fe) = 3 g/L; H_2O_2 = (0 – 100) mM; pH 10; light source = BL).

Figure 3.30 shows that the hydrogen peroxide increases the reaction rate. Furthermore, the complete decolorization is achieved in about 2 hours of irradiation, both in the absence and in the presence of hydrogen peroxide. However, the trend of the curves suggests that the

decolorization was completed in less than 2 hours; therefore, the calculated values of the rate constants of reaction, (in Figure 3.31), k, are not reliable as they overlook the fact that the decolorization was completed in less than 2 hours.

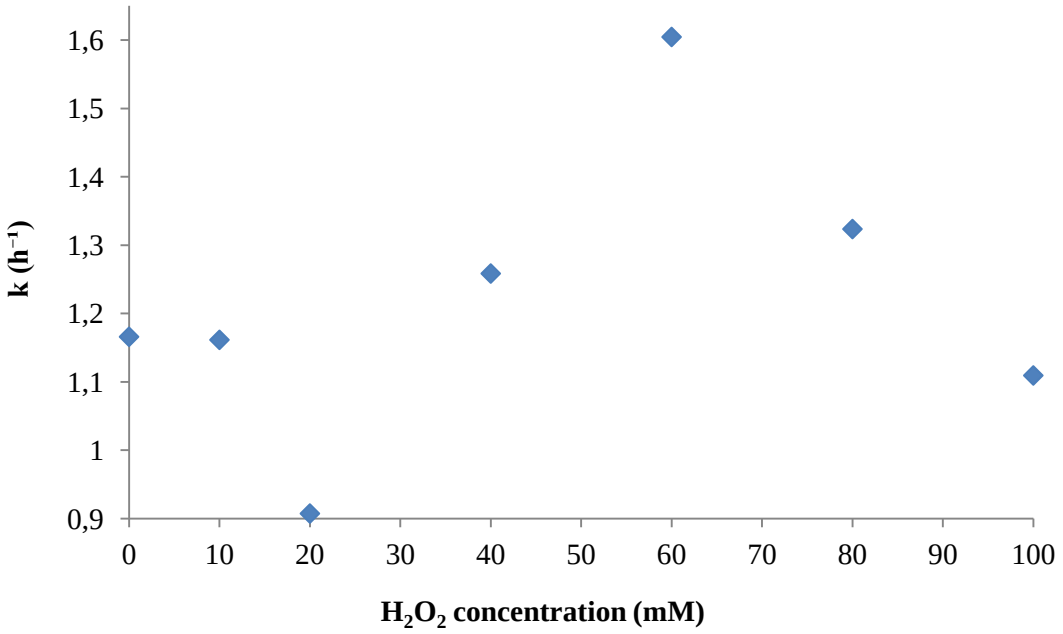

Figure 3.31 – Rate constant of reaction evaluated for each H2O2 concentration (C_{RV5} = 30 ppm; Fe-TiO_2(50 mg Fe) = 3 g/L; H_2O_2 = (0 – 100) mM; pH 10; light source = BL).

For these reasons, the Initial Rate Method was used to calculate the initial rate of each reaction, as a function of the hydrogen peroxide concentration. As unit of time, the first half hour of exposure to blue LEDs was chosen. In Table 3.10 the initial rate values have been reported.

Table 3.10 – Initial rate values calculated for each concentration of H_2O_2 (C_{RV5} = 30 ppm; Fe-TiO_2(50 mg Fe) = 3 g/L; H_2O_2 = (0 – 100) mM; pH 10; light source = BL).

H_2O_2 concentration (mM)	**m (h^{-1})**
0	0.130
10	0.246
20	0.338
40	0.414
60	0.472
80	0.384
100	0.28

In Figure 3.32 the trend of the initial rate of reaction, as a function of the hydrogen peroxide concentration, is shown.

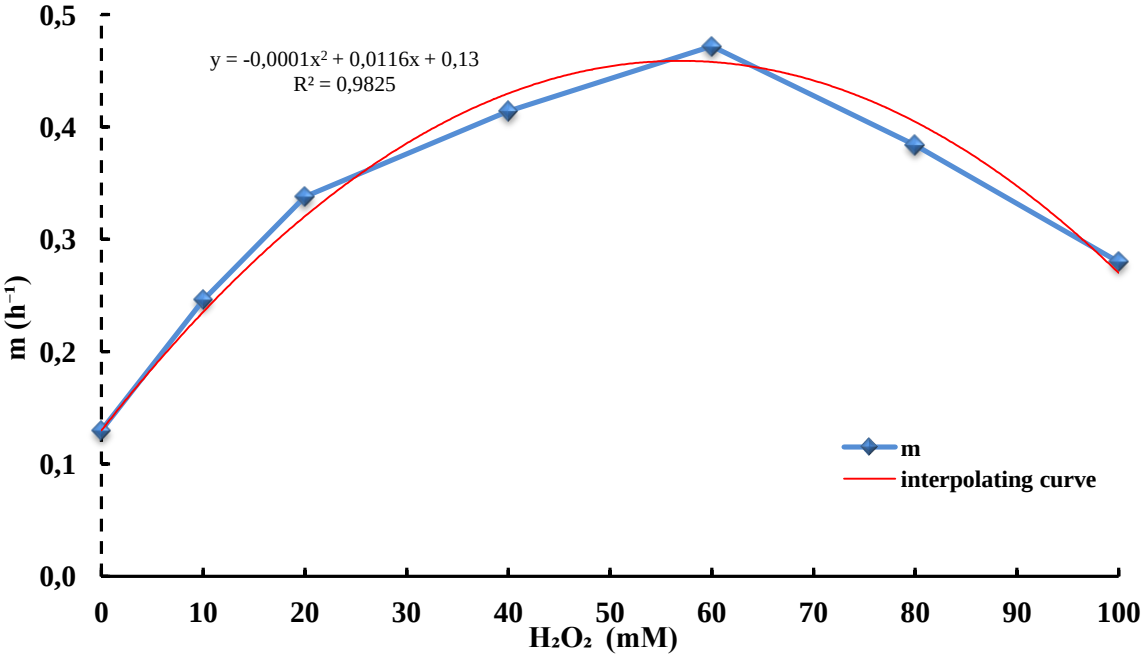

Figure 3.32 – Trend of the initial rate of reaction as a function of the hydrogen peroxide concentration (C_{RV5} = 30 ppm; pH 10; Fe-TiO_2(50 mg Fe) = 3 g/L; light source = BL).

Figure 3.32 shows that as the hydrogen peroxide concentration increases, the initial rate of reaction also increases up to 60 mM H_2O_2 concentration. When the hydrogen peroxide exceeds 60 mM, the initial rate of reaction decreases. Therefore 60 mM can be selected as the optimal hydrogen peroxide concentration.

At low concentrations, hydrogen peroxide enhances the decolorization rate of Reactive Violet 5, because:

- hydrogen peroxide is a better electron acceptor than molecular oxygen, it can act as a trap of the conduction band electrons (Eq. (3.7)) preventing the hole-electron pairs recombination [231] and thus increasing the chances of formation of hydroxyl radicals on the surface of the catalyst [232, 233].
- it can also produce hydroxyl radicals via photodecomposition (Eq. (3.9));
- it can react with the superoxide radical producing other hydroxyl radicals (Eq. (3.8));

$$H_2O_2 + e_{CB}^- \rightarrow \cdot OH + OH^- \quad (3.7)$$

$$H_2O_2 + O^{\cdot -}_2 \rightarrow \cdot OH + OH^- + O_2 \quad (3.8)$$

$$H_2O_2 \rightarrow 2\ \cdot OH \quad (3.9)$$

However, for H_2O_2 concentrations greater than the critical one, it may react with hydroxyl radicals (Eqs. (3.10) and (3.11)), and also act as scavenger of the photoproduced holes.

$$H_2O_2 + \cdot OH \rightarrow HO_2^{\cdot} + H_2O \quad (3.10)$$

$$HO_2^{\cdot} + \cdot OH \rightarrow H_2O + O_2 \quad (3.11)$$

Moreover, at high concentration, hydrogen peroxide could modify the catalyst surface [234]. A combination of these positive and negative effects could be responsible for the observed maximum in Figure 3.32. However, the existence of an optimum H_2O_2 concentration was reported in several other studies on azo dyes [84; 156; 161; 165; 171].

3.9 Discussion

It may be interesting to compare the present results with those obtained in other studies on Reactive Violet 5 degradation.

Chung et Chen (2008) [159] investigated the photocatalytic degradation of Reactive Violet 5 using titanium dioxide (TiO_2) nanoparticles. The experiments were carried out in a quartz beaker with a magnetic stirrer, which was placed in the center of the UV photo-reactor. The reactor was equipped with four Xenon 254 nm lamps. Under optimized conditions, the photodegradation efficiency was 90% after 20 minutes of irradiation and reached nearly 100% after 80 minutes.

Cabansag et al. (2013) [164] studied the photocatalysis of Reactive Violet 5 using ZnO particles. Irradiation was carried out inside a closed rectangular box with two UV lamps having emission peak at 365 nm. Under optimized conditions, a colour removal of 74% was obtained after 30 minutes of irradiation, whereas, after 90 minutes, the solution was totally decolorized.

In 2012, Kunal et al. [240] studied the decolorization and degradation of Reactive Violet 5 using an acclimatized indigenous bacterial mixed cultures-SB4 isolated from anthropogenic

dye contaminated soil. They obtained the complete dye removal within 18 hours, under the best working conditions.

Ayed et al. (2017) [241] evaluated the decolourization and the degradation efficiency of Reactive Violet 5 using a novel bacterial consortium. It was found that under optimal conditions, the bacterial consortium was able to decolourize the dye completely (> 99%) within 8 h.

Therefore, the treatment of Reactive Violet 5, in the presence of catalyst and under exposure to visible light, can lead to removal efficiencies that are comparable or higher than those reported for UV- photocatalysis or microbial degradation of Reactive Violet 5. Moreover, compared to the microbial degradation processes, the examined method seems to be simpler to implement and more flexible in operation.

Finally, a comparison with the results obtained by applying the vis-photocatalytic process to other dyes [142; 177; 179; 180] provides further support to the view that the treatment efficiency, in terms of decolorization, depends strongly on the nature of the dye.

Conclusions and future developments

Conclusions

The photocatalytic decolorization of three reactive dyes, Reactive Blue 4, Reactive Red 120 and Reactive Violet 5, under exposure to visible LEDs, was investigated in this study. The photocatalytic process was carried out in a cylindrical photoreactor. The solution, containing the catalyst as an aqueous suspension, was irradiated by visible blue LEDs.

Reactive Blue 4 was found to be not stable under irradiation of blue LEDs. In fact it could be decolorized by exposure to light even in the absence of catalyst. A Reactive Blue 4 100 ppm solution, buffered at pH 10, was treated under exposure to visible light emitted by LEDs for 9 hours, in the absence of catalyst and in the presence of 1 g/L of Fe-TiO_2(10 mg Fe) and TiO_2, respectively. It was found that the trends of the curves describing the TiO_2/LEDs and Fe-TiO_2(10 mg Fe)/LEDs systems were identical, whereas the curve describing the system in the absence of catalyst followed another path, although all the three systems achieved the same colour removal percentages. These results suggest that the Reactive Blue 4 dye decolorization seems to be mainly influenced by the light source and the contribution of the catalysts to the photocatalysis is almost negligible. This means that there could be a strong relationship between the light of the LEDs and the dye, which are both blue. It could be hypothesized that the Reactive Blue 4 absorbs a large part of the light emitted by the LEDs, therefore there are not enough light photons available to excite the catalyst nanoparticles.

Preliminary experiments were carried out to evaluate the behaviour of the Reactive Red 120 dye. The experimental conditions were the same adopted for the Reactive Blue 4 dye. It was found that in the absence of catalyst the LEDs are not able to decolorize the dye, in fact there was no colour removal even after 5 hours of irradiation. It was also found that the dye could not be decolorized even in the presence of catalysts. These results suggest that Reactive Red 120 is a very stable dye and probably it need to be treated by other processes.

Preliminary experiments carried out on the Reactive Violet 5 dye indicated that it was resistant to direct photolysis and it could be successfully treated by photocatalysis. The

subsequent experiments were carried out using a dye concentration of 30 ppm and a catalyst concentration of 3 g/L. Fe-TiO_2(50 mg Fe) was found to be an efficient catalyst for the decolorization of Reactive Violet 5 in the presence of visible light. Fe-TiO_2(50 mg Fe) showed superior photocatalytic activity compared to other catalysts such as undoped TiO_2, P-25 Degussa, N-doped TiO_2, Fe-TiO_2(10 mg Fe) and Fe-TiO_2(100 mg Fe). The influence of the pH was, then, evaluated. It was found that Reactive Violet 5 photocatalysis in the presence of Fe-TiO_2(50 mg Fe) was strongly favoured in alkaline conditions. pH 10 was selected as the optimal; at pH 10 the solution could be totally decolorized after only 2 hours of irradiation. At optimized pH of 10 a series of experiments were carried out using different concentrations of the Fe-TiO_2(50 mg Fe) catalyst varying from 0 to 6 g/L. 3 g/L was selected as the optimal catalyst concentration. Finally, the influence of the hydrogen peroxide on the photocatalytic decolorization of Reactive Violet 5 was evaluated. A hydrogen peroxide concentration of 60 mM was selected as the optimal. Under the best conditions the complete decolorization was achieved in less than 2 hours of exposure to blue LEDs.

After a comparison of the present results with those obtained in other studies on Reactive Violet 5 decolorization, it was found that Reactive Violet 5 photocatalysis under visible LEDs allows to achieve better results than the microbial treatments and results comparable to those achieved under traditional UV photocatalysis.

It was observed that blue LEDs offer a practical alternative dye treatment at lower cost: they are small, they can be used in different types of photocatalytic reactor set-ups and they have a low operative temperature, whereas UV irradiation sources can waste up to 80% of the light that they produce.

It can be concluded that visible LEDs could be used for development of an economic and energy efficient photocatalytic reactor.

Future developments

In this work the photocatalytic decolorization of Reactive Blue 4, Reactive Red 120 and Reactive Violet 5 was studied, but only the Reactive Violet 5 photocatalysis was optimized.

A detailed study of the Reactive Blue 4 and Reactive Red 120 behaviour under blue LEDs irradiation, in the presence and in the absence of catalysts, could be a research topic.

It may be interesting studying the mineralization of Reactive Violet 5 and finding the optimal conditions for the highest T.O.C. removal. Future works may explore the removal of these dyes from real waste streams using the same procedures.

In the present study, the experimentation was planned varying the level of a single parameter (catalyst concentration, hydrogen peroxide concentration) each time. It may become important to understand, not only the effects of the individual factors, but also the possible interactions and dependencies between the various factors. It could be evaluated the effect of several factors simultaneously, each with different levels; in this case the experimentation could be planned using a Definitive Screening Design, and then a Central Composite Design could be used.

Moreover in order to assess the feasibility of the process on a larger scale, further research is required focusing on the mechanisms of dye degradation and mineralization together with a detailed cost–benefit analysis.

Appendix A

Table A1- Influence of the BL/TiO_2 system on the Reactive Blue 4 decolorization: experimental conditions and absorbances.

Name test	V_{sol} (mL)	pH	C_{RB4} (ppm)	TiO_2 (g/L)	Q_{air} (l/h)	Rpm	dark time (min)	irradiation time (min)	n° of samplings
1	50	uncontrolled	100	**1**	15	900	60	180	6

time (min)	A (595 nm)	A (256 nm)	A (370 nm)	A (750 nm)
-60	0,6304	2,312	0,3586	0,017
0	0,5337	1,9362	0,3002	0,019
30	0,5209	2,0643	0,318	0,0031
60	0,5104	2,095	0,3299	0,0073
120	0,4661	2,0536	0,3349	0,0116
180	0,3994	1,9431	0,3294	0,0118

Table A2- Influence of the BL/Fe-TiO_2 (10 mg Fe) system on the Reactive Blue 4 decolorization: experimental conditions and absorbances.

Name test	V_{sol} (mL)	pH	C_{RB4} (ppm)	Fe-TiO_2 (10 mg Fe) (g/L)	Q_{air} (l/h)	Rpm	dark time (min)	irradiation time (min)	n° of samplings
2	50	uncontrolled	100	1	15	900	60	180	7

time (min)	A (595 nm)	A (256 nm)	A (370 nm)	A (750 nm)
-60	0,666	2,4324	0,3873	0,024
0	0,5817	2,1362	0,3306	0,0102
30	0,5775	2,1624	0,3674	0,025
60	0,5153	2,1932	0,3562	0,0087
90	0,5048	2,1873	0,3839	0,0251
120	0,4143	2,0526	0,3198	-0,0107
180	0,3775	1,9835	0,338	0,0096

Table A3- Influence of the BL/Fe-TiO_2 (50 mg Fe) system on the Reactive Blue 4 decolorization: experimental conditions and absorbances.

Test name	V_{sol} (mL)	pH	C_{RB4} (ppm)	Fe-TiO_2 (50 mg Fe) (g/L)	Q_{air} (l/h)	Rpm	dark time (min)	irradiation time (min)	n° of samplings
3	**50**	uncontrolled	100	1	15	900	60	180	7

time (min)	A (595 nm)	A (256 nm)	A (370 nm)	A (750 nm)
-60	0,6959	2,539	0,3696	0,0037
0	0,6265	2,122	0,3189	0,0149
30	0,5755	2,3968	0,3838	0,0052
60	0,6049	2,3973	0,3981	0,0228
90	0,5385	1,5371	0,3796	0,0184
120	0,5223	2,2987	0,3903	0,0172
180	0,4313	2,1556	0,339	-0,0012

Table A4- Influence of the BL/Fe-TiO_2 (100 mg Fe) system on the Reactive Blue 4 decolorization: experimental conditions and absorbances.

Test name	V_{sol} (mL)	pH	C_{RB4} (ppm)	Fe-TiO_2 (100 mg Fe) (g/L)	Q_{air} (l/h)	Rpm	dark time (min)	irradiation time (min)	n° of samplings
4	**50**	uncontrolled	100	1	15	900	60	180	7

time (min)	A (595 nm)	A (256 nm)	A (370 nm)	A (750 nm)
-60	0,7133	2,6464	0,401	0,0093
0	0,602	2,2108	0,3438	0,0097
30	0,592	2,2449	0,3476	0,0063
60	0,5805	2,2673	0,3592	0,0101
90	0,5305	2,2104	0,3618	0,0115
120	0,4957	2,1936	0,399	0,0285
180	0,3996	2,0429	0,3512	0,0129

Table A5- Influence of the BL/Fe-TiO_2 (100 mg Fe) system on the Reactive Blue 4 decolorization: experimental conditions and absorbances.

Test name	V_{sol} (mL)	pH	C_{RB4} (ppm)	Fe-TiO_2 (100 mg Fe) (g/L)	Q_{air} (l/h)	Rpm	dark time (min)	irradiation time (min)	n° of samplings
5	**50**	uncontrolled	100	**1**	15	900	60	180	11

time (min)	A (595 nm)	A (256 nm)	A (370 nm)	A (750 nm)
-60	0,6882	2,5678	0,3962	0,0104
0	0,5652	2,1448	0,347	0,0168
30	0,5747	2,2506	0,3513	0,0024
60	0,5438	2,2212	0,358	0,0082
90	0,4811	2,1583	0,3614	0,0116
120	0,4452	2,1387	0,3678	0,0145
180	0,3755	2,0313	0,3442	0,0098
240	0,3553	2,0089	0,3555	0,0225
300	0,3128	1,9258	0,3137	0,007
360	0,3012	1,9106	0,31	0,0098
390	0,2856	1,8811	0,2983	0,0056

Table A6- Influence of the BL/N-doped TiO_2 system on the Reactive Blue 4 decolorization: experimental conditions and absorbances.

Test name	V_{sol} (mL)	pH	C_{RB4} (ppm)	N-doped TiO_2 (g/L)	Q_{air} (l/h)	Rpm	dark time (min)	irradiation time (min)	n° of samplings
6	**50**	uncontrolled	100	**1**	15	900	60	180	7

time (min)	A (595 nm)	A (256 nm)	A (370 nm)	A (750 nm)
-60	0,7127	2,591	0,3933	0,0109
0	0,6848	2,3838	0,353	0,0031
30	0,6388	2,5416	0,3755	0,0029
60	0,6276	2,4661	0,386	0,0119
90	0,601	2,4201	0,3927	0,015
120	0,5182	2,3143	0,3573	-0,001
180	0,4466	2,2668	0,3819	0,0146

Table A6- Influence of the BL/N-doped TiO_2 system on the Reactive Blue 4 decolorization: experimental conditions and absorbances.

Test name	**V_{sol} (mL)**	**pH**	**C_{RB4} (ppm)**	**N-doped TiO_2 (g/L)**	**Q_{air} (l/h)**	**Rpm**	**dark time (min)**	**irradiation time (min)**	**n° of samplings**
6-bis	**50**	uncontrolled	100	**1**	15	900	60	180	5

time (min)	**A (595 nm)**	**A (256 nm)**	**A (370 nm)**	**A (750 nm)**
-60	0,6595	2,3656	0,3579	0,0098
0	0,6193	2,3189	0,3064	-0,0284
60	0,5999	2,2521	0,3308	0,0088
120	0,5124	2,1373	0,3291	0,0114
180	0,3917	1,9737	0,3099	0,0108

Table A7- Effect of blue LEDs on the Reactive Blue 4 decolorization: experimental conditions and absorbances.

Test name	**V_{sol} (mL)**	**pH**	**C_{RB4} (ppm)**	**catalyst (g/L)**	**Q_{air} (l/h)**	**Rpm**	**dark time (min)**	**irradiation time (min)**	**n° of samplings**
7	**50**	uncontrolled	100	**absent**	15	900	0	180	4

time (min)	**A (595 nm)**	**A (256 nm)**	**A (370 nm)**	**A (750 nm)**
0	0,632	2,2756	0,3474	0,0102
120	0,5956	2,2991	0,3845	0,0246
150	0,5399	2,23	0,3709	0,0188
180	0,4996	2,1574	0,378	0,0314

Table A8- Influence of pH on the Reactive Blue 4 decolorization carried out in the presence of the BL/Fe-TiO_2 (10 mg Fe) system: experimental conditions and absorbances.

Test name	V_{sol} (mL)	pH	C_{RB4} (ppm)	Fe-TiO_2 (10 mg Fe) (g/L)	Q_{air} (l/h)	rpm	dark time (min)	irradiation time (min)	n° of samplings
8	50	**4**	100	1	15	900	60	180	5

time (min)	A (595 nm)	A (256 nm)	A (370 nm)	A (750 nm)
-60	0,628	2,2281	0,3314	-0,0006
0	0,3891	1,2792	0,1784	-0,0078
60	0,5413	2,115	0,3338	0,0154
120	0,5579	2,2609	0,378	-0,0002
180	0,5216	2,193	0,3623	0,0027

Table A9 - Influence of pH on the Reactive Blue 4 decolorization carried out in the presence of the BL/Fe-TiO_2 (10 mg Fe) system: experimental conditions and absorbances.

Test name	V_{sol} (mL)	pH	C_{RB4} (ppm)	Fe-TiO_2 (10 mg Fe) (g/L)	Q_{air} (l/h)	rpm	dark time (min)	irradiation time (min)	n° of samplings
9	50	**6**	100	1	15	900	60	180	5

time (min)	A (595 nm)	A (256 nm)	A (370 nm)	A (750 nm)
-60	0,5881	2,2253	0,3398	0,0107
0	0,6074	2,4593	0,3777	0,0205
60	0,6158	3,6799	0,5499	0,0056
120	0,5465	5,742	0,7853	0,0131
180	0,4175	6,4441	0,8355	-0,0315

Table A10 - Influence of pH on the Reactive Blue 4 decolorization carried out in the presence of the BL/Fe-TiO_2 (10 mg Fe) system: experimental conditions and absorbances.

Test name	V_{sol} (mL)	pH	C_{RB4} (ppm)	Fe-TiO_2 (10 mg Fe) (g/L)	Q_{air} (l/h)	Rpm	dark time (min)	irradiation time (min)	n° of samplings
10	50	**8**	100	1	15	900	60	180	5

time (min)	A (595 nm)	A (256 nm)	A (370 nm)	A (750 nm)
-60	0,6737	2,4862	0,3731	0,0129
0	0,6538	2,4206	0,3547	0,007
60	0,6363	2,4144	0,3558	0,0075
120	0,5336	2,2751	0,3507	0,014
180	0,4273	2,1294	0,3407	0,0174

Table A11 - Influence of pH on the Reactive Blue 4 decolorization carried out in the presence of the BL/Fe-TiO_2 (10 mg Fe) system: experimental conditions and absorbances.

Test name	V_{sol} (mL)	pH	C_{RB4} (ppm)	Fe-TiO_2 (10 mg Fe) (g/L)	Q_{air} (l/h)	rpm	dark time (min)	irradiation time (min)	n° of samplings
11	**50**	**10**	100	1	15	900	60	180	5

time (min)	A (595 nm)	A (256 nm)	A (370 nm)	A (750 nm)
-60	0,6501	2,3915	0,3489	0,0106
0	0,6251	2,3183	0,3287	0,0052
60	0,6027	2,3303	0,3373	0,0046
120	0,5267	2,2711	0,3385	0,0083
180	0,3636	2,0237	0,298	0,007

Table A12 - Influence of pH on the Reactive Blue 4 decolorization carried out in the presence of the BL/Fe-TiO_2 (10 mg Fe) system: experimental conditions and absorbances.

Test name	V_{sol} (mL)	pH	C_{RB4} (ppm)	Fe-TiO_2 (10 mg Fe) (g/L)	Q_{air} (l/h)	Rpm	dark time (min)	irradiation time (min)	n° of samplings
12	50	**12**	100	1	15	900	60	180	5

time (min)	A (595 nm)	A (256 nm)	A (370 nm)	A (750 nm)
-60	0,6406	2,2633	0,3272	0,0096
0	0,6354	2,2805	0,3287	0,0119
60	0,5793	2,3386	0,3235	-0,0099
120	0,5536	2,2981	0,3403	0,012
180	0,495	2,2233	0,3075	-0,0028

Table A13 - Influence of pH on the Reactive Blue 4 decolorization carried out in the presence of the BL/Fe-TiO_2 (10 mg Fe) system: experimental conditions and absorbances.

Test name	V_{sol} (mL)	pH	C_{RB4} (ppm)	Fe-TiO_2 (10 mg Fe) (g/L)	Q_{air} (l/h)	Rpm	dark time (min)	irradiation time (min)	n° of samplings
12-bis	50	**12**	100	1	15	900	60	180	5

time (min)	A (595 nm)	A (256 nm)	A (370 nm)	A (750 nm)
-60	0,7815	2,8867	0,43	0,0307
0	0,7762	2,8758	0,4343	0,0225
60	0,7369	2,9308	0,4488	0,021
120	0,6534	2,7319	0,3692	-0,0039
180	0,5972	2,6427	0,3282	-0,0207

Table A14 – Reactive Blue 4 decolorization carried out at the optimal pH and in the presence of the BL/Fe-TiO_2 (10 mg Fe) system: experimental conditions and absorbances.

Test name	V_{sol} (mL)	pH	C_{RB4} (ppm)	Fe-TiO_2 (10 mg Fe) (g/L)	Q_{air} (l/h)	rpm	dark time (h)	irradiation time (h)	n° of samplings
11-bis	50	10	100	1	15	900	1	9	11

time (h)	A (595 nm)	A (256 nm)	A (370 nm)	A (750 nm)
-1	0,5871	2,1321	0,2991	0,0064
0	0,5776	2,127	0,2989	0,0025
1	0,5667	2,1808	0,3206	0,0103
2	0,4727	2,0539	0,2904	-0,001
3	0,3216	1,8264	0,2696	0,0038
4	0,2056	1,6206	0,2335	0,0032
5	0,1384	1,4774	0,2023	-0,0007
6	0,1123	1,4064	0,1954	0,0022
7	0,0933	1,3403	0,1841	0,003
8	0,0853	1,3031	0,1813	0,0055
9	0,0673	1,2065	0,1602	0,0004

Table A15 – Reactive Blue 4 decolorization carried out at the optimal pH and in the presence of the BL/ TiO_2 system: experimental conditions and absorbances.

Test name	V_{sol} (mL)	pH	C_{RB4} (ppm)	TiO_2 (g/L)	Q_{air} (l/h)	Rpm	dark time (h)	irradiation time (h)	n° of samplings
13	**50**	10	100	1	15	900	1	9	11

time (h)	A (595 nm)	A (256 nm)	A (370 nm)	A (750 nm)
-1	0,6573	2,4331	0,345	0,0072
0	0,6622	2,4496	0,346	0,0052
1	0,6367	2,4123	0,3632	0,0134
2	0,5158	2,2504	0,3309	0,0063
3	0,3558	2,0242	0,2989	0,0053
4	0,2419	1,8529	0,2667	0,0042
5	0,1841	1,6877	0,2363	0,0032
6	0,1517	1,6042	0,2199	0,0028
7	0,1286	1,5391	0,2081	0,0024
8	0,1093	1,4615	0,1941	0,002
9	0,1056	1,4773	0,1955	0,002

Table A16 – Reactive Blue 4 decolorization carried out at the optimal pH and under exposure to BL: experimental conditions and absorbances.

Test name	V_{sol} (mL)	pH	C_{RB4} (ppm)	catalyst (g/L)	Q_{air} (l/h)	rpm	dark time (h)	irradiation time (h)	n° of samplings
14	**50**	10	100	absent	15	900	0	9	10

time (h)	A (595 nm)	A (256 nm)	A (370 nm)	A (750 nm)
0	0,6606	2,354	0,3324	0,0069
1	0,6606	2,354	0,3324	0,0069
2	0,5958	2,223	0,3393	0,0182
3	0,5439	2,0963	0,3171	0,0166
4	0,4868	2,0128	0,2973	0,0122
5	0,4295	1,9378	0,3049	0,0201
6	0,3314	1,817	0,2784	0,0084
7	0,259	1,7441	0,269	0,0159
8	0,1906	1,6256	0,2456	0,0121
9	0,1302	1,4698	0,2212	0,01

Table A17 – Reactive Blue 4 decolorization carried out at the optimal pH and in the presence of the BL/Fe-TiO_2 (10 mg Fe) system: experimental conditions and absorbances.

Test name	V_{sol} (mL)	pH	C_{RB4} (ppm)	Fe-TiO_2 (10 mg Fe) (g/L)	Q_{air} (l/h)	Rpm	dark time (h)	irradiation time (h)	n° of samplings
15	50	10	300	3	15	900	1	5	7

time (h)	A (595 nm)	A (256 nm)	A (370 nm)	A (750 nm)
-1	1,877	5,2955	0,9798	0,0153
0	1,877	5,2955	0,9798	0,0153
1	1,8223	10	1,0197	0,0202
2	1,1961	5,471	0,9357	0,0164
3	0,5736	5,2609	0,7331	0,0092
4	0,3499	4,4798	0,6286	0,0072
5	0,2523	4,5301	0,6313	0,0093

Table A18 – Reactive Blue 4 decolorization carried out at the optimal pH and under exposure to BL: experimental conditions and absorbances.

Test name	**V_{sol} (mL)**	**pH**	**C_{RB4} (ppm)**	**catalyst (g/L)**	**Q_{air} (l/h)**	**rpm**	**dark time (h)**	**irradiation time (h)**	**n° of samplings**
16	50	10	300	absent	15	900	0	5	6

time (h)	**A (595 nm)**	**A (256 nm)**	**A (370 nm)**	**A (750 nm)**
-1	1,8769	4,3981	1,0067	0,024
0	1,8769	10	1,0429	0,028
1	1,8299	> 10	0,9957	0,0296
2	1,4025	> 10	0,8544	0,0322
3	0,8476	> 10	0,707	0,0226
4	0,5532	4,925	0,6371	0,0141
5	0,3948	4,6174	0,6109	0,0125

Appendix B

Table B1 – Reactive Red 120 decolorization carried out at pH 10 and under exposure to BL: experimental conditions and absorbances.

Test name	V_{sol} (mL)	pH	C_{RR120} (ppm)	catalyst (g/L)	Q_{air} (l/h)	Rpm	dark time (h)	irradiation time (h)	n° of samplings
17	50	10	100	absent	15	900	0	6	7

time (h)	A (510 nm)	A (291 nm)	A (238 nm)	A (373 nm)	A (750 nm)
0	2,5458	3,1703	2,8688	0,7194	0,0015
1	2,471	3,24	2,9782	0,7194	0,0015
2	2,4947	3,2502	2,9722	0,7282	0,0056
3	2,4659	3,2198	2,9564	0,7259	0,0057
4	2,3968	3,147	2,8949	0,722	0,0039
5	2,4461	3,2074	2,955	0,7074	0,005
6	2,438	3,2131	2,964	0,7385	0,0275

Table B2 – Reactive Red 120 decolorization carried out at pH 10 and in the presence of the BL/Fe-TiO_2 (10 mg Fe) system: experimental conditions and absorbances.

Test name	V_{sol} (mL)	pH	C_{RR120} (ppm)	Fe-TiO_2 (10 mg Fe) (g/L)	Q_{air} (l/h)	rpm	dark time (h)	irradiation time (h)	n° of samplings
18	50	10	100	1	15	900	1	2	4

time (h)	A (510 nm)	A (291 nm)	A (238 nm)	A (373 nm)	A (750 nm)
-1	2,3561	2,9936	2,6915	0,6711	0,0015
0	2,2809	2,8383	2,5612	0,6308	-0,0037
1	2,2792	2,8985	2,5992	0,6408	0,0005
2	2,3203	2,9714	2,6849	0,6572	-0,0017

Table B3 – Reactive Red 120 decolorization carried out at pH 10 and in the presence of the BL/Fe-TiO_2 (10 mg Fe) system: experimental conditions and absorbances.

Test name	**V_{sol} (mL)**	**pH**	**C_{RR120} (ppm)**	**TiO_2 (g/L)**	**Q_{air} (l/h)**	**Rpm**	**dark time (h)**	**irradiation time (h)**	**n° of samplings**
19	50	10	100	1	15	900	1	2	4

time (h)	**A (510 nm)**	**A (291 nm)**	**A (238 nm)**	**A (373 nm)**	**A (750 nm)**
-1	2,3561	2,9936	2,6915	0,6711	0,0015
0	2,298	2,9427	2,6503	0,6572	-0,0003
1	2,3149	2,9714	2,6676	0,6632	0,0089
2	2,3119	2,9677	2,6742	0,6327	-0,006

Appendix C

Table C1 – Reactive Violet 5 decolorization carried out at pH 10 and in the presence of the BL/Fe-TiO_2 (10 mg Fe) system: experimental conditions and absorbances.

Test name	V_{sol} (mL)	pH	C_{RV5} (ppm)	Fe-TiO_2 (10 mg Fe) (g/L)	Q_{air} (l/h)	rpm	dark time (h)	irradiation time (h)	n° of samplings
20	50	10	100	3	15	900	1	2	4

time (h)	A (559 nm)	A (221 nm)	A (327 nm)	A (750 nm)
-1	1,6982	2,0915	1,0991	0,0209
0	1,5317	1,9307	0,9985	-0,0001
1	1,3499	1,9007	0,8847	0,012
2	1,1684	1,824	0,7924	0,0113

Table C2 – Reactive Violet 5 decolorization carried out at pH 10 and under exposure to BL: experimental conditions and absorbances.

Test name	V_{sol} (mL)	pH	C_{RV5} (ppm)	Catalyst (g/L)	Q_{air} (l/h)	rpm	dark time (h)	irradiation time (h)	n° of samplings
21	50	10	100	Absent	15	900	0	4	5

time (h)	A (559 nm)	A (221 nm)	A (327 nm)	A (750 nm)
0	1,7173	2,0466	1,0999	0,0181
1	1,6914	2,1148	1,0681	0,0095
2	1,6442	2,1366	1,0571	0,019
3	1,5792	2,1216	1,0284	0,0218
4	1,5485	2,0161	1,014	0,0179

Table C3 – Reactive Violet 5 decolorization carried out under uncontrolled pH and exposure to BL: experimental conditions and absorbances.

Test name	V_{sol} (mL)	pH	C_{RV5} (ppm)	catalyst (g/L)	Q_{air} (l/h)	Rpm	dark time (h)	irradiation time (h)	n° of samplings
22	50	**uncontrolled**	100	absent	15	900	0	9	10

time (h)	A (559 nm)	A (221 nm)	A (327 nm)	A (750 nm)
0	1,6785	1,7436	1,0186	0,0179
1	1,6785	1,7436	1,0186	0,0179
2	1,6318	1,7974	1,0065	0,0217
3	1,6047	1,852	1,0069	0,0194
4	1,6448	1,9311	1,03	0,0186
5	1,6386	1,946	1,02	0,0161
6	1,5985	1,8809	0,9853	0,0188
7	1,6274	1,9439	1,0112	0,0178
8	1,6236	1,9443	1,0092	0,0158
9	1,626	1,9439	1,0069	0,0177

Table C4 – Reactive Violet 5 decolorization carried out under uncontrolled pH and in the presence of the BL/Fe-TiO_2 (10 mg Fe) system: experimental conditions and absorbances.

Test name	V_{sol} (mL)	pH	C_{RV5} (ppm)	Fe-TiO_2 (10 mg Fe) (g/L)	Q_{air} (l/h)	Rpm	dark time (h)	irradiation time (h)	n° of samplings
23	50	**uncontrolled**	100	1	15	900	1	9	11

time (h)	A (559 nm)	A (221 nm)	A (327 nm)	A (750 nm)
-1	1,8327	1,8535	0,9666	0,0155
0	1,8327	1,8535	0,9666	0,0155
1	1,7445	1,9023	1,109	0,015
2	1,6894	1,8728	1,0609	0,0145
3	1,6846	1,8604	1,0263	0,0162
4	1,6617	1,8933	1,0244	0,0148
5	1,6466	1,907	1,0247	0,0149
6	1,6338	1,9213	1,0263	0,0149
7	1,6047	1,8999	1,0052	0,0141
8	1,5974	1,8567	0,9786	0,0145
9	1,5809	1,8678	0,9772	0,0141

Table C5 – Reactive Violet 5 decolorization carried out under uncontrolled pH and in the presence of the BL/ TiO_2 system: experimental conditions and absorbances.

Test name	V_{sol} (mL)	pH	C_{RV5} (ppm)	TiO_2 (g/L)	Q_{air} (l/h)	Rpm	dark time (h)	irradiation time (h)	n° of samplings
23	50	**uncontrolled**	100	1	15	900	1	9	11

time (h)	A (559 nm)	A (221 nm)	A (327 nm)	A (750 nm)
-1	1,8939	1,9096	1,1372	0,0124
0	1,8415	1,8289	1,0898	0,0087
1	1,8415	1,9575	1,1202	0,0163
2	1,8408	2,0472	1,1332	0,0271
3	1,8138	2,0759	1,1319	0,0162
4	1,7843	2,006	1,0752	0,0094
5	1,7703	2,043	1,0863	0,0195
6	1,761	2,0177	1,0686	0,0129
7	1,7366	2,004	1,0588	0,0135
8	1,7281	1,9955	1,0503	0,0129
9	1,7174	1,9934	1,0482	0,0135

Table C6 – Effect of the BL/ TiO_2 system on Reactive Violet 5 decolorization: experimental conditions and absorbances.

Test name	V_{sol} (mL)	pH	C_{RV5} (ppm)	TiO_2 (g/L)	Q_{air} (l/h)	Rpm	dark time (h)	irradiation time (h)	n° of samplings
24	50	uncontrolled	30	**3**	15	900	1	9	11

time (h)	A (559 nm)	A (221 nm)	A (327 nm)	A(750 nm)
-1	0,5813	0,6245	0,3589	0,0065
0	0,5702	0,596	0,3495	0,0104
1	0,5347	0,6599	0,3435	0,0067
2	0,4904	0,599	0,3014	0,0016
3	0,4579	0,6031	0,2906	0,0043
4	0,4422	0,6157	0,2823	0,0035
5	0,4162	0,6121	0,2689	0,0027
6	0,3821	0,594	0,2492	-0,0007
7	0,3623	0,5844	0,2373	-0,0001
8	0,3283	0,5458	0,2135	-0,0036
9	0,3299	0,5635	0,22	0,0022

Table C7 – Effect of the BL/ N-doped TiO_2 system on Reactive Violet 5 decolorization: experimental conditions and absorbances.

Test name	V_{sol} (mL)	pH	C_{RV5} (ppm)	N-doped TiO_2 (g/L)	Q_{air} (l/h)	Rpm	dark time (h)	irradiation time (h)	n° of samplings
25	50	uncontrolled	30	**3**	15	900	1	9	11

time (h)	A (559 nm)	A (221 nm)	A (327 nm)	A(750 nm)
-1	0,5578	0,5845	0,3353	0,0056
0	0,5531	0,5885	0,3376	0,0045
1	0,5302	0,5988	0,3222	0,0022
2	0,5168	0,5881	0,3084	0,0018
3	0,501	0,6106	0,3083	0,0045
4	0,4964	0,6319	0,3097	0,0039
5	0,4927	0,6338	0,3072	0,0041
6	0,4761	0,6249	0,2985	0,0049
7	0,4617	0,6192	0,2888	0,0037
8	0,4472	0,6134	0,282	0,0035
9	0,4296	0,5983	0,2696	0,0031

Table C8 – Effect of the BL/ P-25 Degussa TiO_2 system on Reactive Violet 5 decolorization: experimental conditions and absorbances.

Test name	V_{sol} (mL)	pH	C_{RV5} (ppm)	(P-25 Degussa) TiO_2 (g/L)	Q_{air} (l/h)	Rpm	dark time (h)	irradiation time (h)	n° of samplings
26	50	uncontrolled	30	**3**	15	900	1	9	11

time (h)	A (559 nm)	A (221 nm)	A (327 nm)	A (750 nm)
-1	0,5633	0,6063	0,3507	0,0076
0	0,5725	0,6571	0,3446	0,0053
1	0,5675	0,7182	0,3478	0,0058
2	0,5467	0,7326	0,3387	0,0046
3	0,5178	0,7272	0,319	-0,0001
4	0,5167	0,7537	0,3215	0,004
5	0,5044	0,7628	0,3132	0,0012
6	0,4976	0,8026	0,3185	0,0045
7	0,4713	0,7944	0,3065	0,0045
8	0,4573	0,7942	0,2985	0,0058
9	0,4351	0,7853	0,2895	0,0073

Table C9 – Effect of the BL/ Fe- TiO_2 (10 mg Fe) system on Reactive Violet 5 decolorization: experimental conditions and absorbances.

Test name	V_{sol} (mL)	pH	C_{RV5} (ppm)	Fe-TiO_2 (10 mg Fe) (g/L)	Q_{air} (l/h)	Rpm	dark time (h)	irradiation time (h)	n° of samplings
27	50	uncontrolled	30	**3**	15	900	1	9	11

time (h)	A (559 nm)	A (221 nm)	A (327 nm)	A (750 nm)
-1	0,5597	0,5736	0,3466	0,0075
0	0,5382	0,5566	0,3243	0,0044
1	0,5031	0,5563	0,309	0,0047
2	0,46	0,5424	0,2869	0,0054
3	0,4529	0,5711	0,2851	0,0075
4	0,4403	0,5903	0,2815	0,0043
5	0,4138	0,5839	0,267	0,004
6	0,401	0,5901	0,2619	0,0048
7	0,3875	0,5911	0,2549	0,0039
8	0,3775	0,5973	0,2504	0,0054
9	0,3483	0,586	0,2354	0,0046

Table C10 – Effect of the BL/ Fe- TiO_2 (10 mg Fe) system on Reactive Violet 5 decolorization: experimental conditions and absorbances.

Test name	V_{sol} (mL)	pH	C_{RV5} (ppm)	Fe-TiO_2 (10 mg Fe) (g/L)	Q_{air} (l/h)	Rpm	dark time (h)	irradiation time (h)	n° of samplings
27-bis	50	uncontrolled	30	**3**	15	900	1	9	11

time (h)	A (559 nm)	A (221 nm)	A (327 nm)	A (750 nm)
-1	0,552	0,5803	0,3378	0,0065
0	0,5424	0,5547	0,3254	0,0042
1	0,503	0,5563	0,3081	0,0045
2	0,4681	0,5759	0,2964	0,007
3	0,4346	0,5796	0,2784	0,0051
4	0,4112	0,5914	0,2688	0,005
5	0,3872	0,5951	0,256	0,004
6	0,365	0,5932	0,2449	0,0039
7	0,3437	0,5724	0,2258	0,0014
8	0,323	0,5822	0,2224	0,0036
9	0,3172	0,5883	0,22	0,0036

Table C11 – Effect of the BL/ Fe- TiO_2 (50 mg Fe) system on Reactive Violet 5 decolorization: experimental conditions and absorbances.

Test name	V_{sol} (mL)	pH	C_{RV5} (ppm)	Fe-TiO_2 (50 mg Fe) (g/L)	Q_{air} (l/h)	rpm	dark time (h)	irradiation time (h)	n° of samplings
28	50	uncontrolled	30	**3**	15	900	1	9	11

time (h)	A (559 nm)	A (221 nm)	A (327 nm)	A(750 nm)
-1	0,5373	0,5633	0,3268	0,0032
0	0,562	0,5855	0,3389	-0,004
1	0,5412	0,6477	0,3332	0,0128
2	0,4816	0,6554	0,3051	0,003
3	0,4594	0,6874	0,3005	0,0053
4	0,4274	0,6769	0,2821	0,0042
5	0,4052	0,6823	0,2702	0,0036
6	0,3748	0,6759	0,2504	0,0019
7	0,3449	0,6701	0,2519	0,0013
8	0,3234	0,6455	0,2115	0,0044
9	0,2997	0,6504	0,2265	0,0031

Table C12 – Effect of the BL/ Fe- TiO_2 (50 mg Fe) system on Reactive Violet 5 decolorization: experimental conditions and absorbances.

Test name	V_{sol} (mL)	pH	C_{RV5} (ppm)	Fe-TiO_2 (50 mg Fe) (g/L)	Q_{air} (l/h)	rpm	dark time (h)	irradiation time (h)	n° of samplings
28-bis	50	uncontrolled	30	**3**	15	900	1	9	11

time (h)	A (559 nm)	A (221 nm)	A (327 nm)	A(750 nm)
-1	0,5545	0,6001	0,3443	0,0084
0	0,5261	0,5492	0,3156	0,0041
1	0,4987	0,5844	0,3069	0,0049
2	0,4645	0,6002	0,293	0,0051
3	0,4269	0,598	0,2733	0,0042
4	0,3984	0,595	0,2587	0,0043
5	0,3864	0,6138	0,256	0,0049
6	0,3693	0,6032	0,2455	0,0038
7	0,3559	0,5997	0,2364	0,004
8	0,3388	0,597	0,2266	0,0069
9	0,2944	0,5841	0,2038	0,0032

Table C13 – Effect of the BL/ Fe- TiO_2 (100 mg Fe) system on Reactive Violet 5 decolorization: experimental conditions and absorbances.

Test name	V_{sol} (mL)	pH	C_{RV5} (ppm)	Fe-TiO_2 (100 mg Fe) (g/L)	Q_{air} (l/h)	Rpm	dark time (h)	irradiation time (h)	n° samples
29	50	uncontrolled	30	**3**	15	900	1	9	11

time (h)	A (559 nm)	A (221 nm)	A (327 nm)	A(750 nm)
-1	0,5293	0,5595	0,3228	0,0048
0	0,5122	0,5239	0,3065	0,0049
1	0,4661	0,5465	0,2911	0,006
2	0,4497	0,5603	0,2857	0,0066
3	0,4086	0,5393	0,2588	0,0034
4	0,3879	0,5945	0,2687	0,004
5	0,3696	0,5474	0,2417	0,0034
6	0,3552	0,5689	0,2371	0,0048
7	0,3428	0,5793	0,2422	0,0099
8	0,3101	0,5347	0,2106	0,003
9	0,2954	0,5341	0,2047	0,0069

Table C14 – Effect of the BL on Reactive Violet 5 decolorization: experimental conditions and absorbances.

Test name	V_{sol} (mL)	pH	C_{RV5} (ppm)	catalyst (g/L)	Q_{air} (l/h)	Rpm	dark time (h)	irradiation time (h)	n° of samplings
30	50	uncontrolled	30	**absent**	15	900	0	9	10

time (h)	A (559 nm)	A (221 nm)	A (327 nm)	A (750 nm)
0	0,5607	0,5675	0,3412	0,008
1	0,5373	0,589	0,324	0,0047
2	0,531	0,5836	0,3169	0,0004
3	0,535	0,6161	0,3241	0,0039
4	0,5316	0,6273	0,3238	0,0046
5	0,5481	0,6559	0,3353	0,0051
6	0,5452	0,6566	0,3354	0,0053
7	0,5459	0,6571	0,3357	0,0053
8	0,5476	0,6579	0,3367	0,0049
9	0,5481	0,6588	0,3372	0,0051

Table C15 – Effect of the pH on the Reactive Violet 5 decolorization carried out in the presence of the BL/Fe-TiO_2 (50 mg Fe) system: experimental conditions and absorbances.

Test name	V_{sol} (mL)	pH	C_{RV5} (ppm)	Fe-TiO_2 (50 mg Fe) (g/L)	Q_{air} (l/h)	Rpm	dark time (h)	irradiation time (h)	n° of samplings
31	50	**12**	30	3	15	900	1	9	11

time (h)	A (559 nm)	A (221 nm)	A (327 nm)	A (750 nm)
-1	0,6275	1,0382	0,4058	0,0084
0	0,5884	0,997	0,3786	-0,0006
1	0,5905	1,2702	0,4042	0,0056
2	0,5645	1,4406	0,4061	0,0053
3	0,5076	1,5416	0,3885	0,0053
4	0,4531	1,6531	0,3641	0,004
5	0,3709	1,6629	0,3184	0,0043
6	0,281	1,7391	0,2841	0,0036
7	0,2073	1,7446	0,2504	0,004
8	0,1433	1,7178	0,2123	0,0028
9	0,098	1,692	0,1852	0,0019

Table C16 – Effect of the pH on the Reactive Violet 5 decolorization carried out in the presence of the BL/Fe-TiO_2 (50 mg Fe) system: experimental conditions and absorbances.

Test name	V_{sol} (mL)	pH	C_{RV5} (ppm)	Fe-TiO_2 (50 mg Fe) (g/L)	Q_{air} (l/h)	Rpm	dark time (h)	irradiation time (h)	n° of samplings
31-bis	50	**12**	30	3	15	900	1	9	11

time (h)	A (559 nm)	A (221 nm)	A (327 nm)	A (750 nm)
-1	0,5626	0,9695	0,3716	0,0108
0	0,5452	0,9415	0,3436	0,0018
1	0,4959	1,3537	0,3566	0,006
2	0,4871	1,5714	0,3647	0,004
3	0,4687	1,6825	0,3671	0,0057
4	0,408	1,6632	0,311	-0,0041
5	0,3718	1,6887	0,3081	0,0115
6	0,2902	1,7694	0,2963	0,004
7	0,1968	1,7186	0,293	0,002
8	0,1517	1,5278	0,2489	0,0037
9	0,1064	0,9897	0,1374	0,0016

Table C17 – Effect of the pH on the Reactive Violet 5 decolorization carried out in the presence of the BL/Fe-TiO_2 (50 mg Fe) system: experimental conditions and absorbances.

Test name	V_{sol} (mL)	pH	C_{RV5} (ppm)	Fe-TiO_2 (50 mg Fe) (g/L)	Q_{air} (l/h)	rpm	dark time (h)	irradiation time (h)	n° of samplings
32	50	**4**	30	3	15	900	1	9	11

time (h)	A (559 nm)	A (221 nm)	A (327 nm)	A (750 nm)
-1	0,5624	2,5127	0,3409	0,0043
0	0,5252	2,3867	0,3141	0,003
1	0,5046	2,3579	0,3066	0,0106
2	0,5087	2,4413	0,3112	0,0039
3	0,4967	2,3987	0,3059	0,0042
4	0,5134	2,478	0,3289	0,0062
5	0,5032	2,4593	0,3249	0,007
6	0,4968	2,4119	0,3091	0,0062
7	0,4925	2,4099	0,3063	0,005
8	0,4868	2,3919	0,3041	0,0046
9	0,5071	2,4353	0,3193	0,0153

Table C18 – Effect of the pH on the Reactive Violet 5 decolorization carried out in the presence of the BL/Fe-TiO_2 (50 mg Fe) system: experimental conditions and absorbances.

Test name	V_{sol} (mL)	pH	C_{RV5} (ppm)	Fe-TiO_2 (50 mg Fe) (g/L)	Q_{air} (l/h)	Rpm	dark time (h)	irradiation time (h)	n° of samplings
34	50	**6**	30	3	15	900	1	9	11

time (h)	A (559 nm)	A (221 nm)	A (327 nm)	A (750 nm)
-1	0,6224	0,7288	0,3793	0,0062
0	0,6302	0,7762	0,3907	0,0054
1	0,6176	0,7736	0,3806	0,0064
2	0,6096	0,7608	0,3747	0,0083
3	0,5904	0,7448	0,3616	0,0051
4	0,5783	0,7242	0,3422	-0,0043
5	0,594	0,7831	0,371	0,0066
6	0,5945	0,7928	0,376	0,012
7	0,5804	0,772	0,3623	-0,0036
8	0,5812	0,776	0,3604	0,004
9	0,5991	0,7916	0,3688	0,0033

Table C19 – Effect of the pH on the Reactive Violet 5 decolorization carried out in the presence of the BL/Fe-TiO_2 (50 mg Fe) system: experimental conditions and absorbances.

Test name	V_{sol} (mL)	pH	C_{RV5} (ppm)	Fe-TiO_2 (50 mg Fe) (g/L)	Q_{air} (l/h)	Rpm	dark time (h)	irradiation time (h)	n° of samplings
35	50	**8**	30	3	15	900	1	9	11

time (h)	A (559 nm)	A (221 nm)	A (327 nm)	A (750 nm)
-1	0,6782	0,7653	0,4261	0,008
0	0,6583	0,7275	0,41	0,0098
1	0,6433	0,7571	0,4007	0,0027
2	0,6544	0,8213	0,4176	0,0087
3	0,638	0,7824	0,3963	0,0031
4	0,6223	0,8374	0,4216	0,0193
5	0,6163	0,8222	0,4089	0,0068
6	0,6132	0,8056	0,3932	0,0055
7	0,6126	0,8206	0,3996	0,0002
8	0,5952	0,7951	0,3842	0,0049
9	0,5942	0,7936	0,3903	0,0034

Table C20 – Effect of the pH on the Reactive Violet 5 decolorization carried out in the presence of the BL/Fe-TiO_2 (50 mg Fe) system: experimental conditions and absorbances.

Test name	V_{sol} (mL)	pH	C_{RV5} (ppm)	Fe-TiO_2 (50 mg Fe) (g/L)	Q_{air} (l/h)	Rpm	dark time (h)	irradiation time (h)	n° of samplings
35-bis	50	**8**	30	3	15	900	1	9	11

time (h)	A (559 nm)	A (221 nm)	A (327 nm)	A (750 nm)
-1	0,6349	0,7263	0,4082	0,0125
0	0,6179	0,6692	0,3792	0,0053
1	0,6083	0,7265	0,3768	0,005
2	0,5899	0,7806	0,3701	0,0068
3	0,5936	0,7886	0,3736	0,005
4	0,563	0,7468	0,3575	0,0061
5	0,5821	0,8042	0,3699	0,0076
6	0,5847	0,82	0,3805	0,0147
7	0,5518	0,7907	0,3587	0,0074
8	0,5386	0,7357	0,33	0,0003
9	0,5382	0,6889	0,3128	-0,0049

Table C21 – Effect of the pH on the Reactive Violet 5 decolorization carried out in the presence of the BL/Fe-TiO_2 (50 mg Fe) system: experimental conditions and absorbances.

Test name	V_{sol} (mL)	pH	C_{RV5} (ppm)	Fe-TiO_2 (50 mg Fe) (g/L)	Q_{air} (l/h)	Rpm	dark time (h)	irradiation time (h)	n° of samplings
36	50	**10**	30	3	15	900	1	2	4

time (h)	A (559 nm)	A (221 nm)	A (327 nm)	A (750 nm)
-1	0,5036	0,999	0,3167	0,0071
0	0,4921	1,0741	0,3549	0,0033
1	0,1512	0,9529	0,1791	0,0083
2	0,0218	0,7499	0,0739	0,0008

Table C22 – Effect of the pH on the Reactive Violet 5 decolorization carried out in the presence of the BL/Fe-TiO_2 (50 mg Fe) system: experimental conditions and absorbances.

Test name	V_{sol} (mL)	pH	C_{RV5} (ppm)	Fe-TiO_2 (50 mg Fe) (g/L)	Q_{air} (l/h)	rpm	dark time (h)	irradiation time (h)	n° of samplings
36-bis	50	**10**	30	3	15	900	1	2	4

time (h)	A (559 nm)	A (221 nm)	A (327 nm)	A (750 nm)
-1	0,5026	0,9743	0,3118	0,0042
0	0,4861	0,9873	0,3435	0,0093
1	0,158	0,8748	0,1745	0,0063
2	0,0315	0,7528	0,091	0,0024

Table C23 – Effect of the catalyst concentration on the Reactive Violet 5 decolorization carried out in the presence of the BL/Fe-TiO_2 (50 mg Fe) system: experimental conditions and absorbances.

Test name	V_{sol} (mL)	pH	C_{RV5} (ppm)	Fe-TiO_2 (50 mg Fe) (g/L)	Q_{air} (l/h)	Rpm	dark time (h)	irradiation time (h)	n° of samplings
37	50	10	30	**6**	15	900	1	2	4

time (h)	A (559 nm)	A (221 nm)	A (327 nm)	A (750 nm)
-1	0,5095	1,0988	0,321	0,0052
0	0,5063	1,1774	0,4402	0,0058
1	0,1232	0,9366	0,1648	0,0062
2	0,0113	0,8526	0,0798	0,0012

Table C24 – Effect of the catalyst concentration on the Reactive Violet 5 decolorization carried out in the presence of the BL/Fe-TiO_2 (50 mg Fe) system: experimental conditions and absorbances.

Test name	V_{sol} (mL)	pH	C_{RV5} (ppm)	Fe-TiO_2 (50 mg Fe) (g/L)	Q_{air} (l/h)	Rpm	dark time (h)	irradiation time (h)	n° of samplings
37-bis	50	10	30	**6**	15	900	1	2	4

time (h)	A (559 nm)	A (221 nm)	A (327 nm)	A (750 nm)
-1	0,5026	0,9743	0,3118	0,0042
0	0,4526	0,9742	0,3234	0,0065
1	0,0932	0,8246	0,149	0,0103
2	0,016	0,7619	0,0866	0,0049

Table C25 – Effect of the catalyst concentration on the Reactive Violet 5 decolorization carried out in the presence of the BL/Fe-TiO_2 (50 mg Fe) system: experimental conditions and absorbances.

Test name	V_{sol} (mL)	pH	C_{RV5} (ppm)	Fe-TiO_2 (50 mg Fe) (g/L)	Q_{air} (l/h)	Rpm	dark time (h)	irradiation time (h)	n° of samplings
38	50	10	30	**1.5**	15	900	1	2.5	5

time (h)	A (559 nm)	A (221 nm)	A (327 nm)	A (750 nm)
-1	0,4969	1,0103	0,3084	0,0044
0	0,4943	1,0231	0,3195	0,003
1	0,296	0,9984	0,2205	0,0051
2	0,1195	0,9246	0,1333	0,0032
2,5	0,0537	0,9043	0,0995	0,0038

Table C26 – Effect of the catalyst concentration on the Reactive Violet 5 decolorization carried out in the presence of the BL/Fe-TiO_2 (50 mg Fe) system: experimental conditions and absorbances.

Test name	V_{sol} (mL)	pH	C_{RV5} (ppm)	Fe-TiO_2 (50 mg Fe) (g/L)	Q_{air} (l/h)	Rpm	dark time (h)	irradiation time (h)	n° of samplings
38-bis	50	10	30	**1.5**	15	900	1	2.5	5

time (h)	A (559 nm)	A (221 nm)	A (327 nm)	A (750 nm)
-1	0,5251	1,1115	0,3308	0,0044
0	0,5334	1,2698	0,4172	0,0054
1	0,2942	1,0826	0,2567	0,0058
2	0,1046	0,9534	0,1364	0,0044
2,5	0,0462	0,9167	0,1024	0,0039

Table C27 – Effect of the catalyst concentration on the Reactive Violet 5 decolorization carried out in the presence of the BL/Fe-TiO_2 (50 mg Fe) system: experimental conditions and absorbances.

Test name	V_{sol} (mL)	pH	C_{RV5} (ppm)	Fe-TiO_2 (50 mg Fe) (g/L)	Q_{air} (l/h)	rpm	dark time (h)	irradiation time (h)	n° samplings
39	50	10	30	**4.5**	15	900	1	2	4

time (h)	A (559 nm)	A (221 nm)	A (327 nm)	A (750 nm)
-1	0,5026	0,9743	0,3118	0,0042
0	0,4806	1,0899	0,3677	0,0057
1	0,1237	0,862	0,1514	0,0034
2	0,0187	0,7787	0,0872	0,0045

Table C28 – Effect of the catalyst concentration on the Reactive Violet 5 decolorization carried out in the presence of the BL/Fe-TiO_2 (50 mg Fe) system: experimental conditions and absorbances.

Test name	V_{sol} (mL)	pH	C_{RV5} (ppm)	Fe-TiO_2 (50 mg Fe) (g/L)	Q_{air} (l/h)	Rpm	dark time (h)	irradiation time (h)	n° of samplings
40	50	10	30	**0.5**	15	900	1	4	7

time (h)	A (559 nm)	A (221 nm)	A (327 nm)	A (750 nm)
-1	0,5102	1,019	0,3119	0,0007
0	0,495	1,0049	0,3091	0,0039
1	0,3602	0,963	0,2339	0,0006
2	0,1835	0,9039	0,1584	0,006
3	0,0925	0,9063	0,1134	0,0019
3,5	0,065	0,8954	0,0985	0,0017
4	0,0338	0,4448	0,0506	0

Table C29 – Effect of the catalyst concentration on the Reactive Violet 5 decolorization carried out in the presence of the BL/Fe-TiO_2 (50 mg Fe) system: experimental conditions and absorbances.

Test name	V_{sol} (mL)	pH	C_{RV5} (ppm)	Fe-TiO_2 (50 mg Fe) (g/L)	Q_{air} (l/h)	Rpm	dark time (h)	irradiation time (h)	n° of samplings
36	50	10	30	**3**	15	900	1	2	4

time (h)	A (559 nm)	A (221 nm)	A (327 nm)	A (750 nm)
-1	0,5036	0,999	0,3167	0,0071
0	0,4921	1,0741	0,3549	0,0033
1	0,1512	0,9529	0,1791	0,0083
2	0,0218	0,7499	0,0739	0,0008

Table C30 – Effect of the catalyst concentration on the Reactive Violet 5 decolorization carried out in the presence of the BL/Fe-TiO_2 (50 mg Fe) system: experimental conditions and absorbances.

Test name	V_{sol} (mL)	pH	C_{RV5} (ppm)	Fe-TiO_2 (50 mg Fe) (g/L)	Q_{air} (l/h)	Rpm	dark time (h)	irradiation time (h)	n° of samplings
36-bis	50	10	30	**3**	15	900	1	2	4

time (h)	A (559 nm)	A (221 nm)	A (327 nm)	A (750 nm)
-1	0,5026	0,9743	0,3118	0,0042
0	0,4861	0,9873	0,3435	0,0093
1	0,158	0,8748	0,1745	0,0063
2	0,0315	0,7528	0,091	0,0024

Table C31 –Reactive Violet 5 decolorization carried out under exposure to BL: experimental conditions and absorbances.

Test name	V_{sol} (mL)	pH	C_{RV5} (ppm)	catalyst (g/L)	Q_{air} (l/h)	Rpm	dark time (h)	irradiation time (h)	n° of samplings
41	50	10	30	**Absent**	15	900	0	9	10

time (h)	A (559 nm)	A (221 nm)	A (327 nm)	A (750 nm)
0	0,4844	0,7803	0,3068	0,0081
1	0,462	0,8354	0,2951	0,0074
2	0,4362	0,8821	0,3042	0,0186
3	0,3586	0,8835	0,2427	-0,0037
4	0,3003	0,8084	0,2126	0,0094
5	0,2785	0,9269	0,2416	0,0184
6	0,2057	0,8225	0,1701	0,0049
7	0,1679	0,8194	0,1536	0,0051
8	0,1317	0,7569	0,1337	0,0039
9	0,1085	0,7937	0,1216	0,0047

Table C32 – Effect of the H_2O_2 concentration on the Reactive Violet 5 decolorization carried out in the presence of the BL/Fe-TiO_2 (50 mg Fe) system: experimental conditions and absorbances.

Test name	V_{sol} (mL)	pH	C_{RV5} (ppm)	H_2O_2 (mM)	Fe-TiO_2 (50 mg Fe) (g/L)	Q_{air} (l/h)	rpm	dark time (h)	irradiation time (h)	n° of samplings
42	50	10	30	**60**	3	15	900	1	2	6

time (h)	A (559 nm)	A (221 nm)	A (327 nm)	A (750 nm)
-1	0,6044	1,1749	0,3813	0,0041
0	0,623	10	0,9222	0,0186
0,5	0,5007	5,9295	1,1569	0,0384
1	0,2236	2,0651	0,7627	0,0188
1,5	0,061	1,0933	0,2349	0,0076
2	0,0202	0,9681	0,1593	0,0035

Table C33 – Effect of the H_2O_2 concentration on the Reactive Violet 5 decolorization carried out in the presence of the BL/Fe-TiO_2 (50 mg Fe) system: experimental conditions and absorbances.

Test name	V_{sol} (mL)	pH	C_{RV5} (ppm)	H_2O_2 (mM)	Fe-TiO_2 (50 mg Fe) (g/L)	Q_{air} (l/h)	rpm	dark time (h)	irradiation time (h)	n° of samplings
42-bis	50	10	30	**60**	3	15	900	1	2	6

time (h)	A (559 nm)	A (221 nm)	A (327 nm)	A (750 nm)
-1	0,599	1,0531	0,3687	0,0059
0	0,6167	10	0,8476	0,0144
0,5	0,4964	5,7442	0,9238	0,0201
1	0,3066	2,115	0,8004	0,022
1,5	0,0781	1,3767	0,3996	0,0171
2	0,0178	0,932	0,1082	0,0007

Table C34 – Effect of the H_2O_2 concentration on the Reactive Violet 5 decolorization carried out in the presence of the BL/Fe-TiO_2 (50 mg Fe) system: experimental conditions and absorbances.

Test name	V_{sol} (mL)	pH	C_{RV5} (ppm)	H_2O_2 (mM)	Fe-TiO_2 (50 mg Fe) (g/L)	Q_{air} (l/h)	rpm	dark time (h)	irradiation time (h)	n° of samplings
43	50	10	30	**40**	3	15	900	1	2	6

time (h)	A (559 nm)	A (221 nm)	A (327 nm)	A (750 nm)
-1	0,4561	0,9451	0,2904	0,0044
0	0,4561	3,9623	0,3113	0,0001
0,5	0,3715	3,1162	0,3505	0,0041
1	0,2185	1,1545	0,2496	0,0029
1,5	0,0744	0,9391	0,121	0,0014
2	0,0241	1,0218	0,1552	0,0043

Table C35 – Effect of the H_2O_2 concentration on the Reactive Violet 5 decolorization carried out in the presence of the BL/Fe-TiO_2 (50 mg Fe) system: experimental conditions and absorbances.

Test name	V_{sol} (mL)	pH	C_{RV5} (ppm)	H_2O_2 (mM)	Fe-TiO_2 (50 mg Fe) (g/L)	Q_{air} (l/h)	rpm	dark time (h)	irradiation time (h)	n° of samplings
44	50	10	30	**20**	3	15	900	1	2	6

time (h)	A (559 nm)	A (221 nm)	A (327 nm)	A (750 nm)
-1	0,6122	1,12	0,3807	0,0071
0	0,6059	2,9565	0,5723	0,0104
0,5	0,4985	2,0665	0,7814	0,015
1	0,2496	1,2942	0,4041	0,0086
1,5	0,0658	0,1927	0,0651	0,0081
2	0,0658	1,0342	0,1931	0,0011

Table C36 – Effect of the H_2O_2 concentration on the Reactive Violet 5 decolorization carried out in the presence of the BL/Fe-TiO_2 (50 mg Fe) system: experimental conditions and absorbances.

Test name	V_{sol} (mL)	pH	C_{RV5} (ppm)	H_2O_2 (mM)	Fe-TiO_2 (50 mg Fe) (g/L)	Q_{air} (l/h)	rpm	dark time (h)	irradiation time (h)	n° of samplings
44-bis	50	10	30	**20**	3	15	900	1	2	6

time (h)	A (559 nm)	A (221 nm)	A (327 nm)	A (750 nm)
-1	0,6044	1,1749	0,3813	0,0041
0	0,6347	3,2251	0,7459	0,0135
0,5	0,5533	2,5109	0,9854	0,0261
1	0,2917	1,6965	0,6944	0,028
1,5	0,0766	1,1801	0,3029	0,0083
2	0,0242	1,0435	0,1684	0,0035

Table C37 – Effect of the H_2O_2 concentration on the Reactive Violet 5 decolorization carried out in the presence of the BL/Fe-TiO_2 (50 mg Fe) system: experimental conditions and absorbances.

Test name	V_{sol} (mL)	pH	C_{RV5} (ppm)	H_2O_2 (mM)	Fe-TiO_2 (50 mg Fe) (g/L)	Q_{air} (l/h)	rpm	dark time (h)	irradiation time (h)	n° of samplings
44-ter	50	10	30	**20**	3	15	900	1	2	6

time (h)	A (559 nm)	A (221 nm)	A (327 nm)	A (750 nm)
-1	0,6122	1,12	0,3807	0,0071
0	0,6188	3,1344	0,7245	0,0112
0,5	0,5402	2,2104	0,72	0,0141
1	0,3145	1,2258	0,3875	0,0096
1,5	0,1174	0,9699	0,1813	0,0038
2	0,0271	0,9632	0,1381	0,0012

Table C38 – Effect of the H_2O_2 concentration on the Reactive Violet 5 decolorization carried out in the presence of the BL/Fe-TiO_2 (50 mg Fe) system: experimental conditions and absorbances.

Test name	V_{sol} (mL)	pH	C_{RV5} (ppm)	H_2O_2 (mM)	Fe-TiO_2 (50 mg Fe) (g/L)	Q_{air} (l/h)	rpm	dark time (h)	irradiation time (h)	n° of samplings
45	50	10	30	**80**	3	15	900	1	2	6

time (h)	A (559 nm)	A (221 nm)	A (327 nm)	A (750 nm)
-1	0,5353	1,0468	0,3338	0,0036
0	0,5235	5,7988	0,4288	0,0028
0,5	0,4231	10	0,6266	0,0023
1	0,2746	5,617	0,5956	0,0045
1,5	0,095	1,6795	0,3539	0,0026
2	0,019	1,1463	0,166	-0,0005

Table C39 – Effect of the H_2O_2 concentration on the Reactive Violet 5 decolorization carried out in the presence of the BL/Fe-TiO_2 (50 mg Fe) system: experimental conditions and absorbances.

Test name	V_{sol} (mL)	pH	C_{RV5} (ppm)	H_2O_2 (mM)	Fe-TiO_2 (50 mg Fe) (g/L)	Q_{air} (l/h)	rpm	dark time (h)	irradiation time (h)	n° of samplings
46	50	10	30	**100**	3	15	900	1	2	6

time (h)	A (559 nm)	A (221 nm)	A (327 nm)	A (750 nm)
-1	0,5	1,0685	0,4545	0,0044
0	0,4915	10	0,9563	0,0047
0,5	0,4393	10	0,9459	0,0205
1	0,306	3,8448	0,6265	0,0253
1,5	0,1131	1,8138	0,9451	0,0137
2	0,0431	1,3289	0,6265	0,0089

Table C40 – Effect of the H_2O_2 concentration on the Reactive Violet 5 decolorization carried out in the presence of the BL/Fe-TiO_2 (50 mg Fe) system: experimental conditions and absorbances.

Test name	V_{sol} (mL)	pH	C_{RV5} (ppm)	H_2O_2 (mM)	Fe-TiO_2 (50 mg Fe) (g/L)	Q_{air} (l/h)	rpm	dark time (h)	irradiation time (h)	n° of samplings
46-bis	50	10	30	**100**	3	15	900	1	2	4

time (h)	A (559 nm)	A (221 nm)	A (327 nm)	A (750 nm)
-1	0,5367	0,9983	0,3431	0,0125
0	0,5104	10	0,4359	0,005
1	0,2634	5,4523	0,6691	0,0025
2	0,052	1,3737	0,2612	0,0051

Table C41 – Effect of the H_2O_2 concentration on the Reactive Violet 5 decolorization carried out in the presence of the BL/Fe-TiO_2 (50 mg Fe) system: experimental conditions and absorbances.

Test name	V_{sol} (mL)	pH	C_{RV5} (ppm)	H_2O_2 (mM)	Fe-TiO_2 (50 mg Fe) (g/L)	Q_{air} (l/h)	rpm	dark time (h)	irradiation time (h)	n° of samplings
47	50	10	30	**10**	3	15	900	1	2	6

time (h)	A (559 nm)	A (221 nm)	A (327 nm)	A (750 nm)
-1	0,4864	0,9693	0,3045	0,0051
0	0,4864	1,973	0,6316	0,0069
0,5	0,4269	1,395	0,6565	0,0112
1	0,2601	1,0057	0,2756	0,0049
1,5	0,1038	0,908	0,1805	0,002
2	0,0281	0,8706	0,1281	0,0031

Table C42 – Effect of the H_2O_2 concentration on the Reactive Violet 5 decolorization carried out in the presence of the BL/Fe-TiO_2 (50 mg Fe) system: experimental conditions and absorbances.

Test name	V_{sol} (mL)	pH	C_{RV5} (ppm)	H_2O_2 (mM)	Fe-TiO_2 (50 mg Fe) (g/L)	Q_{air} (l/h)	rpm	dark time (h)	irradiation time (h)	n° of samplings
47-bis	50	10	30	**10**	3	15	900	1	2	6

time (h)	A (559 nm)	A (221 nm)	A (327 nm)	A (750 nm)
-1	0,5393	1,0606	0,3372	0,0051
0	0,5493	2,0645	0,5231	0,0069
0,5	0,4831	1,5274	0,5701	0,0112
1	0,3120	1,1376	0,3283	0,0049
1,5	0,1149	0,9703	0,1535	0,002
2	0,0323	0,9382	0,1021	0,0031

Table C43 – Effect of the H_2O_2 concentration on the Reactive Violet 5 decolorization carried out in the presence of the BL/Fe-TiO_2 (50 mg Fe) system: experimental conditions and absorbances.

Test name	V_{sol} (mL)	pH	C_{RV5} (ppm)	H_2O_2 (mM)	Fe-TiO_2 (50 mg Fe) (g/L)	Q_{air} (l/h)	rpm	dark time (h)	irradiation time (h)	n° of samplings
48	50	10	30	**0**	3	15	900	1	2	6

time (h)	A (559 nm)	A (221 nm)	A (327 nm)	A (750 nm)
-1	0,4853	0,9744	0,3059	0,0082
0	0,4815	1,0223	0,3389	0,003
0,5	0,4553	1,18	0,3434	0,0079
1	0,2934	1,0554	0,2406	0,003
1,5	0,1301	1,0043	0,1725	0,006
2	0,0452	0,9543	0,1192	0,0042

References

[1] Zollinger, H. (1987). Synthesis, properties of organic dyes and pigments. *Color Chemistry*. New York, USA: VCH Publishers, 92-102.

[2] Ogugbue, C.J. & Sawidis T. (2011). Bioremediation and detoxification of synthetic wastewater containing triarylmethane dyes by aeromonas hydrophila isolated from industrial effluent. *Biotechnology Research International*, DOI 10.4061/2011/967925.

[3] Couto, S.R. (2009). Dye removal by immobilised fungi. *Biotechnology Advance, 27* (3), 227-235.

[4] O'Neill, C., Hawkes, F. R., Hawkes, D. L., Lourenço, N. D., Pinheiro, H. M., Delée, W. (1999). Colour in textile effluents – sources, measurement, discharge consents and simulation: a review. *Journal of Chemical Technology and Biotechnology, 174* (11), 1009-1018.

[5] Forgacs, E., Cserháti, T., Oros, G. (2004). Removal of synthetic dyes from wastewaters: a review. *Environment International, 30* (7), 953- 971.

[6] Przystaś, W., Zabłocka-Godlewska, E., Grabińska-Sota, E. (2012). Biological removal of azo and triphenylmethane dyes and toxicity of process by-products. *Water Air Soil Pollut., 223* (4), 1581-1592.

[7] Ibrahim, M. B., Poonam, N., Datel, S., Roger, M. (1996). Microbial decolorization of textile dyecontaining effluents: a review. *Bioresource Technology, 58* (3), 217-227.

[8] Wijetunga, S., Li, X. F., Jian, C. (2010). Effect of organic load on decolourization of textile wastewater containing acid dyes in upflow anaerobic sludge blanket reactor. *Journal of Hazardous Materials, 177* (1-3), 792-798.

[9] Chung, K. T. & Cerniglia, C. E. (1992). Mutagenicity of azo dyes: structure-activity relationships. *Mutation Research, 277* (3), 201-220.

[10] Pinheiro, H. M., Touraud, E., Thomas, O. (2004). Aromatic amines from azo dye reduction: status review with emphasis on direct UV spectrophotometric detection in textile industry wastewaters. *Dyes and Pigments, 61* (2), 121-139.

[11] Hao, O. J., Kim, H., Chiang, P. C. (2000). Decolorization of wastewater. *Critical Reviews in Environmental Science and Technology, 30* (4), 449-505.

[12] Firmino, P. I. M., Silva, M. E. R., Cervantes, F. J., Santos, A. B. (2010). Colour removal of dyes from synthetic and real textile wastewaters in one- and two-stage anaerobic systems. *Bioresource Technology, 101*(20), 7773-7779.

[13] Carneiro, P. A., Umbuzeiro, G. A., Oliveira, D. P., Zanoni, M. V. B. (2010). Assessment of water contamination caused by a mutagenic textile effluent/dyehouse effluent bearing disperse dyes. *Journal of Hazardous Materials, 174* (1-3), 694-699.

[14] Allen, R. L. M. (1971). *Colour Chemistry*. London: Thomas Nelson and Sons Ltd. pp 11–13.

[15] Choy, K. K. H., McKay, G., Porter, J.F. (1999). Sorption of acid dyes from effluents using activated carbon. *Resour. Conserv. Recy. 27*, 57-71.

[16] Slokar, Y. M., Le Marechal, A. M. (1997). Methods of decoloration of textile wastewaters. *Dyes Pigments 37*, 335-356.

[17] Kumar, M. N. V. R., Sridhari, T. R., Bhavani, K. D., Dutta, P. K. (1998). Trends in color removal from textile mill effluents. *Colorage 40*, 25-34.

[18] Raghavacharya, C., (1997). Colour removal from industrial effluents – a comparative review of available technologies. *Chem. Eng. World 32*, 53-54.

[19] Rao, K. L. L. N., Krishnaiah, K., Ashutush, (1994). Colour removal from a dye-stuff□industry effluent using activated carbon. *Indian J. Chem. Technol. 1*, 13-19.

[20] Poots, V. J. P., McKay, J. J., (1976). The removal of acid dye from effluent using natural adsorbents. - *I Peat. Water Res. 10*, 1061-1066.

[21] Nigam, P., Armour, G., Banat, I. M., Singh, D., Marchant, R. (2000). Physical removal of textile dyes and solid state fermentation of dye adsorbed agricultural residues. *Bioresour. Technol. 72*, 219-226.

[22] Nigam, P., Banat, I. M., Singh, D., Marchant, R., (1996). Microbial process for the decolorisation of textile effluent containing azo, diazo and reactive dyes. *Process Biochem. 31*, 435-442.

[23] Nigam, P., Marchant, R. (1995). Selection of the substratum for composing biofilm system of textile decolourizing bacteria. *Biotechnol. Lett. 17,* 993-996.

[24] Nawar, S. S., Doma, H. S. (1989). Removal of dyes from effluents using low cost agricultural by-products. *Sci. Tot. Environ. 79,* 271-279.

[25] Nasser, N. M., El-Geundi, M. (1991). Comparative cost of colour removal from textile effuents using natural adsorbents. *J. Chem. Technol. Biotechnol. 50*, 257-264.

[26] Mishra, G., Tripathy, M. (1993). A critical review of the treatments for decolourization of textile effluent. *Colourage 40,* 35-38.

[27] Xu, Y., Lebrun, R. E. (1999). Treatment of textile dye plant effluent by nanofiltration membrane. *Separ. Sci. Technol. 34,* 2501-2519.

[28] Hosono, M., Arai, H., Aizawa, M., Yamamoto, I., Shimizu, K., Sugiyama, M. (1993). Decolorisation and degradation of azo dye in aqueous solution of supersaturated with oxygen by irradiation of high-energy electron beams. *Appl. Rad. Iso. 44*, 1199-1203.

[29] Barr, D. P., Aust, S.D. (1994). Mechanisms white rot fungi use to degrade pollutants. Environ. *Sci. Technol. 28,* 320-328.

[30] Archibald, F., Roy, B. (1992). Production of marganic chelates by laccase from the lignin degrading fungus Trametes versicolor. *Appl. Environ. Microbiol. 58,* 1496-1499.

[31] Thurston, C.F. (1994). The structure and function of fungal laccases. *Microbiology 140,* 19-26.

[32] Kirby, N. (1999). Bioremediation of textile industry wastewater by white rot fungi. D.Phil. Thesis, University of Ulster, Coleraine, UK.

[33] Schliephake, K., Lonergan, G.T. (1996). Laccase variation during dye decolourisation in a 200 L packed-bed bioreactor. *Biotechnol. Lett. 18,* 881-886.

[34] Paszczynski, A., Crawford, R.C. (1995). Potential for bioremediation of xenobiotic compounds by the white-rot fungus Phanerochaete chrysosporium. *Biotechnol. Progr. 11,* 368-379.

[35] Banat, I.M., McMullan, G., Meehan, C., Kirby, N., Nigam, P., Smyth, W.F., Marchant, R. (1999). Microbial decolorization of textile dyes present in textile industries effuent. In: Proceedings of the Industrial Waste Technical Conference, Indianapolis, USA, pp. 1-16.

[36] Banat, I. M., Nigam, P., McMullan, G., Marchant, R., Singh, D. (1997). The isolation of thermophilic bacterial cultures capable of textile dyes decolorization. *Environ. Int. 23,* 547-551.

[37] Banat, I.M., Nigam, P., Singh, D., Marchant, R. (1996). Microbial decolorization of textile-dye-containing effluents: a review. *Bioresour. Technol. 58,* 217-227.

[38] Knapp, J. S., Newby, P. S. (1995). The microbiological decolorization of an industrial effluent containing a diazo-linked chromophore. *Water Res. 7,* 1807-1809.

[39] Nigam, P., Marchant, R., (1995). Selection of the substratum for composing biofilm system of textile decolourizing bacteria. *Biotechnol. Lett. 17,* 993-996.

[40] Ogawa, T., Yatome, C. (1990). Biodegradation of azo dyes in multistage rotating biological contractor immobilized by assimilating bacteria. *Bull. Environ. Contam. Toxicol. 44,* 561-566.

[41] Kulla, M. G. (1981). Aerobic bacterial degradation of azo dyes. Microbial degradation of xerobiotics and recalcitrant compounds. In: Leisinger, T., Cook, A.M., Hutter, R., Nuesch, J. (Eds.), FEMS Symposium, 12. Academic Press, London, pp. 387-399.

[42] Hu, T. L. (1996). Removal of reactive dyes from aqueous solution by different bacterial genera. *Water Sci. Technol. 34,* 89-95.

[43] Hu, T. L. (1992). Sorption of reactive dyes by Aeromonas biomass. *Water Sci. Technol. 26,* 357-366.

[44] Tsezos, M., Bell, J. P. (1989). Comparison of the biosorption and desorption of hazardous organic pollutants by live and dead biomass. *Water Res. 23,* 561-568.

[45] Bustard, M., McHale, A.P. (1998). Biosorpion of heavy metals by distillery-derived biomass. *Bioprocesss Eng. 19,* 351-353.

[46] Modak, A., Natarajan, K. A. (1995). Biosorption of metals using non-living biomass - a review. *Min. Metall. Proc. November,* 189-195.

[47] Zhou, W., Zimmerman, W. (1993). Decolorisation of industrial effluents containing reactive dyes by actinomyces. *Microbiol. Lett. FEMS 107,* 157-162.

[48] Carliell, C. M., Barclay, S. J., Buckley, C. A. (1996). Treatment of exhausted reactive dye bath effluent using anaerobic digestion: laboratory and full scale trials. *Water S.A. 22,* 225-233.

[49] Carliell, C. M., Barclay, S. J., Naidoo, N., Buckely, C. A., Mulholland, D. A, Senior, E. (1995). Microbial decolourisation of reactive azo dye under anaerobic conditions. *Water S.A. 21,* 61-69.

[50] Carliell, C. M., Barclay, S. J, Naidoo, N., Buckely, C. A., Mulholland, D. A, Senior, E. (1994). Anaerobic decolourisation of reactive dyes in conventional sewage treatment processes. *Water S.A. 20,* 341-345.

[51] Slokar, Y. M., Le Marechal, A. M. (1997). Methods of decoloration of textile wastewaters. *Dyes Pigments 37,* 335-356.

[52] Raghavacharya, C. (1997). Colour removal from industrial effluents – a comparative review of available technologies. *Chem. Eng. World 32,* 53-54.

[53] Lin, S. H., Lin, C. M. (1993). Treatment of textile waste effluents by ozonation and chemical coagulation. *Water Res. 27,* 1743-1748.

[54] Ince, N. H., Gonenc, D. T. (1997). Treatability of a textile azo dye by UV/H_2O_2. *Environ. Technol. 18,* 179-185.

[55] Gahr, F., Hermanutz, F., Opperman, W. (1994). Ozonation – an important technique to comply with new German law for textile wastewater treatment. *Water Sci. Technol. 30,* 255-263.

[56] Lopez, A., Ricco, G., Ciannarella, R., Rozzi, A., Di Pinto, A. C., Possino, R. (1999). Textile wastewater reuse: ozonation of membrane concentrated secondary effluent. *Water Sci. Technol. 40,* 99-105.

[57] Groff, K. A., Byung, R. K. (1989). Textile wastes. *J. WPCF 61,* 872-876.

[58] Yang, Y., Wyatt II., D.T., Bahorsky, M. (1998). Decolorization of dyes using UV/H_2O_2 photochemical oxidation. *Text. Chem. Color. 30,* 27-35.

[59] Peralto-Zamora, P., Kunz, A., De Morales, G. S., Pelegrini, R., De Capos Moleiro, P., Reyes, J., Duran, N. (1999). Degradation of reactive dyes: a comparative study of ozonation, enzymatic and photochemical processes. *Chemosphere 38,* 835-852.

[60] Qiao, R. P., Ma, Y. M., Qi, X. H., Li, N., Jin, X. C., Wang, Q. S., Zhuang, Y. Y. (2005). Degradation of microcystin-RR by combination of UV/H_2O_2 technique. *Chin. Chem. Lett., 16* (9), 1271-1274.

[61] Shu, H. Y., & Chang, M. C. (2006). Development of a rate expression for predicting decolorization of C. I. Acid Black 1 in a UV/H_2O_2 process. *Dyes Pigm., 70* (1), 31-37.

[62] Igwe, J. C., Abia, A. A., Ibeh, C. A. (2008). Adsorption kinetics and intraparticulate diffusivities of Hg, As and Pb ions on unmodified and thiolated coconut fiber. *Int. J. Environ. Sci. Tech., 5* (1), 83-92.

[63] Shah, B. A., Shah, V. A., Singh, R. R. (2009). Sorption isotherms and kinetics of chromium uptake from wastewater using natural sorbent material. *Int. J. Environ. Sci. Tech., 6* (1), 77-90.

[64] Alshamsi, F. A., Albadwawi, A. S., Alnuaimi, M. M., Rauf, M. A., Ashraf, S. S. (2007). Comparative efficiencies of the degradation of crystal violet using UV/hydrogen peroxide and fenton's reagent. *Dyes Pigm., 74* (2), 283-287.

[65] C.A. Martínez-Huitle, & E. Brillas, Decontamination of wastewaters containing synthetic organic dyes by electrochemical methods: a general review. *Appl. Catal. B 87* 105–145.

[66] Vlyssides, A.G., Papaioannou, D., Loizidoy, M., Karlis, P.K. & Zorpas, A. A. (2000). Testing an electrochemical method fortreatment of textile dye wastewater. *Waste Manag. 20*, 569-574.

[67] Martínez-Huitle, C. A. And Ferro, S. (2006). Electrochemical oxidation of organic pollutants for the wastewater treatment: direct and indirect processes. *Chem. Soc. Rev. 35*, 1324–1340.

[68] Panizza, M., & Cerisola, G. (2009). Direct and mediated anodic oxidation of organic pollutants. *Chem. Rev. 109*, 6541–6569.

[69] Cañizares, P., Sáez, C., Sánchez-Carretero, A., Rodrigo, M.A. (2009). Synthesis of novel oxidants by electrochemical technology. *J. Appl. Electrochem. 39*, 2143–2149.

[70] Cheng, C.Y. and Kelsall, G. H. (2007). Models of hypochlorite production in electrochemical reactors with plate and porous anodes. *J. Appl. Electrochem. 37*, 1203–1217.

[71] Panizza, M., Kapalka, A., Comninellis, C. (2008). Oxidation of organic pollutants on BDD anodes using modulated current electrolysis. *Electrochim. Acta 53*, 2289–2295.

[72] Scialdone, O., Randazzo, S., Galia, A., Silvestri, G. (2009). Electrochemical oxidation of organics in water: role of operative parameters in the absence and in the presence of NaCl. *Water Res. 43*, 2260–2272.

[73] Polcaro, A.M., Vacca, A., Mascia, M., Palmas, S., Ruiz, J. R. (2009). Electrochemical treatment of waters with BDD anodes: kinetics of the reactions involving chlorides. *J. Appl. Electrochem. 39*, 2083–2092.

[74] Andrade, L. S., Tasso, T. T., Silva, D. L., Rocha-Filho, R. C., Bocchi, N., Biaggio S. R. (2009). On the performances of lead dioxide and boron-doped diamond electrodes in the anodic

oxidation of simulated wastewater containing the Reactive Orange 16 dye. *Electrochim. Acta 54,* 2024–2030.

[75] Saien, J., and Soleymani, A. R. (2007). Degradation and mineralization of Direct Blue 71 in a circulating upflow reactor by UV/TiO_2 process and employing a new method in kinetic study. *J. Hazard. Mater. 144,* 506-512.

[76] Aarthi, T., Narahari, P., Madras, G. (2007). Photocatalytic degradation of Azure and Sudan dyes using nano TiO_2. *J. Hazard. Mater. 149,* 725-734.

[77] Saquib, M., Abu Tariq, M., Haque, M.M., Muneer, M. (2008). Photocatalytic degradation of disperse blue 1 using UV/TiO_2/H_2O_2 process. *J. Environ. Manage. 88,* 300-306.

[78] Huang, M., Xu, C., Wu, Z., Huang, Y., Lin, J., Wu, J. (2008). Photocatalytic discolorization of methylorange solution by Pt modified TiO2 loaded on natural zeolite. *Dyes Pigm.77*, 327-334.

[79] Andronic, L., & Duta, A. (2007). TiO_2 thin films for dyes photodegradation. *Thin Solid Films 515*, 6294-6297.

[80] Liu, H. L., and Chiou, Y. R. (2005). Optimal decolorization efficiency of Reactive Red 239 by UV/TiO_2 photocatalytic process coupled with response surface methodology. *Chem. Eng. J. 112*, 173-179.

[81] Bergamini, R. B. M., Azevedo, E. B., Araújo, L. R. R. (2009). Heterogeneous photocatalytic degradation of reactive dyes in aqueous TiO_2 suspensions: Decolorization kinetics. *Chem. Eng. J. 149*, 215-220.

[82] Zielinska, B., Grzechulska, J., Grzmil, B., Morawski, A. W. (2001). Photocatalytic degradation of Reactive Black 5. A comparison between TiO_2-Tytanpol A11 and TiO_2-Degussa P25 photocatalysts. *Appl. Catal. B 35,* L1-L7.

[83] Alaton, I.A., & Balcioglu, I.A. (2001). Photochemical and heterogeneous photocatalytic degradation of waste vinylsulphone dyes: a case study with hydrolysed Reactive Black 5. *J. Photochem. Photobiol. A Chem. 141*, 247-254.

[84] Muruganandham, M., Sobana, N., Swaminathan, M. (2006). Solar assisted photocatalytic and photochemical degradation of Reactive Black 5. *J. Hazard. Mater. 137,* 1371-1376.

[85] Tang, C., & Chen, V. (2004). The photocatalytic degradation of Reactive Black 5 using TiO_2/UV in an annular photoreactor. *Water Res. 38,* 2775-2781.

[86] Zuorro A., & Lavecchia R. (2014). Evaluation of UV/H_2O_2 advanced oxidation process (AOP) for the degradation of diazo dye Reactive Green 19 in aqueous solution. *Desalination and Water Treatment, 52* (7-9), 1571-1577.

[87] Rajamanickam, D., & Shanthi, M. (2016). Photocatalytic degradation of an organic pollutant by zinc oxide – solar process. *Arabian Journal of Chemistry, 9* (2), S1858-S1868.

[88] Fujishima, A., Rao, T. N., Tryk, D. A. (2000). Titanium dioxide photocatalysis. Jo*urnal of Photochemistry and Photobiology, C 1* (1), 1–21.

[89] Linsebigler, A. L., Lu, G., Yates, J. T. (1995). Photocatalysis on TiO_2 surfaces: principles, mechanisms, and selected results. *Chemical Reviews, 95* (3), 735–758.

[90] Tada, H., Yamamoto, M., Ito, S. (1999). Promoting effect of MgO_x submonolayer coverage of TiO_2 on the photoinduced oxidation of anionic surfactants. *Langmuir, 15* (11), 3699–3702.

[91] Shang, G., Fu, H., Yang, S., Xu, T. (2011). Mechanistic study of visible-light-induced photodegradation of 4-chlorophenol by $TiO_2{-}xN_x$ with low nitrogen concentration. I*nternational Journal of Photoenergy, vol. 2012,* Article ID 759306, 9 pages.

[92] Li, S., Lin, S., Liao, J., Pan, N., Li, D., Li, J. (2012). Nitrogen-doped TiO_2 nanotube arrays with enhanced photoelectrochemical property. *International Journal of Photoenergy, vol. 2012,* Article ID 794207, 7 pages.

[93] Xiang, Q., Yu, J., Wang, W., Jaroniec, M. (2011). Nitrogen self-doped nanosized TiO_2 sheets with exposed 001 facets for enhanced visible-light photocatalytic activity. *Chemical Communications, 47* (24), 6906–6908.

[94] Li, K. Wang, H., Pan, C., Wei, J., Xiong, R., Shi, J. (2012). Enhanced photoactivity of Fe + N codoped anatase-rutile TiO_2 nanowire film under visible light irradiation. *International Journal of Photoenergy, vol. 2012,* Article ID 398508, 8 pages, 2012.

[95] Hu, J., Tang, H., Lin X., et al. (2012). Doped titanium dioxide films prepared by pulsed laser deposition method. *International Journal of Photoenergy, vol. 2012,* Article ID 758539, 8 pages.

[96] Qian, J., Cui, G., Jing, M., Wang, Y., Zhang, M., Yang, J. (2012). Hydrothermal synthesis of nitrogen-doped titanium dioxide and evaluation of its visible light photocatalytic activity. *International Journal of Photoenergy, vol. 2012,* Article ID 198497, 6 pages.

[97] Hu, C. C., Hsu, T.C., Kao, L. H., (2012). One-step cohydrothermal synthesis of nitrogen-doped titanium oxide nanotubes with enhanced visible light photocatalytic activity. *International Journal of Photoenergy, vol. 2012,* Article ID 391958, 9 pages, 2012.

[98] Emeline, A. V., Kuznetsov, V. N., Rybchuk, V. K., Serpone, N. (2008). Visible-light-active titania photocatalysts: the case of N-doped TiO_2 s-properties and some fundamental issues. *International Journal of Photoenergy, vol. 2008,* Article ID 258394, 19 pages.

[99] Wang, J. A., Limas-Ballesteros, R., Lopez, T. et al., (2001). Quantitative determination of titanium lattice defects and solid-state reaction mechanism in iron-doped TiO_2 photocatalysts. *Journal of Physical Chemistry, 105* (40), 9692–9698.

[100] Yu, J. C., Yu, J. G., Zhao J. C. (2002). Enhanced photocatalytic activity of mesoporous and ordinary TiO_2 thin films by sulfuric acid treatment. *Applied Catalysis, 36* (1), 31–43.

[101] Tayade, R. J., Suroliya, P. K., Kulkarni, R. G., Jasra, R. V. (2007). Photocatalytic degradation of dyes and organic contaminants in water using nanocrystalline anatase and rutile TiO_2. *Science and Technology of Advanced Materials, 8* (6), 455–462.

[102] Asahi, R., Morikawa, T., Ohwaki, T., Aoki, K., Taga, Y. (2001). Visible-light photocatalysis in nitrogen-doped titanium oxides. *Science, 293* (5528), 269–271.

[103] H. Irie, Y. Watanabe, and K. Hashimoto, "Nitrogenconcentration dependence on photocatalytic activity of TiO_{2-x} Nx powders," The Journal of Physical Chemistry, vol. 107, no. 23, pp. 5483–5486, 2003.

[104] Sacco, O., Stoller, M., Vaiano, V., Ciambelli, P., Chianese, A., Sannino, D. (2012). Photocatalytic degradation of organic dyes under visible light on N-doped TiO_2 photocatalysts. *International Journal of Photoenergy Volume 2012,* Article ID 626759, 8 pages.

[105] Sato, S. (1986). Photocatalytic activity of NO_x-doped TiO_2 in the visible light region. *Chemical Physics Letters, 123* (1–2), 126-128..

[106] Sakthivel, S., Janczarek, M., Kisch, H. (2004). Visible light activity and photoelectrochemical properties of Nitrogen-Doped TiO_2. *J. Phys. Chem. B, 108* (50), 19384–19387.

[107] Sato, S., Nakamura, R., Abe, S. (2005). Visible-light sensitization of TiO_2 photocatalysts by wet-method N doping. *Applied Catalysis A: General*, *284* (1–2), 131-137 .

[108] Chen, X., & Burda, C. (2004). Photoelectron spectroscopic investigation of Nitrogen-Doped Titania nanoparticles. *J. Phys. Chem. B, 108* (40), 15446–15449.

[109] Sakatani, Y. , Nunoshige, J., Ando, H., Okusako, K., Koike, H., Takata, T., Kondo, J.N., Hara, M., Domen, K. (2003). Photocatalytic decomposition of acetaldehyde under visible light irradiation over La^{3+} and N Co-doped TiO_2. *Chem. Lett., 32* (12) 1156-1157.

[110] Di Valentin, C., Pacchioni, G., Selloni, A., Livraghi, S., Giamello, E. (2005). Characterization of paramagnetic species in N-Doped TiO_2 powders by EPR spectroscopy and DFT calculations. *J. Phys. Chem. B, 109* (23), 11414–11419.

[111] Asahi, R., Morikawa, T., Ohwaki, T., Aoki, K., Taga Y. (2001). Visible-light photocatalysis in Nitrogen-Doped Titanium Oxides. *Science, 293* (5528), 269-271.

[112] Miyauchi, M., Ikezawa, A., Tobimatsu, H., Irie, H., Hashimoto, K. (2004). Zeta potential and photocatalytic activity of nitrogen doped TiO_2 thin films. *Phys. Chem. Chem. Phys. 6*, 865-870.

[113] Lin, Z., Orlov, A., Lambert, R.M., Payne, M.C. (2005). New insights into the origin of visible light photocatalytic activity of nitrogen-doped and oxygen-deficient Anatase TiO_2. *J. Phys. Chem. B, 109* (44), 20948–20952.

[114] Diwald, O., Thompson, T.L., Goralski, E.G., Walck, S.D., Yates, J.T. (2004). The effect of nitrogen ion implantation on the photoactivity of TiO_2 Rutile single crystals. *J. Phys. Chem. B, 108* (1), 52-57.

[115] Diwald, O., Thompson, T.L., Zubkov, T., Goralski, E.G., Walck, S.D., Yates, J.T. (2004). Photochemical activity of Nitrogen-Doped Rutile TiO_2(110) in visible light. *J. Phys. Chem. B, 108* (19) 6004-6008.

[116] Thompson, T.L., & Yates J.T. (2006). Surface science studies of the photoactivation of TiO_2-new photochemical processes. *Chem. Rev., 106* (10) 4428-4453.

[117] Serpone, N. (2006). Is the band gap of pristine TiO_2 narrowed by anion- and cation-doping of Titanium Dioxide in second-generation photocatalysts? *J. Phys. Chem. B, 110* (48), 24287–24293.

[118] Morikawa, T., Asahi, R., Ohwaki, T., Aoki, K., Taga, Y. (2001). Band-gap narrowing of Titanium Dioxide by Nitrogen doping. *Japanese Journal of Applied Physics, 40* (2), Number 6A.

[119] Nakano, Y., Morikawa, T., Ohwaki, T., Taga, Y. (2005). Deep-level optical spectroscopy investigation of N-doped TiO_2 films. *Appl. Phys. Lett., 86* (13), id.132104, 3 pages.

[120] Irie, H., Watanabe, Y., Hashimoto, K. (2003). Nitrogen-concentration dependence on photocatalytic activity of TiO_{2-x} N_x powders. *J. Phys. Chem. B, 107* (23), 5483–5486.

[121] Sathish, M., Viswanathan, B., Viswanath, R.P., Gopinath, C.S. (2005). Synthesis, characterization, electronic structure, and photocatalytic activity of Nitrogen-doped TiO_2 nanocatalyst. *Chem. Mater., 17* (25), 6349–6353.

[122] Yates, H.M., Nolan, M.G., Sheel, D.W., Pemble, M.E. (2006). The role of nitrogen doping on the development of visible light-induced photocatalytic activity in thin TiO_2 films grown on glass by chemical vapour deposition. *Journal of Photochemistry and Photobiology A: Chemistry, 179* (1–2), 213-223.

[123] Banash, M.A., & Croll, S.G. (1999). A quantitative study of polymeric dispersant adsorption onto oxide-coted titania pigments. *Prog. Org. Coat., 35,* 37–44.

[124] Terwilliger, C.D., & Chiang, Y.M. (1993). Characterization of chemically and physically-derived nano-phase titanium dioxide. *Nanostructured Materials, 2,* 37–45.

[125] Hyeok, C., Stathatos, E., Dionysiou, D. (2007). Effect of surfactant in a modified sol on the physicochemical properties and photocatalytic activity of crystalline TiO_2 nanoparticles. *Top. Catal., 44,* 513–521.

[126] Yamahoto, M., & Ohata, M. (1996). New macromolecular silane coupling agents synthesized by living anionic polymerization: grafting of these polymers onto inorganic particles and metals. *Prog. Org. Coat.*, *27*, 277–285.

[127] Shao, Q., Wang, C.G., Zhu,Y.F., Ge, S.S. (2006). Surface modification and characterization of nanometer TiO_2 for nanometer styrene - acrylate emulsion polymerization. *Funct. Mater.*, *37*, 642–645.

[128] Chen, J., Zhou, Y., Nan, Q.L., Sun, Y.Q., Ye, X.Y., Wang, Z.Q. (2007). Synthesis, characterization and infrared emissivity study of polyurethane/TiO_2 nanocomposites. *Appl. Surf. Sci.*, *253*, 9154–9158.

[129] Hojjati, B., Sui, R., Charpentier, P.A. (2007). Synthesis of TiO_2/PAA nanocomposite by RAFT polymerization. *Polymer*, *48*, 5850–5858.

[130] Chio, W.Y., Termin, A., Hoffmann, M.R. (1994). The role of metal ion dopants in quantum-sized TiO_2: correlation between photoreactivity and charge carrier recombination dynamics. *J. Phys. Chem. 98*, 13669–13679.

[131] Chio, W.Y., Termin, A., Hoffmann, M.R. (1994). Effects of metal-ion dopants on the photocatalytic reactivity of quantum-sized TiO_2 particles. *Angew. Chem. Int. Ed.*, *33* (10), 1091–1092.

[132] Zhao,W., Chen, C., Li, X., Zhao, J., Hidaka, H., Serpone, N. (2002). Photodegradation of sulforhodamine-B dye in platinized titania dispersions under visible light irradiation: influence of platinum as a functional co-catalyst. *J. Phys. Chem., B, 106*, 5022–5028.

[133] Liu, Y., Liu, C.Y., Rong, Q., Zhang, Z. (2003). Characteristics of the silver-doped TiO_2 nanoparticles. *Appl. Surf. Sci., 220*, 7–11.

[134] Li, G., Liu, C., Liu, Y. (2006). Different effects of cerium ions doping on properties of anatase and rutile TiO_2. *Appl. Surf. Sci., 253*, 2481–2486.

[135] Chen, X.B., Mao, S.S. (2007). Titanium dioxide nanomaterials: synthesis, properties, modifications, and applications. *Chem. Rev., 107,* 2891–2959.

[136] Belver, C., Bellod, R., Fuerte, A., Fernández-García, M. (2006). Nitrogen containing TiO_2 photocatalysts: part 1. synthesis and solid characterization. *Appl. Catal. B: Environ., 65,* 301–308.

[137] Irie, H., Watanabe,Y.,Hashimoto, K. (2003). Nitrogen-concentration dependence on photocatalytic activity of $TiO_{2-x}N_x$ powders. *J. Phys. Chem. B, 107,* 5483–5486.

[138] Yuan, F.G., Li, P.F., Weng, C.D. (2010). Surface modification of nanosized titanium dioxide with metal- acetylacetonate complexes. *J. Mol. Sci., 26,* 127–135.

[139] Tayade, R. J., Natarajan, T. S., Bajaj, H. C. (2009). Photocatalytic degradation of Methylene Blue dye using ultraviolet light emitting diodes. *Ind. Eng. Chem. Res., 48* (23), 10262–10267.

[140] Chen, D. H., Ye X. J., Li, K.Y. (2005). Oxidation of PCE with a UV LED photocatalytic reactor. *Chem. Eng. Technol., 28,* 95-97.

[141] Autin, O., Romelot, C., Rust, L., Hart, J., Jarvis, P., Mac Adam, J., Parsons, S. A., Jefferson, B. (2013) Evaluation of a UV-light emitting diodes unit for the removal of micropollutants in water for low energy advanced oxidation processes. *Chemosphere, 92* (6) 745-751.

[142] Repo, E., Rengaraj, S., Pulkka, S., Castangnoli, E., Suihkonen, S., Sopanen, M., Sillanpää, M. (2013). Photocatalytic degradation of dyes by CdS microspheres under near UV and blue LED radiation. Separation *and Purification Technology 120,* 206–214

[143] Dai, K., Lu, L., Dawson, G. (2013). Development of UV-LED/TiO_2 device and their application for photocatalytic degradation of methylene blue. *J. Mater. Eng. Perform., 22* (4), 1035-1040.

[144] Joonwichien, S., Yamasue, E., Okumura, H., Ishihara, K. (2011). Effects of magnetic field on photodegradation of Methylene Blue over ZnO and TiO_2 powders using UV-LED as a light source. *J. Chem. Chem. Eng. 5,* 729-737.

[145] Thillai, S. N., Natarajan, K., Bajaj, H. C., Tayade, R. J. (2013). *Advanced functional polymers and composites: materials, devices and allied applications.* Nova Science Pub Inc., vol. 2, UK ed. edition.

[146] Natarajan, K., Thillai, S. N., Bajaj, H. C., Tayade, R. J. (2011). Photocatalytic reactor based on UV-LED/TiO_2 coated quartz tube for degradation of dyes. *Chemical Engineering Journal 178,* 40–49.

[147] Loetscher, L. H., Carey, J. M., Skiles, S. L., Carey, V. M., Boyd, J. E. (2009). Titania−acrylic coil reactor for photocatalytic water purification and sterilization. *Ind. Eng. Chem. Res. 48* (10), 4697–4702.

[148] Dai, K., Lu, L., Zhu, G., Liu, Z., Liu, Q., Chen, Z. (2012). A scalable synthesis technique of novel AgBr microcrystal and its visible light photocatalytic performance. *Materials Letters 87,* 94-96.

[149] Kroeze, J. E., Koehorst, R. B. M., Savenije, T. J. (2004). Singlet and triplet exciton diffusion in a self-organizing porphyrin antenna layer. *Advanced Functional Materials, 14* (10), 992–998.

[150] Winnischofer, H., Formiga, A. L. B., Nakamura, M., Toma, H. E., Araki, K., Nogueira, A.F. (2005) Conduction and photoelectrochemical properties of monomeric and electropolymerized tetraruthenated porphyrin films. *Photochem Photobiol Sci, 4* (4), 359–366.

[151] Ingrosso, C., Petrella, A., Curri, M. L., Striccoli, M., Cosma, P., Cozzoli, P. D., Agostiano, A. (2005). Photoelectrochemical properties of Zn(II) phthalocyanine/ZnO nanocrystals heterojunctions: nanocrystal surface chemistry effect. *Applied Surface Science, 246* (4), 367-371.

[152] Iliev, V. (2002). Phthalocyanine modified titania, catalyst for photooxidation of phenols by irradiation with visible light. *Journal of Photochemistry and Photobiology A: Chemistry, 151* (1-3), 195-199.

[153] Burgeth, G. and Kisch, H. (2002). Photocatalytic and photoelectrochemical properties of titaniachloroplatinate (IV). *Coord. Chem. Rev., 230,* 41–47. 224.

[154] Vaiano, V., Sacco, O., Sannino, D., Ciambelli. P. (2015). Photocatalytic removal of spiramycin from wastewater under visible light with N-doped TiO_2 photocatalysts. C*hemical Engineering Journal, 261*, 3–8.

[155] Souza, M. C. P., Lenzi, G. G., Colpini, L. M. S., Jorge, L. M. M., Santos, O. A. A. (2011). Photocatalytic discoloration of Reactive Blue 5G dye in the presence of mixed of iron and silver. *Brazilian Journal of Chemical Engineering, 28* (3), 393-402.

[156] Gonçalves, M. S. T., Pinto, E. M.S., Nkeonye, P., Oliveira-Campos, A. M .F. (2005). Degradation of C.I. Reactive Orange 4 and its simulated dyebath wastewater by heterogeneous photocatalysis. *Dyes and Pigments, 64* (2), 135-139.

[157] Chatterjee, D., Patnam V. R., Sikdar, A., Joshi, P., Misra, R., Raob, N. N. (2008). Kinetics of the decoloration of reactive dyes over visible light-irradiated TiO_2 semiconductor photocatalyst. *Journal of Hazardous Materials, 156,* 435–441.

[158] Rupa V., Manikandan, A., Divakar, D., Sivakumar, T. (2007). Effect of deposition of Ag on TiO_2 nanoparticles on the photodegradation of Reactive Yellow-17. *Journal of Hazardous Materials, 14* (7), 906–913.

[159] Chung, Y. C. and Chen, C. Y. (2009). Degradation of azo dye reactive violet 5 by TiO_2 photocatalysis. *Environ. Chem. Lett., 7*, 347–352.

[160] Souza, M. C. P., Lenzi, G. G, Colpini, L. M. S., Jorge L. M. M., Santos, O. A. A. (2011). Photocatalytic discoloration of Reactive Blue 5G dye in the presence of mixed oxides and with the addiction of iron and siver. *Brazilian Journal of Chemical Engineering, 28* (3), 393-402.

[161] Thi Dung, N., Van Khoa, N., Herrmann J. M. (2005). Photocatalytic degradation of reactive dye RED-3BA in aqueous TiO_2 suspension under UV-visible light. *International Journal of Photoenergy, 7* (1), 11-15.

[162] Kavitha, S. K. K. and Palanisamy P.N. (2011). Photocatalytic and sonophotocatalytic degradation of Reactive Red 120 using dye sensitized TiO_2 under visible light. *International Journal of Chemical, Molecular, Nuclear, Materials and Metallurgical Engineering, 5* (1), 1-6.

[163] Mendes Saggioro E., Sousa Oliveira A., Pavesi T., Gil Maia C. G., Vieira Ferreira L. F., and Costa Moreira J. (2011). Use of Titanium Dioxide photocatalysis on the remediation of model textile wastewaters containing azo dyes. *Molecules, 16* (12), 10370-10386.

[164] Cabansag, J. L J., Dumelod, J. C., Alfaro, J. C. O., Arsenal, J. D., Sambot, J. C., Enerva, L. T., and Leaño Jr, J. L. (2013). Photocatalytic degradation of aqueous C.I. Reactive Violet 5 using bulk zinc oxide (ZnO) slurry. *Philippine Journal of Science, 142* (1), 77-85.

[165] Saquib, M. And Muneer M. (2002). Semiconductor mediated photocatalysed degradation of an anthraquinone dye, Remazol Brilliant Blue R under sunlight and artificial light source. *Dyes and Pigments 53,* 237–249.

[166] Liu,Y., Chen, X., Li, J., Burda, C. (2005). Photocatalytic degradation of azo dyes by nitrogen-doped TiO_2 nanocatalysts. *Chemosphere, 61,* 11–18.

[167] Chatzisymeon, E., Petrou, C., Mantzavinos, D. (2013). Photocatalytic treatment of textile dyehouse effluents with simulated and natural light. *Global NEST Journal, 15* (1), 21-28.

[168] Khanna, A., & Shetty, V. K. (2014). Solar light induced photocatalytic degradation of Reactive Blue 220 (RB-220) dye with highly efficient $Ag@TiO_2$ core–shell nanoparticles: a comparison with UV photocatalysis. *Solar Energy, 99,* 67–76.

[169] Samsudin, E. M., Goh, S. N., Wu, T. Y., Ling, T. T., Hamid, S. B. A., Juan, J. C. (2015). Evaluation on the photocatalytic degradation activity of Reactive Blue 4 using pure Anatase nano-TiO_2. *Sains Malaysiana, 44* (7), 1011–1019.

[170] Thamaraiselvi, K. & Sivakumar, T. (2017). Photocatalytic activities of novel $SrTiO_3$–BiOBr heterojunction catalysts towards the degradation of reactive dyes. *Applied Catalysis B: Environmental 207*, 218–232.

[171] Neppolian, B., Choi H. C., Sakthivel S,. Arabindoo B,. Murugesan, V. (2002). Solar light induced and TiO_2 assisted degradation of textile dye reactive blue 4. *Chemosphere, 46*, 1173–1181.

[172] Giwa, A., Nkeyone, P. O., Bello, K. A., Kolawole, E. G. (2012). Solar photocatalytic degradation of Reactive Yellow 81 and Reactive Violet 1 in aqueous solution containing semiconductor oxides. *International Journal of Applied Science and Technology, 2* (4), 90-105.

[173] Badawy, M. I., Mahmoudb, F. A., Abdel-Khalekc, A. A., Gad-Allaha, T. A., Abdel Samad, A. A. (2013). Solar photocatalytic activity of sol–gel prepared Ag-doped ZnO thin films. *Desalination and Water Treatment, 52*, 2601–2608.

[174] Wang, W. Y. and Ku, Y. (2006). Photocatalytic degradation of Reactive Red 22 in aqueous solution by UV-LED radiation. *Water Res., 40* (12), 2249-58.

[175] Tayade R. J., Sivakumar, T. N., Bajaj H. C. (2009). Photocatalytic degradation of Methylene Blue dye using ultraviolet light emitting diodes. *Ind. Eng. Chem. Res., 48* (23), 10262–10267.

[176] Stefanov, B. I., Kaneva, N.V., Puma, G. L., Dushkin, C. D. (2011). Novel integrated reactor for evaluation of activity of supported photocatalytic thin films: case of Methylene Blue degradation on TiO_2 and nickel modified TiO_2 under UV and visible light. *Colloid Surface A,* 382, 219-225.

[177] Eskandari, P., Kazemi, F., Azizian-Kalandaragh, Y. (2013). Convenient preparation of CdS nanostructures as a highly efficient photocatalyst under blue LED and solar light irradiation. *Separation and Purification Technology 120,* 180–185.

[178] Dai, K., Lü, J. L., Lu, L. H., Liu, Q., Zhu, G. P., Li, D. P. (2014). Synthesis of micro-nano heterostructure AgBr/ZnO composite for advanced visible light photocatalysis. *Materials Letters, 130,* 5-8.

[179] Kuo,Y. L., Su, T. L., Kung, F. C., Wu, T. J. (2011). A study of parameter setting and characterization of visible-light driven nitrogen-modified commercial TiO_2 photocatalysts. *Journal of Hazardous Materials, 190,* 938–944.

[180] Jo, W. K., Tayade R. J. (2014). New generation energy-efficient light source for photocatalysis: LEDs for environmental applications. *Industrial & Engineering Chemistry Research, 53* (6), 2073-2084.

[181] Zhang, W. and Wu, C. W. (2014). Dyeing of multiple types of fabrics with a single reactive azo disperse dye. *Chem Papers., 68,* 330–335.

[182] Nagai, S. (1959). Induction of the respiration-deficient mutation in yeast by various synthetic dyes. *Science, 130* (3383), 1188–1189.

[183] Heinfling, A., Martinez, M. J., Martinez, A. T., Bergbauer, M., Szewzyk, U. (1998). Transformation of industrial dyes by manganese peroxidases from Bjerkandera adusta and Pleurotus eryngii in a manganese-independent reaction. *Applied and Environmental Microbiology, 64* (8), 2788–2793.

[184] Hsiao, Y.-C., Wu, T.-F., Wang, Y.-S., Hu, C.-C., Huang, C. (2014). Evaluating the sentizing effect on the photocatalytic degradation of dyes using anatase-TiO_2. *Applied Catalysis B, 148,* 250–257.

[185] Zhang, S. (2014). Preparation of controlled shape ZnS microcrystals and photocatalytic property. *Ceramics International, 40,* 4553–4557.

[186] Zhang, X., Chen, W., Lin, Z., Yao, J., Tan, S. (2011). Preparation and photocatalysis properties of bacterial cellulose/TiO_2 composite membrane doped with rare earth elements. *Synthesis and Reactivity in Inorganic, Metal-Organic and Nano-Metal Chemistry, 41* (8), 997–1004.

[187] Khataee A. R., and Kasiri, M. B. (2010). Photocatalytic degradation of organic dyes in the presence of nanostructured titanium dioxide: influence of the chemical structure of dyes. *Journal of Molecular Catalysis A, 328* (1-2), 8–26.

[188] Jie, R.-H., Guo, G.-B., Zhao, W.-G., An, S.-L. (2013). Preparation and photocatalytic degradation of methyl orange of nano-powder TiO_2 by hydrothermal method supported on activated carbon. *Journal of Synthetic Crystals, 42,* 2144–2149.

[189] Bouberka, Z., Benobbou, K. A., Khenifi, A., Maschke, U. (2014). Degradation by irradiation of an Acid Orange 7 on colloidal TiO_2/(LDHs). *Journal of Photochemistry and Photobiology A, 275,* 21–29.

[190] Prasannan, A. and Imae, T. (2013). One-pot synthesis of fluorescent carbon dots from orange waste peels. *Industrial & Engineering Chemistry Research, 52,* 15673–15678.

[191] Devi, L. G. and Arunakumari, M. L. (2013). Enhanced photocatalytic performance of Hemin (chloro(protoporhyinato) iron (III)) anchored TiO_2 photocatalyst for methyl orange degradation: a surface modification method. *Applied Surface Science, 276,* 521–528.

[192] Abadulla, E., Tzanov, T., Costa, S., Robra, K.-H., Cavaco-Paulo, A., Gubitz, G. M. (2000). Decolorization and detoxification of textile dyes with a laccase from Trametes hirsuta. *Applied and Environmental Microbiology, 66* (8), 3357–3362.

[193] Sakkayawong, N., Thiravetyan, P., Nakbanpote, W. (2005). Adsorption mechanism of synthetic reactive dye wastewater by chitosan. *Journal of Colloid and Interface Science, 286* (1), 36–42.

[194] Wang, Y. Wang, G., Wang, H., Liang, C., Cai, W., Zhang, L. (2010). Chemical-template synthesis of micro/nanoscale magnesium silicate hollow spheres for waste-water treatment. *Chemistry: A European Journal, 16,* (11), 3497–3503.

[195] Gong, J.-L., Wang, B., Zeng, G.-M., et al., (2009). Removal of cationic dyes from aqueous solution using magnetic multi-wall carbon nanotube nanocomposite as adsorbent. *Journal of Hazardous Materials, 164* (2-3), 1517–1522.

[196] Peralta-Hernándeza, J. M., Meas-Vong, Y., Rodríguez, F. J., Chapman, T. W., Maldonado, M. I., Godínez, L. A. (2008). Comparison of hydrogen peroxide-based processes for treating dye-containing wastewater: decolorization and destruction of Orange II azo dye in dilute solution. Dyes & Pigments, 76(3), 656–662.

[197] Ikhtiyarova, G. A., Özcan, A. S., Gök, O., Özcan, A. (2012). Characterization of natural- and organo-bentonite by XRD, SEM, FT-IR and thermal analysis techniques and its adsorption behaviour in aqueous solutions. *Clay Minerals, 47,* 31–44.

[198] Rashmi, S. and V. Preeti, V. (2013). Decolorisation of aqueous dye solutions by low-cost adsorbents: a review. *Coloration Technology, 129,* 85–108.

[199] Hussein, F. H. (2013). Effect of photocatalytic treatments on physical and biological properties of textile dyeing wastewater. *Asian Journal of Chemistry, 25,* 9387–9392.

[200] Moon, J., Yun, C. Y., Chung, K.-W., Kang, M.-S., Yi, J. (2003). Photocatalytic activation of TiO_2 under visible light using Acid Red 44. *Catalysis Today, 87* (1–4), 77–86.

[201] Abdelaal, M. Y., and Mohamed, R. M. (2013). Novel Pd/TiO_2 nanocomposite prepared by modified sol-gel method for photocatalytic degradation of methylene blue dye under visible light irradiation. *Journal of Alloys and Compounds, 576,* 201–207.

[202] M. G. Weinbauer, C. Beckmann, and M. G. Höfle, (1998). Utility of green fluorescent nucleic acid dyes and aluminum oxide membrane filters for rapid epifluorescence enumeration of soil and sediment bacteria. *Applied and Environmental Microbiology, 64* (12), 5000–5003.

[203] Mohamed, A., Alberto, S., Victor, M.-F., Luis, E. (2013). Removal of basic yellow cationic dye by an aqueous dispersion of Moroccan stevensite. *Applied Clay Science, 80,* 46–51.

[204] Kavitha S. K., and Palanisamy, P. N. (2010). Solar photocatalitic degradation of Vat Yellow 4 dye in aqueous suspension of TiO_2-optimization of operational parameters. *Advances in Environmental Sciences, 2,* 189–202.

[205] Buitrón, G., Quezada, M., Moreno, G. (2004). Aerobic degradation of the azo dye acid red 151 in a sequencing batch biofilter. *Bioresource Technology, 92*(2), 143–149.

[206] Lachheb, H., Puzenat, E., Houas, A. et al. (2004). Photocatalytic degradation of various types of dyes (Alizarin S, Crocein Orange G, Methyl Red, Congo Red, Methylene Blue) in water by UV irradiated titania. *Applied Catalysis B, 39* (1), 75–90.

[207] Krishnakumar, B., Subash, B., Swaminathan, M. (2012). AgBr−ZnO - an efficient nano-photocatalyst for the mineralization of Acid Black 1 with UV light. *Sep. Purif. Technol., 85,* 35−44.

[208] Velmurugan, R., Selvam, K., Krishnakumar, B., Swaminathan, M. (2011). An efficient reusable and antiphotocorrosive nano ZnO for the mineralization of Reactive Orange 4 under UV-A light. Sep. *Purif. Technol., 80* (1), 119−124.

[209] Kiwi, J., Pulgarin, C., Peringer, P., Gratzel, M. (1993). Beneficial-effects of heterogeneous photocatalysis on the biodegradation of anthraquinone sulfonate observed in waste-water treatment. *New journal of chemistry, 17* (7), 487-494.

[210] Pichat, P., Guillard, C., Amalric, L., Renard, A-C., Plaidy, O. (1995). Assessment of the importance of the role of H_2O_2 and $O_2^{\cdot-}$ in the photocatalytic degradation of 1,2-dimethoxybenzene. *Solar Energy Materials and Solar Cells, 38,* 391-399.

[211] Muruganandham, M., Sobana, N., Swaminathan, M. (2006). Solar assisted photocatalytic and photochemical degradation of Reactive Black 5. *Journal of Hazardous Materials,* 1371-1377.

[212] Subash, B., Krishnakumar, B., Swaminathan, M., Shanthi, M. (2013). Highly efficient, solar active, and reusable photocatalyst: Zr-Loaded Ag−ZnO for Reactive Red 120 dye degradation with synergistic effect and dye-sensitized mechanism. *Langmuir, 29* (3), 939–949.

[213] Wawrzyniak, B. and Morawski A.W. (2005). Solar-light-induced photocatalytic decomposition of two azo dyes on new TiO_2 photocatalyst containing nitrogen. *Applied Catalysis B: Environmental, 62,* 150–158.

[214] Zhou, Y., Lu, S. X., Xua, W. G. (2008). Photocatalytic activity of Nd-doped ZnO for the degradation of C.I. Reactive Blue 4 in aqueous suspension. *Environmental Progress & Sustainable Energy, 28* (2), 226-233.

[215] Sakthivel, S., Neppolian, B., Shanker, M.V., Arabindoo, B., Palanichamy, M., & Murugesan, V. (2003). Solar photocatalytic degradation of azo dye comparison of photocatalytic efficiency of ZnO and TiO_2. *Solar Energy Materials and Solar Cells, 77*, 65–82.

[216] Di Paola, A., Ikeda, S., Marcì, G., Othani, B., Palmisano, L. (2001). Transition metal doped TiO_2: physical properties and photocatalytic behaviour. *International Journal of Photoenergy, 3,* 171-176.

[217] Rys, P., & Zollinger, H. (1992). Fundamentals of the chemistry and application of dyes. *Wiley-Interscience*, New York.

[218] Tusi, S.M., Chu, W. (2001). Quantum yield study of the photodegradation of hydrophobic dyes in the presence of acetone sensitizer. *Chemosphere, 44*, 17–22.

[219] Gozmen, B., Kayan, B., Gizir, A.M., Hesenov, A. (2009). Oxidative degradations of reactive blue 4 dye by different advanced oxidation methods. *Journal of Hazardous Materials, 168* (1), 129-136.

[220] Sivakumar, T. And Shanthi, K. (2000). Photocatalytic studies on some textile reactive dyes using TiO_2. *Indian, J. Environ. Protect., 21*, 101–104.

[221] Annadurai, G. Sivakumar, T. Babu, S. R. (2000). Photocatalytic decolurisation of congo red over ZnO powder using Box–Behnken design of experiments. *Bio Process Eng., 23*, 0167–0170.

[222] Sivakumar, T., Shanthi, K., Newton Samuel, T. (2000). Photocatalysed decomposition of anthraquinone sulphonic acid (sodium salt) using ZnO. *Bio Process Eng., 23*, 579–583.

[223] Ganesh, R., Boardman, G. D., Michelsen, D. (1994). Fate of azo dyes in sludges. *Water Research, 28* (6), 1367-1376.

[224] Navio, J. A, Testa, J. J, Djedjeian, P., Padron, J. R., Rodriguez D. (1999). Iron-doped titania powders prepared by a sol–gel method: part II: photocatalytic properties. *Appl. Catal. Gen., 178*, 191–203.

[225] Serpone, N., Lawless, D., Disdier, D. (1994). Spectroscopic, photoconductivity, and photocatalytic studies of TiO_2 colloids: naked and with the lattice doped with Cr^{3+}, Fe^{3+}, and V^{5+}. *Cations. Langmuir, 10* (3), 643–652.

[226] Carp, O., Hiusman C. L., Realler A. (2004). Photoinduced reactivity of titanium dioxide. *Progress in Solid State Chemistry, 32*, 33–177.

[227] Irie, H., Watanabe, Y., Hashimoto, K. (2003). Nitrogen - concentration dependence on photocatalytic activity on TiO_{2-x} N_x powders. *J. Phys. Chem. B, 107*, 5483–5486.

[228] A. Selvaraj, S. Sivakumar, A. Ramasamy and V. Balasubramanian, (2013). Photocatalytic degradation of triazine dyes over N-doped TiO_2 in solar radiation. *Res. Chem. Intermed*., *39,* 2287–2302.

[229] Muruganandham, M., and Swaminathan, M. (2004). Solar photocatalytic degradation of a reactive azo dye in TiO_2-suspension. *Solar Energy Materials and Solar Cells, 81* (4), 439-457.

[230] Fox, M. A., and Dulay, M. T. (1993). Heterogeneous photocatalysis. *Chem. Rev.*, *93* (1), 341–357.

[231] Mahmoodi, N. M., Arami, M., Limaee, N. Y., Gharanjig, K., Ardejani, F. D. (2006). Decolorization and mineralization of texile dyes at solution bulk by heterogeneous nanophtocatalysis using immobilizer nanoparticles of titanium dioxide. *Colloids Surf., A, 290*, 125-131.

[232] Prado, A. G. S., Bolzon, L. B., Pedroso, C. P., Moura, A. O., Costa L. L. (2008). Nb_2O_5 as efficient and recyclable photocatalyst for indigo carmine degradation. *Appl. Catal. A, 82*, 219-224.

[233] Aguedacha, A., Brosillonb, S., Morvanb, J., Lhadi, E. K. (2005). Photocatalytic degradation of azo-dyes reactive black 5 and reactive yellow 145 in water over a newly deposited titanium dioxide. *Appl.Catal. B, 57*, 55-62.

[234] Zhu, C., Wang, L., Kong, L., Yang, X., Wang, L., Zheng, S., Chen, F., Maizhi, F., Zong, H. (2000). Photocatalytic degradation of AZO dyes by supported TiO_2/UV in acqueous solution. *Chemosphere, 41*, 303-309.

[235] Sumandeep Kaur Vasundhara Singha (2007). TiO_2 mediated photocatalytic degradation studies of Reactive Red 198 by UV irradiation. *Journal of Hazardous Materials, 141* (1), 230-236.

[236] Qamar, M., Saquib, M., Muneer, M. (2005). Photocatalytic degradation of two selected dye derivatives, chromotrope 2B and amido black 10B, in aqueous suspensions of titanium dioxide. *Dyes and Pigments, 65* (1), 1-9.

[237] Jiang, Y., Sun, Y., Liu, H., Zhu, F., Yin, H. (2008). Solar photocatalytic decolorization of C.I. Basic Blue 41 in an aqueous suspension of TiO_2–ZnO. *Dyes and Pigments, 78* (1), 77-83.

[238] Zielinska, B., Grzechulska, J., Morawski, A.W. (2003). Photocatalytic decomposition of textile dyes on TiO_2-Tytanpol A11 and TiO_2-Degussa P25. *Journal of Photochemistry and Photobiology A: Chemistry 157*, 65–70.

[239] Calimana, A.F., Cojocarua, C., Antoniadis, A., Poulios, I. (2007). Optimized photocatalytic degradation of Alcian Blue 8 GX in the presence of TiO_2 suspensions. *Journal of Hazardous Materials, 144* (1–2), 265-273.

[240] Kunal, J., Varun, S., Digantkumar, C., Datta, M. (2012). Decolorization and degradation of azo dye – Reactive Violet 5R by an acclimatized indigenous bacterial mixed cultures-SB4 isolated from anthropogenic dye contaminated soil. *Journal of Hazardous Materials, 213– 214,* 378– 386.

[241] Ayed, L., Bekir, K., Achour, S., Cheref, A., Bakhrouf, A. (2017). Exploring bioaugmentation strategies for azo dye CI Reactive Violet 5 decolourization using bacterial mixture: dye response surface methodology. *Water and Environment Journal, 31,* 80–89.

[242] Jo, W.K., Park, G.T., Tayade, R. J. (2015). Synergetic effect of adsorption on degradation of malachite green dye under blue LED irradiation using spiral-shaped photocatalytic reactor. *J. Chem. Technol. Biotechnol., 90, 2280–2289.*

[243] Kulkarni, S. V., Blackwell, C. D., Blackard, A. L., Stackhouse, C. W., Alexander M. W. (1985). Textile Dyes and Dyeing Equipment : Classification, Properties, and

Environmental Aspects. US Environmental Protection Agency, Research Triangle Park NC 27711.

[244] Booth, Gerald (2000). *Dyes, General Survey*. Wiley-VCH Verlag GmbH & Co. KGaA.

[245] IUPAC, Compendium of Chemical Terminology, 2nd ed. (the "Gold Book") (1997).

[246] Hunger, K., Mischke, P., Rieper, W., Raue, R., Kunde, K., Engel, A (2005). Azo Dyes. *Ullmann's Encyclopedia of Industrial Chemistry*. Wiley-VCH, Weinheim.

[247] Baker, John R., (1958) Principles of biological microtechnique Methuen, London, UK.

[248] Phipps, Elena (2010). Cochineal Red The Art History of a Color, p34. Yale University Press, New Haven and London. ISBN 978-0-300-15513-6. Textile Organic Dyes.

[249] Zaharia, C. And Suteu, D. (2012). Characteristics, Polluting Effects and Separation/Elimination Procedures from Industrial Effluents – A Critical Overview. *Organic Pollutants Ten Years After the Stockholm Convention - Environmental and Analytical Update*, 55-86.

[250] Tappe, H., Helmling, W., Mischke, P., Rebsamen, K., Reiher, U., Russ, W., Schläfer, L., Vermehren, P. (2000). Reactive Dyes. *Ullmann's Encyclopedia of Industrial Chemistry*. Wiley-VCH, Weinheim.

[251] Farah Maria Drumond Chequer, Gisele Augusto Rodrigues de Oliveira, Elisa Raquel Anastácio Ferraz, Juliano Carvalho Cardoso, Maria Valnice Boldrin Zanoni and Danielle Palma de Oliveira (2013). Textile Dyes: Dyeing Process and Environmental Impact. *Eco-Friendly Textile Dyeing and Finishing*. Chapter 6, 151-176.

[252] Ohsaka, T., Izumi, F., Fujiki, Y. (1978). Raman spectrum of anatase, TiO_2. *Journal of Raman Spectroscopy*, 7 (6), 321–324.

[253] Aita, C. R. (2007). Raman scattering by thin film nanomosaic rutile TiO_2. *Applied Physics Letters,. 90,* (21), 213112–213113.